INVESTIGATION OF RANK DISTANCE PROPERTIES OF CYCLIC, ABELIAN CODES AND STUDY OF THEIR APPLICABILITY FOR ERROR CORRECTION IN WIRELESS DEVICES
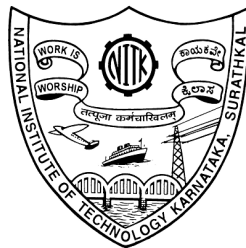
Thesis

Submitted in partial fulfillment of the requirements for the degree of

DOCTOR OF PHILOSOPHY

by

GODKHINDI SHRUTKIRTHI S.

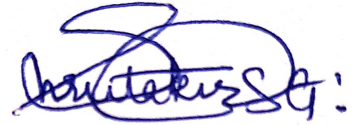DEPARTMENT OF ELECTRONICS AND COMMUNICATION ENGINEERING

NATIONAL INSTITUTE OF TECHNOLOGY KARNATAKA

SURATHKAL, MANGALORE - 575025

JULY, 2021

DECLARATION

I hereby *declare* that the Research Thesis entitled "**INVESTIGATION OF RANK DISTANCE PROPERTIES OF CYCLIC, ABELIAN CODES AND STUDY OF THEIR APPLICABILITY FOR ERROR CORRECTION IN WIRELESS DEVICES**" which is being submitted to the **National Institute of Technology Karnataka, Surathkal** in partial fulfillment of the requirements for the award of the Degree of **Doctor of Philosophy** in **Electronics and Communication Engineering** is a *bonafide report of the research work carried out by me*. The material contained in this Research Thesis has not been submitted to any University or Institution for the award of any degree.

Godkhindi Shrutkirthi S.

Reg. No.: 155081 EC15F01

Department of Electronics and Communication Engineering

Place: NITK, Surathkal.

Date: 22-07-2021

CERTIFICATE

This is to certify that the Research Thesis entitled **"INVESTIGATION OF RANK DISTANCE PROPERTIES OF CYCLIC, ABELIAN CODES AND STUDY OF THEIR APPLICABILITY FOR ERROR CORRECTION IN WIRELESS DEVICES"** submitted by **GODKHINDI SHRUTKIRTHI S.** (Reg. No.: 155081EC15F01) as the record of the research work carried out by her, is *accepted as the Research Thesis submission* in partial fulfillment of the requirements for the award of degree of **Doctor of Philosophy**.

U. Sripati Acharya
Research Supervisor

(Prof. U. Shripathi Acharya)

21|1|24
Chairman - DRPC

(Prof. Ashvini Chaturvedi)

PROF & HEAD
Department
N.I.T.K. Surathkal
MANGALORE - 575 025

ACKNOWLEDGMENT

I am grateful to all my faculties and teachers throughout my life, for their encouragement and guidance in both technical and personal life.

This thesis is dedicated to my family for their unfailing love, countless encouragements and patience. I am deeply indebted to my parents, Shashikant G. and Sangeeta G. for their immense love, consideration, care, time and motivation, without their blessing my journey would never have been possible. My special thanks to my dear sister, Bhargavi B. for being with me always and patiently listening to me every time. I would like to express my love and thanks to her and my grandma, Suhasini K., for their trust, unwavering love, enthusiasm and support throughout my journey. I am very grateful to my husband Bharath K. and my in-laws, for their continuous support, reassurance, motivation and trust in me.

Finally, I would like to thank God for helping me through all the difficult times, providing me a path at each and every step, for blessing me with good health, guidance and bliss during my research work.

Place: NITK, Surathkal   Godkhindi Shrutkirthi S.

Date: 22-07-2021

Dedicated to

My Parents and Family.

Abstract

The use of multiple-antenna configurations coupled with suitable signal processing techniques is one of the most promising technique to achieve high data rates and improved quality of service in wireless communication systems. Over the years many Multiple-Input Multiple-Output (MIMO) techniques have been proposed to achieve high spectral efficiencies, higher data rates and improved reliability of communication. MIMO techniques have been broadly divided into two broad categories; Spatial Multiplexing techniques (SMX) [Foschini (1996)], which is employed to enhance the capacity of system and Space Time Coding Techniques (STC) [Tarokh et al. (1998)], which have been employed to improve the reliability of communications. In SMX, independent streams of information are radiated from multiple transmit antennas. SMX achieves higher multiplexing gain, but this technique is not suitable for large scale MIMO, due to increased decoding complexity at the receiver. Space Time Block Codes (STBCs) are channel codes which maximize spatial diversity. STBCs are capable of providing improved coding gain for same spectral efficiency compared with equivalent diversity schemes. This in turn enhances the overall reliability of the wireless communication system. STBCs combat channel imperfections and improve the integrity of data transfer by combining coding gain with diversity gain [Alamouti (1998)].

Space Time (ST) techniques employing multiple antennas suffer from excess energy consumption, due to the activation of all antennas and their power amplifier chains. A energy efficient MIMO technique namely, Spatial Modulation (SM) was proposed by Mesleh et al. in [Mesleh et al. (2008)]. This technique achieves increased energy efficiency by activating only a single antenna at a time. Spectral efficiency is further improved by conveying information through the medium of active antenna indices [Mesleh et al. (2008)]. Thus SM is an energy conserving technique that utilizes the spatial dimension of multiple antenna configuration to convey additional information. The concept of SM was further improved by appending a STBC with the SM scheme. This

arrangement was introduced by [Basar et al. (2011)] and is known as Space Time Block Coded Spatial Modulation (STBC-SM). Most of the literature on this topic has been devoted to the study and design of Orthogonal STBC-SMs. However, it has been observed that several Non-orthogonal STBCs provide performance (both in terms of Bit Error Rate (BER) and Spectral efficiency) than conventional Orthogonal-STBCs. This has lead us to study the performance of several families of Non-Orthogonal STBCs when employed over different types of channels in this thesis.

The use of error control code enhances the integrity of data transfer, especially when the communication system is operating in an environment perturbed by channel induced distortion and noise. This is done by introducing controlled number of redundant bits into the information bit stream. The discipline of error control codes has evolved from designing binary codes for binary symmetric channels to designing complex symbol oriented codes for various types of channels including semiconductor, optical and magnetic memories [Moon (2005)]. A comprehensive study of the literature has inspired us to explore the use of full rank codes over STBCs, STBC-SM systems and in other evolving applications.

In this thesis we have designed a class of full rank Non orthogonal Space Time Block Codes (NSTBC) which are derived from full rank Cyclic and Abelian codes. It is observed that these NSTBCs outperform conventional STBCs when employed over a variety of channel fading conditions. The description of research work conducted commences in Chapter 3 after a brief description of the state of art (literature survey) given in Chapter 2. In Chapter 3, we have proposed a class of Spatially Modulated Non Orthogonal Space Time Block Codes (SM-NSTBC) designed from $n-$length non-binary Cyclic codes over $GF(q^m)$ where q is a prime and m is order of the extension field ($m \leq n$). The proposed SM-NSTBC outperforms conventional Spatially Modulated Orthogonal Space Time Block Codes (SM-OSTBC), STBC-SM, SM schemes and their variants in terms of average bit error rate (ABER) performance.

In chapter 4, the concept of receive spatial modulation has been explored. The technique of Precoded SM-NSTBC is proposed to attain receive spatial modulation. In this scheme a part of information is conveyed by receive antenna indices in addition to the

conventionally radiated NSTBC symbols. This is achieved by adopting suitable precoding technique at the transmitter. The performance of proposed Precoded SM-NSTBC scheme is synthesized for spatially correlated and spatially uncorrelated Rayleigh fading environments.

The design of a cooperative communication system with Amplify and Forward relaying for Spatially Modulated Non-orthogonal Space Time Block Code (SM-NSTBC-AF) is discussed in Chapter 5. A single relay with multiple antenna elements is assumed to exist between source and destination. The information transmitted by the source is received by the relay in first time slot, in the second time slot this information is amplified and forwarded to the destination. In the proposed scheme, a direct link between source and destination as well as the cooperative link (link between source and destination through a relay) are assumed to exist and operate in tandem. It is observed that this approach provides improved ABER performance over conventional schemes. This scheme has been compared with equivalent schemes employing amplify and forward relaying, namely Cooperative STBC-SM schemes and Cooperative SM schemes.

In Chapter 6, the system and channel model of High Altitude Platforms (HAPs) has been studied. The effect of Imperfect Channel State Information (Imp-CSI) is investigated to obtain insight into the performance of HAP-MIMO links when deployed in real life situations. The performance of full rank SM-NSTBC, STBC-SM and SM-OSTBC schemes over a HAP-MIMO environment is analyzed. It is observed that proposed SM-NSTBC outperforms competing schemes under the conditions of perfect-CSI availability as well as imperfect-CSI.

In the last part of this thesis we have investigated the design of NSTBCs derived from non-binary Abelian codes. First, a description of the transform domain properties and rank-distance properties of Abelian codes has been provided. This is followed by the design and synthesis of Spatially Modulated Non-orthogonal Space Time Block Codes derived from n-length full rank Abelian codes over $GF(q^m)$. It is observed that the proposed Abelian SM-NSTBC provides a performance improvement when compared with Cyclic SM-NSTBC and other conventional STBCs.

In summary, in this thesis we have utilized the rank distance characterization of

Cyclic and Abelian codes. The codewords derived from Cyclic and Abelian codes when viewed as $(m \times n)$ matrices possess full rank. By employing suitable rank preserving maps we have synthesized full rank Non-orthogonal STBCs from these full rank codes. SM-NSTBC schemes which achieve high reliability, high spectral efficiency with moderate decoding complexity have been designed. The performance of proposed schemes have been analyzed under Rayleigh fading environments. Further, we have explored the concept of receive spatial modulation and have synthesized schemes which employ full rank Non-orthogonal STBCs. This is followed by the derivation of a technique which employs cooperative SM-NSTBC with amplify and forward relaying to improve the overall link performance. We have also proposed a MIMO scheme which can be employed on a High Altitude Platform communication system. The performance of this scheme over HAP-MIMO environment has been determined. The design of all systems has been done keeping in view of the 3GPP communication standards.

It is expected that the results contained in this thesis will be useful for the designs of modern communication systems such as 5G and beyond-5G.

Contents

Acronyms and Abbreviations

ABER   Average Bit Error Ratio

AF   Amplify and Forward

AoA   Angle of Arrival

AoD   Angle of Departure

AWGN   Additive White Gaussian Noise

BER   Bit Error Rate

bpcu   bits per channel use

CDF   Cumulative Distribution Function

CSI   Channel State Information

CSIT   Channel State Information at Transmitter

DF   Decode and Forward

ECC   Error correcting codes

GF   Galois Field

GFFT   Galois Field Fourier Transform

GPSM   Generalised Pre-coding aided Spatial Modulation

HAP   High Altitude Platform

IAI   Inter Antenna Interference

ICI   Inter Channel Interference

IGFFT   Inverse Galois Field Fourier Transform

i.i.d   Independent and Identically Distributed

IM   Index Modulation

Imp-CSI   Imperfect Channel State Information

LoS   Line of Sight

L-SM   Layered Spatial Modulation

LTE   Long Term Evolution

MIMO   Multiple Input Multiple Output

ML   Maximum Likelihood

NLoS   Non Line of Sight

NSTBC	Non-Orthogonal Space Time Block Code
OSTBC	Orthogonal Space Time Block Code
QoS	Quality of Service
P-CSI	Perfect Channel State Information
PDF	Probability Density Function
PEP	Pairwise Error Probability
PSM	Precoding aided Spatial Modulation
RS	Reed-Solomon
SC	Spatially Correlated
SD	Sphere Decoding
SISO	Single Input Single Output
SM	Spatial Modulation
SM-OSTBC	Spatially Modulated Orthogonal Space Time Block Code
SM-NSTBC	Spatially Modulated Non-orthogonal Space Time Block Code
SMX	Spatial Multiplexing
SNR	Signal to Noise Ratio
STBC	Space Time Block Codes
STBC-CSM	Space Time Block Coded Spatial Modulation with Cyclic structure
STBC-SM	Space Time Block Coded Spatial Modulation
STBC-TSM	Space Time Block Coded Spatial Modulation with Temporal Modulation
STC	Space Time Codes
STSK	Space Time Shift Keying
TAS	Transmit Antenna Synchronization
UAV	Unmanned Ariel Vehicle
3GPP	3rd Generation Partnership Project
5G	5th Generation

List of Symbols

Symbol	Explanation
$\mathbf{X}$	Transmitted symbol vector
$\mathbf{H}$	Channel Matrix
$\mathbf{Y}$	Received symbol vector
$\mathbf{N}$	Additive White Gaussian Noise random variables
$\mathscr{C}$	Cyclic code
$Rank_q(\cdot)$	Rank of a Cyclic code over $GF(q)$
m	Extension field
n	Length of a cyclic code
$GF(q)$	Galois field of size q
$GF(q^m)$	m^{th} Galois Field extension of $GF(q)$
$\mathbf{a}$	n- tuple value over finite field
$\mathbf{A_j}$	GFFT of $\mathbf{a_i}$
$\mathbf{a_i}$	IGFFT of $\mathbf{A_j}$
p	Characteristic of a finite field element
α	Primitive polynomial
e_j	Size of the Cyclotomic coset
$[c]^d$	Cardinality of c
$\mathscr{Z}_i$	Gaussian integer map of i
$\zeta(i)$	Eisenstein integer map of i
$[\cdot]$	Rounding to the next nearest integer
$\mathbf{X}^T$	Transpose of matrix $\mathbf{X}$
$\mathbf{X}^H$	Matrix Hermitian of $\mathbf{X}$
$\|\mathbf{X}\|_F^2$	Frobenius norm of the matrix
N_t	Number of transmit antennas
N_r	Number of receive antennas
N_a	Number of active antennas

Symbol	Explanation
$\mathbf{M}_{m \times m}$	Full rank $m \times m$ codeword matrices
θ	Angle of rotation
$\mathbf{X_{SM}}$	Spatially modulated transmitted codeword matrix
$\hat{\mathbf{X}}_{\mathbf{SM}}$	Estimated codeword of $\mathbf{X}$
$\tilde{\mathbf{X}}_{SM}$	Set of all possible codewords
η	Spectral Efficiency
n_s	Number of time slots
$\mathbf{H_e}$	Equivalent channel matrix
$Re\{H\}$	Real part of H
$Im\{H\}$	Imaginary part of H
T	Number of time slot
$N(\mathbf{X}_{SM} - \hat{\mathbf{X}}_{SM})$	Number of non-zero elements of matrix of $(\mathbf{X}_{SM} - \hat{\mathbf{X}}_{SM})$
$P(\mathbf{X}_{SM} \to \hat{\mathbf{X}}_{SM})$	Pairwise error probability (PEP)
$E\{\mathbf{c}\}$	Expectation of $\mathbf{c}$
$Q(\cdot)$	Q function
$\mathbf{S}_{SM}$	Information codeword matrix
$\mathbf{P}$	Precoding matrix
$\hat{\mathbf{S}}_{SM}$	Estimation of $\mathbf{S}_{SM}$
β	Normalization factor
$\mathbf{X}$	Transmitted Signal
$\mathbf{H}_c$	Correlated channel matrix
h_{ij}	Channel gain from jth transmit antenna to ith receive antenna
$\mathbf{R}_{Rx}$	Receiver correlation matrix
$\mathbf{R}_{Tx}$	Transmitter correlation matrix
$\otimes$	Kronecker product
ρ	Spatial Correlation coefficient
$d(\mathbf{S_{SM}}, \hat{\mathbf{S}}_{SM})$	Number of non-zero elements of $(\mathbf{S_{SM}} - \hat{\mathbf{S}}_{SM})$
M_α	Moment generating function of α
$f_{(\alpha)}(\alpha)$	Probability density function of α
Γ	The gamma function
N_{re}	Number of relay antennas

Symbol	Explanation
E_s	Symbol energy
$\mathbf{H}_{SR}$	Channel matrix from source to relay
$\mathbf{H}_{SD}$	Channel matrix from source to destination
$\mathbf{Y}_{sr}$	Received signal at the relay
$\mathbf{Y}_{sd}$	Received signal at destination
G	Scaling factor
P_{out}	Outage probability
K	Rician factor
$\mathbf{H}_{LoS}$	Line of sight component of channel
$\mathbf{H}_{NLoS}$	Non-line of sight of channel
σ^2_{LoS}	Power of LoS
σ^2_{NLoS}	Power of NLoS
θ_A	Angle of Arrival
θ_D	Angle-of-Departure

List of Figures

List of Tables

Chapter 1

Introduction

Error control codes are widely employed to reduce impairments in transmission channels caused by packet loss, channel noise, channel fading, and interference. The use of error control codes enhances the robustness against noise and channel induced perturbations by adding controlled redundancy into the information bits. The performance of most classical channel codes is primarily determined by the minimum distance (d_{min}) between two codewords of the code. The most commonly used distance metric is the Hamming metric, which specifies the number of discrepancies in corresponding locations between two codewords. However, for several channels/storage memory models, a distance metric closely matched to the distortion induced by the channel/storage device has to be incorporated, which is more suitable to the interference introduced by the channel. An alternate distance metric that has received considerable attention over the past three decades is the Rank metric. This metric has found application in several domains such as wireless communications, cryptography, storage systems, and network coding. Historically, most classical error control codes were synthesized with the Hamming metric as the distance measure. The Hamming metric is not particularly well suited to the characteristics of many real channels (for example, MIMO-fading channels or certain storage channels). Hence, many researchers have attempted to postulate metrics that match the communication channel/storage device characteristics in a more comprehensive manner. This search has led researchers to come up with the Rank metric. The notion of the Rank metric was first introduced by [Delsarte (1978)]. Rank metric is a distance measure which is well suited to quantify the perturbations introduced by wireless MIMO channels, storage arrays and storage tape drives where information

is represented in the form of rectangular matrices rather than one dimensional n-tuple. Gabidulin has constructed linear codes over the finite field $GF(q)$ for every k, m and n where q is a prime, k, n are parameters of code and m represents order of the extension field [Gabidulin (1985)]. Roth has studied the same problem in the context of coding for storage devices [Roth (1991)]. Sripati et.al [Sripati (2004)] have specified methods to construct full rank $m \times n$ codes over the field $GF(q)$ from the families of Cyclic and Abelian codes. These full rank codes were employed to construct designs for Non-Orthogonal Space Time Block codes (NSTBCs) by using suitable Rank preserving metrics [Sripati et al. (2004), Sripati and Rajan (2003)]. Many researchers have since then used this approach to synthesize NSTBCs for a number of applications [Puchinger et al. (2016), Lusina et al. (2003), Goutham Simha (2018), Mans et al. (2017)]. In this thesis, we have used this approach to synthesize NSTBC designs for a number of modern applications.

The modern era is characterized by ubiquitous connectivity provided by wireless communication systems. Communication infrastructure should be designed for widespread accessibility, high throughput, and reliability. Keeping these objectives in mind, it has become essential for upcoming wireless standards such as 5G and beyond-5G to provide a service, which is reliable in addition to being energy as well as spectrally efficient. The most promising solution capable of supporting the increasing demand for high-quality wireless services is the use of multiple antennas at transmit and receive end, i.e. use of Multiple Input-Multiple Output (MIMO) schemes [Foschini and Gans (1998)]. In order to achieve Multiplexing gain, a MIMO technique named spatial multiplexing (SMX) has been proposed [Foschini (1996)]. Though SMX achieves higher multiplexing gains, it is not suitable for very large scale MIMO and massive MIMO systems due to the increased complexity and cost overheads [Mesleh et al. (2017)]. Space Time Block Codes (STBC) are channel codes designed for use with multiple transmit/receive antennas to improve the reliability of wireless communication. This is done by exploiting the diversity inherent in a MIMO system and augmenting this with the coding gain provided by the channel code [Alamouti (1998)]. The Alamouti code was the first Orthogonal Space Time Block code to be proposed. Orthogonal Space Time

Block Codes achieve rate-one, full diversity for two transmit antenna systems. For systems, which possess more than 2 transmit/receive antennas, Orthogonal STBCs impose a limitation that the maximum achievable symbol rate would reduce to 3/4, which in turn reduces the channel capacity [Tarokh et al. (1998), Su and Xia (2003)]. To increase the reliability of the system other variants of STBCs such as Quasi-Orthogonal STBC, Non-orthogonal STBC and full diversity high-rate STBCs have been proposed in [Li and Wang (2014), Le et al. (2014)].

Spatial Modulation (SM) [Mesleh et al. (2008)] constitutes a low complexity substitute to conventional SMX schemes with the added advantage of improved spectral and energy efficiency. SM is a unique method that achieves higher energy efficiency by activating only a single antenna at a time. Spectral efficiency is improved by conveying information through the medium of antenna indices. Inter channel interference (ICI) is eliminated as a single antenna is activated at the transmitting end over any symbol interval. This scheme was generalized to activate more than one transmit antennas as shown in [Mesleh et al. (2008), Simha et al. (2017)]. SM scheme was further augmented by combining OSTBC with SM (known as Space Time Block Coded Spatial Modulation (STBC-SM)) [Basar et al. (2011)]. STBC-SM has allowed a trade-off between achievable throughput and diversity. In STBC-SM, the information bits are divided into two parts, the first half is used to activate different sets of two transmit antennas, and the other half of information bits are modulated as 2×2 Alamouti STBC and radiated by the activated antennas. Many variants of STBC-SM which achieve high data rates have been proposed in the last few years. One significant example is the class of Spatially Modulated Orthogonal Space Time Block Codes (SM-OSTBC) which incorporated the concept of spatial constellation selection [Le et al. (2014), Wang and Chen (2014)].

1.1 Motivation for this Research work

Algebra has emerged as an important tool to study and analyze error control codes. Channel codes are an essential constituent of modern wired and wireless communication as well as storage systems. There are a wide variety of channels whose characteristics are not well matched to the traditional Hamming metric. Hence, alternate metrics

have been described in the literature, and it has been shown that the Rank distance metric is well matched to correct errors that could be introduced in MIMO channels. The performance of such wireless communication channels can be considerably improved by using matrix codes that have good rank distance properties. A comprehensive study of the literature on Orthogonal and Non-Orthogonal STBCs has inspired us to explore the use of full rank codes in MIMO systems. The primary motivation of this work is to synthesize and evaluate novel NSTBC designs for different MIMO techniques by employing the full rank codes (A full rank code is defined as a code in which all of the codeword matrices other than the all zero codeword matrix possess full rank property). A large amount of existing literature on this topic is dedicated to the use of STBC MIMO techniques with orthogonal property. However it has been observed that several schemes employing non-orthogonal STBCs promise performance improvement [Mans et al. (2017)]. In this thesis we have proposed a class of non-orthogonal STBCs, with full rank property which outperforms conventional STBCs. The concept of synthesizing STBCs from full rank Cyclic was introduced in [Sripati (2004)]. This body of research work has been continued further in this thesis. A number of NSTBC designs for various modern applications arising from full rank Cyclic and Abelian codes have been synthesized. The performance of these designs has been evaluated through analytic means and Monte Carlo simulations. The contributions made by this thesis in various chapters are enumerated below.

Chapter 2 provides a study of the existing literature available. Firstly, the basic model of the MIMO communication system is provided, followed by the description of the Rayleigh channel model. Further, a fundamental insight is provided on the preliminary concepts used in the construction of codes proposed in this thesis. A description of rank as a metric is provided. It is shown that this rank metric can be employed to quantify errors introduced by MIMO channels. Followed by the transform domain description of Cyclic code and its rank-distance properties. Furthermore, a discussion of rank-preserving maps, namely Gaussian Integer Map and Eisenstein Integer Map is provided. These rank preserving maps are employed in this thesis to obtain codeword matrices over the complex number field from the designed Cyclic and Abelian code-

words (defined over a finite field).

Chapter 3 is the first contributory chapter in this thesis. A novel MIMO scheme, namely Spatially Modulated Non Orthogonal Space Time Block Codes (SM-NSTBC), is presented in this chapter. The full rank codewords obtained from Cyclic codes are employed in the design of SM-NSTBC codewords. These full rank codewords matrices are obtained over finite field of $GF(q)$ (q is a prime) are transformed into equivalent full rank matrices over the complex number field by incorporating rank-preserving maps. A theoretical upper bound on the Average Bit Error Rate (ABER) is derived for the proposed scheme. Further, a low complexity sphere decoder for the proposed SM-NSTBC scheme has been presented, and its performance has been evaluated. The performance of this proposed SM-NSTBC is compared with existing conventional schemes, namely SM, SM-OSTBC and STBC-SM schemes. Simulation results show that the proposed SM-NSTBC scheme provides a minimum performance improvement of 1.5 dB over SM-OSTBC schemes and approximately 5 dB over conventional SM scheme.

To further explore the performance of SM-NSTBC scheme, the concept of precoding is incorporated in Chapter 4. The novel idea of Precoded SM-NSTBC for receive antenna activation is proposed. In the Precoded SM-NSTBC scheme, additional information bits are conveyed by the use of receive antenna indices. This technique is mainly preferred for downlink communication as it leads to a reduction in complexity at the receiver end. In order to activate the specific set of receive antennas, a suitable precoding technique has to be incorporated at the transmitter end. A detailed discussion of the precoding algorithm has been provided in this chapter. Here, we assume that the Channel State Information is available at the transmitter end. An analytical upper bound on the ABER is derived for the proposed scheme and the decoding complexity is computed. Followed by a brief description of the mathematical model used to describe Spatially Correlated (SC) channel conditions. With the help of this insight, the performance of proposed Precoded SM-NSTBC is determined for varying values of Spatial Correlation. It is observed that the proposed Precoded SM-NSTBC outperforms precoded SM-OSTBC and precoded STBC-SM by a minimum of 2 dB.

The concept of cooperative communication is explored in Chapter 5. The arrange-

5

ment of multiple antennas at the transmitter and/or receiver is not always possible due to the limitation of size and cost of hardware. In such a framework employing relays achieves the advantage of the MIMO scheme by establishing a virtual MIMO system. The design and performance analysis of cooperative communication with Amplify and Forward relaying scheme for Spatially Modulated Non-orthogonal Space Time Block Code (SM-NSTBC-AF) is provided in this chapter. The cooperative link is established between the transmitter and receiver through a relay. In the proposed SM-NSTBC-AF scheme, a direct link between transmitter and receiver as well as the cooperative link are assumed to be operating simultaneously to ensure better performance than the conventional scheme. The analytical upper bound and outage probability for the proposed SM-NSTBC-AF scheme is evaluated. The performance is compared with equivalent schemes with amplify and forward relaying, namely cooperative STBC-SM and cooperative SM scheme. A performance improvement of ~ 3 dB is observed over the competing schemes.

In the next contributory chapter, a communication scheme operating in conjunction with an Unmanned Ariel Vehicle (UAV) scenario is considered. The channel and system model of High Altitude Platforms (HAP) is studied to understand the various issues affecting communication between UAVs and base stations. Further, the performance of Space Time Block Codes and Spatial Modulation is studied in the context of communication with HAPs. The performance of SM-NSTBC scheme operating over a HAP environment is explored. This performance is compared with other competing schemes, and it is observed that SM-NSTBC achieves higher performance as compared to other schemes. Further, the effect of Imperfect Channel State Information (Imp-CSI) in the presence of spatial correlation is studied to gain a deeper understanding of various practical factors that influence performance. It is observed that the SM-NSTBC scheme outperforms other STBCs with perfect-CSI and Imp-CSI channel conditions.

Chapter 7, is devoted to the design of NSTBCs originating from Abelian codes. First a brief description of Abelian code's characterization and their transform domain description is given. Followed by a discussion of the rank-distance properties of Abelian codes and the method to synthesize full rank distance codes from the class of Abelian

codes is provided. These full rank-distance Abelian codes are then used to synthesize a class of full rank Non-Orthogonal Space Time Block Codes by incorporating rank-preserving maps. The performance of these spatially modulated NSTBCs extracted from Abelian codes are compared with the conventionally synthesized STBC-SM, SM-OSTBC and SM-NSTBC derived from Cyclic codes. It is thus shown that the class of Abelian codes can be a rich source for NSTBC designs.

The last chapter provides a summary of results obtained and further enlists the directions for future research work.

Chapter 2

Literature Survey

In this chapter, background of MIMO communication system is provided. Followed by the introduction of preliminary concept that are incorporated in this thesis is described. The preliminary concepts such as the notion of rank as a metric, the transform domain description of Cyclic codes, Rank distance properties of Cyclic code, construction of full rank Cyclic codes and description of rank preserving maps are discussed.

2.1   Introduction to MIMO communication

The most fundamental mode of wireless communication is the single input single output (SISO) system that employs only a single antenna at transmitter and receiver ends. A multiple antenna system at the transmitter and receiver offers the advantage of increased diversity and possible coding gain over the SISO model of wireless communication.
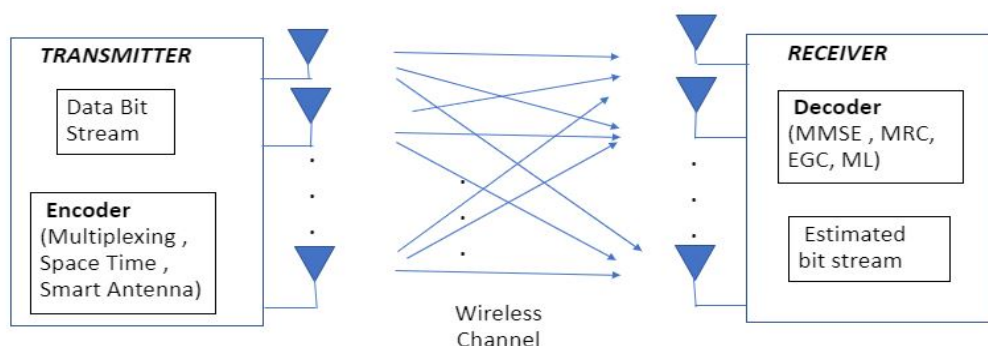
Figure 2.1 Generalized block diagram of MIMO scheme.

Figure 2.1 gives a generalized block diagram of a multiple-input multiple-output

(MIMO) system, a system that has more than one antenna at both transmitter and receiver. In a MIMO system, more than one communication link is established between transmitter and receiver. A MIMO system with N_t number of transmit antennas and N_r number of receive antennas is sketched in Figure (2.1). The received signal is given by Equation (2.1). In this equation, $y_1, y_2, \cdots, y_{N_r}$ represent the N_r received symbols, The coefficients $h_{i,j}$; $0 \le i \le N_t, 0 \le j \le N_r$ represent the channel coefficients, $x_1, x_2, \cdots, x_{N_t}$ represent the transmitted symbols and $n_1, n_2, \cdots, n_{N_r}$ represent the noise symbols.

$$
\begin{bmatrix} y_1 \\ y_2 \\ \vdots \\ y_{N_r} \end{bmatrix} = \begin{bmatrix} h_{11} & h_{12} & \cdots & h_{1N_t} \\ h_{21} & h_{22} & \cdots & h_{2N_t} \\ \vdots & \vdots & \cdots & \vdots \\ h_{N_r 1} & h_{N_r 2} & \cdots & h_{N_r N_t} \end{bmatrix} \begin{bmatrix} x_1 \\ x_2 \\ \vdots \\ x_{N_t} \end{bmatrix} + \begin{bmatrix} n_1 \\ n_2 \\ \vdots \\ n_{N_r} \end{bmatrix} \tag{2.1}
$$

The vector representation of this equation is specified by,

$$
\mathbf{Y} = \mathbf{HX} + \mathbf{N} \tag{2.2}
$$

Here $\mathbf{Y}$ is the received vector, $\mathbf{H}$ represents the channel between transmitter and receiver, $\mathbf{X}$ is the transmitted symbol vector and $\mathbf{N}$ represents independent and identically distributed (i.i.d) circularly symmetric complex Additive White Gaussian Noise (AWGN) random variables with zero mean and unit variance. For any MIMO system, the average transmit power is assumed to be same for all transmit antennas and is normalized to value of unity.

The Spatial Multiplexing (SMX) scheme is one of the most basic examples of a MIMO system. In a SMX system, all the transmit antennas radiate different streams of information, this in turn increases the total spectral efficiency and capacity of the system [Foschini (1996)]. As different symbols are radiated from different transmit antennas, transmit diversity is not achieved. Equation (2.1) gives a representation of a SMX system. The diversity gain of such a system depends only on the number of receive antennas.

The Space Time Block Codes (STBC) is another popular MIMO scheme, which

was first introduced by Alamouti in [Alamouti (1998)]. This code could achieve full diversity at transmitter and could be decoded by simple decoding technique. The temporal as well as the Spatial domains of a MIMO system were exploited by this code to yield results equivalent to that obtained by a 1×2 maximum ratio combining (MRC) system (corresponding to 2×1 Alamouti scheme) or 2×2 MRC system (corresponding to 2×2 Alamouti). This concept of STBC was later explored for higher numbers of transmit and receive antennas.

In general, the transmitted codeword of a STBC employing N_t transmit antennas and spread over T time slots is given by Equation (2.3)

$$\begin{bmatrix} x_{11} & x_{12} & \cdots & x_{1T} \\ x_{21} & x_{22} & \cdots & x_{2T} \\ \vdots & \vdots & \cdots & \vdots \\ x_{N_t 1} & x_{N_t 2} & \cdots & x_{N_t T} \end{bmatrix} \tag{2.3}$$

Later, in 2008 an energy efficient MIMO system was proposed in [Mesleh et al. (2008)] namely Spatial Modulation (SM). In this scheme, addition information is conveyed by the antenna index. The information is transmitted only from a single antenna and not by multiple antennas. This helps in reducing the issue of transmit antenna synchronization (TAS) and inter-antenna interference (IAI).

2.1.1 Channel description of MIMO system

The propagation medium between the transmitter and receiver is exposed to multi-path distortion, attenuation along superposition of noise. Signal distortion is brought about by phenomenon such as reflection, diffraction, refraction and scattering. This results in the creation of several components which arrive at the receiver at different instants, having experienced different amounts of phase shift and attenuation (multi-path components). So it becomes very crucial to estimate the channel coefficients, which specify the phase change and the attenuation suffered by the signal over each of the $N_t \times N_r$ individual propagation channels characterizing a MIMO system. A channel model is usually specified by a particular probability distribution which captures the distortion

introduced by the channel in a precise manner. The Rayleigh, Rician and Nakagami-m probability distributions have been extensively employed in literature to model the perturbations induced by communication channels. The received symbol is often modeled as a complex number with the real (in-phase) component describing the amplitude and the imaginary (quadrature phase) component representing the phase shift. The channel coefficient component defined between a pair of transmit and receive antennas is described by,

$$h = h_r + jh_i \tag{2.4}$$

here h is individual channel coefficient, h_r and h_i are the real and imaginary components of h.

A symbol propagating over a channel containing a large number of scattering and reflecting objects in which a Line of Sight (LoS) component is not supported is usually modeled as perturbed by a Rayleigh distributed random variable. The Rayleigh distribution describes the distortion induced by a multipath fading channel with Non-Line of Sight (NLoS) components accurately. This Rayleigh fading model is one of the most commonly adopted statistical model used to describe the effect of a propagation environment on a radio signal.

In this thesis Rayleigh fading environment is mainly incorporated. The concept of Rank as a distance metric and full rank codewords designed from transform domain description of Cyclic codes are explored in this thesis. An overview of this rank as a metric is provided in following section. This is followed by a description of the Galois field transform domain description of Cyclic codes in section 2.3. In section 2.4 Cyclic codes are synthesized by making use of the transform domain description and their rank properties are analyzed. Section 2.5 gives a brief insight over the rank preserving maps used to transform the Galois field elements of the code to the complex number field which make up the transmitted codeword with symbols from the complex number field.

2.2 Introduction to Rank distance metric in coding theory

The most commonly used distance metric for any error control code is Hamming distance. But there are other metrics which are better suited to the real-time characteristics

of channel conditions. One such example is the Rank metric. The concept of Rank distance and its application as a distance metric to design channel codes originated in the work of Delsarte and Gabidulin [Delsarte (1978), Gabidulin (1985)]. Further, Gabidulin discovered the techniques to synthesize linear codes with good Rank Distance properties. Roth in [Roth (1991)] discovered the class of maximum-rank array codes and applied them to the correction of criss-cross errors found in semiconductor memories and tape drives. Later, [M.Blaum and van Tilborg (1998)] have provided a description of construction, decoding approaches and performance of array codes. In this section we have described the concept of rank distance and its application as a distance metric.

Rank as metric: Let $\mathscr{C}$ be a code defined over $GF(q^m)$. The equivalent matrix of $\mathscr{C}$ can be obtained by expanding each element of $\mathscr{C}$ (which is an element of $GF(q^m)$) as an m-tuple over $GF(q)$. Then the Rank of a vector $\mathscr{C} \in GF(q^m)$ is the rank of equivalent matrix **M**, obtained by expanding each element of $\mathscr{C}$.

Rank distance satisfies all the requirements of a metric as shown below. Let the Rank of vector $\mathscr{C}$ over $GF(q)$ be represented as $Rank_q \mathscr{C}$. Let $\mathscr{C}_1, \mathscr{C}_2, \mathscr{C}_3 \in GF(q^m)$ then,

- $Rank_q \mathscr{C} \geq 0$. The rank can be zero only for all zero vector.

- $Rank_q(\mathscr{C}_1, \mathscr{C}_1) = Rank_q(\mathscr{C}_1 - \mathscr{C}_1) = 0$.

- Triangle inequality : $Rank_q(\mathscr{C}_1, \mathscr{C}_2) \leq Rank_q(\mathscr{C}_1, \mathscr{C}_3) + Rank_q(\mathscr{C}_3, \mathscr{C}_2)$.

- $Rank_q(\mathscr{C}_1, \mathscr{C}_2) = Rank_q(\mathscr{C}_1 - \mathscr{C}_2) = Rank_q(\mathscr{C}_2 - \mathscr{C}_1) = Rank_q(\mathscr{C}_2, \mathscr{C}_1)$

Here $Rank_q \mathscr{C}$ is the Rank of $\mathscr{C}$ over $GF(q)$. The matrix space is defined as the collection of all $m \times n$ matrices with elements $a_{i,j}$ drawn from the finite field $GF(q)$, where m is the order of the extension field and n is the length of the code. The code is a subspace of this vector space constructed using a step by step well determined procedure. The rank distance $Rank_q(X, Y)$ between two codewords X and Y of the code is defined as the rank of difference matrix $(X - Y)$ over $GF(q)$. The minimum value of $Rank_q(X, Y)$ evaluated over all codewords X, Y of the code is termed as the Rank distance of the code.

In many applications such as tape drives, storage devices and several wireless schemes, data is stored in two dimensional arrays. If suitable codewords drawn from a rank metric

code are used to store information in this schemes, then error detection and correction can be enabled by using the rank distance metric.

In order to obtained codes with high error detection and correction property, the codes must satisfy full rank property. One can obtain full rank codewords by using the transform domain description of full rank Cyclic codes. Consider an n-length vector **c** over the field $GF(q^m)$ which is considered as a vector space of dimension m over $GF(q)$. Therefore the vector $\mathbf{c} \in [GF(q^m)]^n$ can also be regarded as a $m \times n$ matrix over $GF(q)$ by expanding each element of $\mathscr{C}$ as an m-tuple along a basis of $GF(q^m)$ over $GF(q)$. The process of obtaining full rank Cyclic codes and its equivalent full rank matrix is explained in the following section.

2.3 Transform domain description of Cyclic codes

Cyclic codes are one of the subclass of linear codes with additional property of cyclic shift. The design of Cyclic codes have close relation to the structure of Galois fields [Blahut (2003)]. This Galois field description of a Cyclic code is employed in encoding and decoding applications.

The Galois Field Fourier Transform (GFFT) for Cyclic codes of length n over $GF(q^m)$ is as follows [Moon (2005)].

- *The GFFT Transform Pair:* Let $\mathbf{a} = (a_0, a_1, \ldots, a_{n-1}) \in GF(q^m)$, where q is prime and $gcd(q, n) = 1$. Let τ be the smallest positive integer such that $n | q^{m\tau} - 1$ and $\alpha \in GF(q^{m\tau})$ be an element of order n. The Galois Field Fourier Transform (GFFT) of $\mathbf{a}$ is given by $\mathbf{A} = (A_0, A_1, \ldots, A_{n-1})$, where the element A_j is defined as given in equation (2.5).

$$A_j = \sum_{i=0}^{n-1} \alpha^{ij} a_i \qquad j = 0, 1, ..., n-1 \tag{2.5}$$

The Inverse Galois Field Fourier Transform (IGFFT) of $\mathbf{A}$ is defined as given in equation (2.6).

$$a_i = \frac{1}{n \; modulo \; p} \sum_{j=0}^{n-1} \alpha^{-ij} A_i \qquad i = 0, 1, ..., n-1 \tag{2.6}$$

14

Here, **a** and **A** are considered to be time domain and transform domain Fourier Transform pair, p is the characteristic of the Galois field $GF(q)$ and its extension fields, α is defined as the nth root of unity [Moon (2005)].

- An $n-$length codeword derived in $GF(q^m)$ is systematically represented as $m \times n$ matrix over $GF(q)$. Consider a codeword **A** of length n over $GF(q^m)$, it is expressed as a $m \times n$ matrix over $GF(q)$ as given below:

$$\mathbf{a} = \begin{bmatrix} a_{0,0} & a_{0,1} & \cdots & a_{0,n-1} \\ a_{1,0} & a_{1,1} & \cdots & a_{1,n-1} \\ \vdots & \vdots & \cdots & \vdots \\ a_{m-1,0} & a_{m-1,1} & \cdots & a_{m-1,n-1} \end{bmatrix} \tag{2.7}$$

In this matrix, $a_{i,j} \in GF(q)$. The rank of this matrix is equivalent to the rank of codeword **a**, where $\mathbf{a} = \{\mathbf{a_0}, \mathbf{a_1}, \ldots, \mathbf{a_{n-1}}\}$ and the individual $\mathbf{a_i} \in GF(q^m)$.

Cyclotomic coset: The cyclotomic cosets modulo n with respect to $GF(q)$ is a partitioning of the integers into sets. Let $I_n = 0, 1, 2, \ldots\ldots\ldots, n-1$, for any $j \in I_n$ and for any divisor d of m the q^d cyclotomic coset of $j \bmod n$ is a set defined by

$$[j]^d = \{i \in I_n | j = iq^{dt} \bmod n \; for \; some \; t \geq 0\} \tag{2.8}$$

Cardinality of the above set is given by $e_j^{(d)}$. When ($d = 1$), we denote the q-cyclotomic coset of $j \bmod n$ by $[j]$ and its cardinality by e_j. The cardinality of a cyclotomic coset is used for the design of full rank Cyclic codes. The structure of Cyclic codes have a close correspondence to the structure of Galois field.

The GFFT of Cyclic codes defined in Equation 2.5 is a linear transform satisfying the properties of conjugacy constraint and cyclic shift [Sripati (2004)]. These properties are described below:

- *Conjugacy Constraint Property* [Sripati (2004)]: Let **a** and **A** are considered to be time domain and transform domain Fourier Transform pair as defined in Equation 2.5. $\mathbf{A} \in GF(q^{m\tau})$ is the GFFT of $\mathbf{a} \in GF(q^m)$ if and only if

$$A_{jq^m \, modulo \, n} = A_j^{q^m} \quad \forall j \in [0, \, n-1] \tag{2.9}$$

This constraint restricts A_j to the subfield $GF(q^{\tau_j})$ of $GF(q^{m\tau})$ where τ_j is the length of $[j]^m = \{j, jq^m, jq^{2m}, \cdots, j(q^{m(\tau_j-1)})\}$. The specific value of A_j uniquely specifies the values of all transform components $A_{j'}$ for $j' \in [j]^m$.

- *Cyclic Shift property* [Sripati (2004)]: If $\mathbf{A} = GFFT(\mathbf{a})$, let $b \in GF(q^m)$, n-tuple such that $b_i = a_{i-1 \, mod \, n} \, \forall \, i \in [0, \, n-1]$ and $\mathbf{B} = GFFT(\mathbf{b})$, then

$$B_j = a^j A_j \quad \forall j \in [0, \, n-1] \tag{2.10}$$

From property 2 for linear Cyclic codes, A_j takes values from $\{0\}$ or $GF(q^{e_j^{(m)}})$. Hence Cyclic code can be considered as a set of inverse GFFT vectors of all the vectors of a subspace of $GFFT(GF(q)) \in GF(q^m)$. Here, transform components in $[j]^m$ of every vector take on only the zero vector or all the values of $GF(q^{e_j^{(m)}})$ and transform components in disjoint $[j_1]^m$ and $[j_2]^m$ take values independently.

In other words, for a linear block code to be classified as a Cyclic codeword, the codeword components in the time domain as well as the transform domain must satisfy the cyclic shift property as indicated above. The elements which are not in same cyclotomic coset are independent. In the following section the Rank properties of Cyclic codes is discussed.

2.4 Rank Properties of Cyclic codes

In this section the Rank distance properties of Cyclic codes have been discussed[Sripati and Rajan (2003), Sripati (2004)]. Full rank Cyclic codes can be designed by incorporating the following.

Lemma [Moon (2005)]: Let $\mathscr{C}$ be a Cyclic code of length n over $GF(q^m)$ with A_0 being one of the free transform domain components. Then $Rank_q(\mathscr{C}) = 1$.

It can be proved by the definition of transform domain, as A_0 has no component multiples by it, for any value of j in definition we get only single value in base field i.e. A_j, forcing the code to become an n repetition code. That has only one independent component.

Theorem 1 [Sripati and Rajan (2003)]: Consider $\mathscr{C}$ to be a Cyclic code of length n, $(n|q^m - 1)$ over $GF(q^m)$, let $A_{jq^s} = A_{[j]}$, $(|[j]| = e_j, \ 0 \le s \le e_j - 1)$ be a single free transform domain component and all other transform components be constrained to zero, then the $Rank_q(\mathscr{C}) = e_j$. Were, e_j is order of the q-cyclotomic coset $[j]$.

When A_{jq^s} is the only free transform domain component and all other $n - 1$ components are constrained to zero, then the inverse Galois Field Fourier Transform (IGFFT) of the components is given by definition as

$$a_i = \frac{1}{n \ modulo \ p} \alpha^{-ijq^s} A_{jq^s} \tag{2.11}$$

We ignore $1/(n \ modulo \ p)$ scaling factor as it does not contribute to rank of the matrix. This implies that, $\mathbf{a} = \{A_{jq^s}(\alpha^0, \alpha^{-jq^s}, \ldots, \alpha^{-(n-1)jq^s})\}$, which tend to have values only from the conjugacy class of α^{jq^s}. So the total $Rank_q(\mathbf{C})$ of the codeword is given same as the order of q-cyclotomic coset $[j]$.

Theorem 2 [Sripati (2004)]: Let $\mathscr{C}$ be a Cyclic code of length n, $(n|q^m - 1)$ over $GF(q^m)$ with a single free transform component $A_{jq^s}, 0 \le s \le e_j - 1$ and all other transform components constrained to zero. For any non-zero codeword $\mathbf{a} = (a_0, a_1, \ldots, a_{e_j-1}, a_{e_j}, \ldots, a_{n-1}) \in \mathscr{C}$ the entries of $(a_{e_j}, a_{e_j+1}, \ldots, a_{n-1})$ can be expressed as a linear combination of the entries $(a_0, a_1, \ldots, a_{e_j-1})$.

Proof: By definition, we know $a_i = \alpha^{-ijq^s} A_{jq^s}$,

$$\mathbf{a} = (A_{jq^s}, \alpha^{-jq^s} A_{jq^s}, \ldots, \alpha^{-e_{j-1}jq^s} A_{jq^s}, \alpha^{e_j jq^s} A_{jq^s}, \ldots, \alpha^{-(n-1)jq^s} A_{jq^s})$$

where e_j is the order of q-cyclotomic coset $[j]$. For simplicity we assume $A_{jq^s} = 1$, so we get

$$\mathbf{a} = (1, \alpha^{-jq^s}, \alpha^{-2jq^s}, \ldots, \alpha^{-e_{j-1}jq^s}, \alpha^{-e_j jq^s}, \ldots, \alpha^{-(n-1)jq^s}).$$

Let $X = (1, \alpha^{-jq^s}, \alpha^{-2jq^s}, \ldots, \alpha^{-e_{j-1}jq^s}, \alpha^{-e_j jq^s}, \ldots, \alpha^{-(n-1)jq^s})$, as $A_{jq^s} \ne 0$ then $Rank_q(a) = e_j$. To decude theorem 2, let $X_1 = (1, \alpha^{-jq^s}, \alpha^{-2jq^s}, \ldots, \alpha^{-e_{j-1}jq^s})$, and all elements of X_1 are independent and the rest element of X i.e. $(\alpha^{-e_j jq^s}, \alpha^{-e_{j+1}jq^s}, \ldots, \alpha^{-(n-1)jq^s})$ are dependent on X_1.

Using the contradiction, assume that, all element of X_1 are not independent. As they are dependent, one can formulate that, there exist set of coefficients $c_0, c_1, c_2, \ldots, c_{e_{j-1}} \in GF(q)$ such that $c_0 + c_1\alpha^{-jq^s} + c_2\alpha^{-2jq^s}, \ldots, c_{e_{j-1}}\alpha^{-e_{j-1}jq^s} = 0$ given that, not all $c_i = 0$.

This implies that the degree of the minimal polynomial of α^{-jq^s} is $\leq e_{j-1}$. But, this disagrees with the basic construction where the degree of minimal polynomial is e_j. This contradicts our assumption that, element of X_1 are dependent. Hence, the first e_j components are independent in X and all other elements can be represented as linear combination of first e_j elements. Hence it's proved that for any non-zero codeword $a = (a_0, a_1, \ldots, a_{e_j-1}, a_{e_j}, \ldots, a_{n-1}) \in C$ the entries of $(a_{e_j}, a_{e_j+1}, \ldots, a_{n-1})$ can be expressed as a linear combination of the entries $(a_0, a_1, \ldots, a_{e_j-1})$. In other words the $Rank_q(\mathbf{a}) =$ number of linearly independent components in $\{a_0, a_1, \ldots, a_{e_j-1}, a_{e_j}\}$.

Thus, all the non-zero codewords of this code $\mathscr{C}$ (which are $m \times n$ matices over $GF(q)$) have rank equal to e_j. The single free transform component is chosen from a full size q-cyclotomic coset of size m.

We know that a $n-$length Cyclic codeword derived in $GF(q^m)$ can be systematically represented as $m \times n$ matrix over $GF(q)$ as shown in equation (2.7). Therefore from theorem 1 and 2, it can be stated that first m columns are linearly independent and the remaining $(n-m)$ columns are linearly dependent on the first m columns. The code can be punctured without a reduction in the rank by dropping the last $(n-m)$ columns of every codeword. Hence, we will henceforth work with the $m \times m$ full rank codeword matrices of the punctured Cyclic code $\mathscr{C}$. Let us illustrate the process of code construction with a suitable example.

Let A_j be the single free transform domain component drawn from a full size q-cyclotomic coset of size m. Making use of the definition of the IGFFT, the time domain vector can be represented as,

$$\mathbf{a} = [A_j, \alpha^{-j}A_j, \alpha^{-2j}A_j, \ldots, \alpha^{-(n-1)j}A_j] \tag{2.12}$$

Here, $A_j \in GF(q^m)$ and α is the nth root of unity. Each of the n coefficients of this vector can be represented as a n tuple over the field $GF(q)$. From Theorem 1, it follows that by arranging these n-tuples as columns one can obtain an $m \times n$ full rank matrix over $GF(q)$. While by Theorem 2, it can be proved that elements $A_0, A_1, \cdots, \alpha^{(e_j-1)j}A_{j-1}$ are linearly independent.

Example 1: *Consider the Cyclic code over $GF(5)$ as the base field and $m = 4, n|q^m - 1$, where $n = 13$. Let A_1 be a free transform domain component and all other compo-*

nents are constrained to zero.

Here, $e_j = 4$, so element A_0 to A_3 are independent and at the same time A_4 to A_{12} can be expressed as linear combinations of A_0 to A_3. By shortening the $m \times n$ matrix to $m \times e_j$ we get a 4×4 matrix. It can be generalized as follows for all possible values of A_1.

$$C = \begin{bmatrix} a_0 & 3a_0 + a_1 + 2a_2 + 2a_3 & 2a_0 + 3a_1 + 2a_2 + 3a_3 & 3a_0 + 4a_1 + 3a_3 \\ a_1 & a_0 + 4a_1 + 3a_2 + 4a_3 & 2a_0 & a_0 + 2a_1 + 4a_2 + 4a_3 \\ a_2 & 4a_0 + 4a_1 + 4a_3 & 4a_0 + a_1 + a_2 + 4a_3 & 3a_1 + 2a_2 + a_3 \\ a_3 & 2a_0 + 4a_1 + 4a_2 & a_0 + 4a_1 + a_2 + a_3 & 3a_0 + 3a_2 + 2a_3 \end{bmatrix}$$

Here a_0, a_1, a_2, a_3 are coefficient of $\alpha^0, \alpha^1, \alpha^2, \alpha^3$ where α is primitive element of $GF(5^4)$ and $a_0, a_1, a_2, a_3 \in GF(5)$. As the free transform domain component selected here is A_1 with its cyclotomic coset given by $[1] = \{1, 5, 12, 8\}$.

Similarly, consider $q = 7$ and $m = 4$. We consider the Cyclic code $\mathscr{C}$ construction of length $n = 5$ over $GF(7^4)$. We select A_1 as the free transform component and constrain all other transform components to zero in order to satisfy the conditions required to define a full rank Cyclic code (i.e a Cyclic code whose non-zero codewords are full rank when viewed as $m \times n$ matrices over the base field $GF(7)$). It has been determined that as $1 \in \{1, 2, 4, 3\}$, a cyclotomic coset of full size in $GF(7^4)$, all the non zero codewords of a Cyclic code with A_1 as the free transform domain component with all other transform components constrained to zero will possess rank equal to $m = 4$. Hence, we allow A_1 to take on values successively from $\{0, 1, \cdots, \alpha^{7^4 - 2}\}$ in the field $GF(7^4)$ and constrain all other transform components to zero. For a given value of A_1, the corresponding codeword matrix can be obtained by computing the Inverse Galois Field Fourier Transform. By making this computation successively for 7^4 values that can be taken on by A_1 from the field $GF(7^4)$, we can compute the entire set of codewords of the Cyclic code.

The full rank code with $m \times m$ matrices over $GF(q)$ can be transformed into an equivalent collection of full rank $m \times m$ matrices over the complex number field by the

use of suitable rank-preserving maps. Two such maps, namely the Gaussian Integer map and the Eisenstein Integer map are described in literature. The Gaussian Integer map is applicable only for prime integers of the form $4K+1$, where K is an integer. The Eisenstein map is applicable only for prime integers of the form $6K+1$, where K is an integer. For codewords over $GF(2)$ one can obtain a map is obtained by mapping the symbols $\{0,1\}$ to a rank preserving map of $\{+1,-1\}$ [Sripati (2004)]. Hence, conventional signal constellations where the number of symbols is a power of 2 cannot be employed in these schemes.

The following sub-section gives brief insight about the rank preserving mapping scheme which can be employed while designing a system with full rank code vectors.

2.5 Rank Preserving Mapping techniques

Gaussian and Eisenstein mapping techniques are bijective, isometric and rank preserving. Lusina et.al, in [Lusina et al. (2003)] proposed the use of rank preserving maps for finite fields, which could retain the full rank property from $GF(q)$ to a complex signal set in designing of STBCs. The mapping was carried by the use of Gaussian Integers ($q = 1\ mod\ 4$). A prime number q which is in the form of $q = 4K+1$, can be expressed as $q = u^2 - v^2$ for suitable u and v. These are known as Gaussian integers which are represented by $\omega = u + iv; u, v \in Z$ [Huber (1994b)]. This map is defined as follows:

$$\mathscr{Z}_i = i\ mod\ \Pi = i - \left[\frac{i\Pi'}{\Pi\Pi'}\right]\Pi; \qquad i = 0, 1, \ldots, q-1 \qquad (2.13)$$

Here, $\Pi = (u + iv)$ and $\Pi' = (u - iv)$, $[\cdot]$ stands for rounding of operation to the nearest integer. The values of ω for $q = 5, 13, 17$ is tabulated in Table 2.1 .

Table 2.1 $q, \Pi, u\ and\ v$ values

q	Π	u	v
5	2+i	-1	1+i
13	3+2i	-2	1+2i
17	4+i	-2	2+i

A similar interpretation for Eisenstein-Jacobi integers was given in [Huber (1994a)],

where a rank preserving map for $GF(q)$, (q is a prime) which can be expressed as $q = 1 \mod 6$ was given. The Eisenstein-Jacobi integer can be expressed as $\omega = \alpha + \rho\beta$, where ρ is a complex number given by $\rho = (-1 + i\sqrt{3})/2$, the Eisenstein-Jacobi prime is given by $q = \alpha^2 + 3\beta^2$ [Puchinger et al. (2016)]. The mapping for Eisenstein map is given as following:

$$\zeta(i) = i \quad \mod \Pi \triangleq i - \left\lceil \frac{i\Pi^*}{\Pi\Pi^*} \right\rceil \Pi \, for \, i = 0, 1, 2, \ldots, q-1 \quad (2.14)$$

Where $\Pi = \alpha + \beta + \rho 2\beta$ and $\Pi^* = \alpha + \beta + \rho^2 2\beta$. The values $GF(q)$ represented using the Gaussian and Eisenstein integer maps for certain values of q are listed in Table 2.2

Table 2.2 q', Π, α and β values

q'	Π	α	β
7	3+2ρ	2	1
13	3+4ρ	1	2
19	5+2ρ	4	1

This technique of constructing full rank Cyclic codes can be used to synthesize binary as well as non-binary Cyclic codes [Sripati et al. (2004)]. We have used this technique to synthesize full rank codes over $GF(5), GF(7), GF(13)$ and $GF(17)$. These full rank codes further mapped using rank preserving maps have been used to derive suitable NSTBC designs as described in following chapters. The rank preserving maps incorporated for $GF(5), GF(13), GF(17)$ is Gaussian integer map, and for $GF(7)$ is Eisenstein Integer map. The map and the constellation diagram of $GF(5)$, $GF(7)$, $GF(13)$ and $GF(17)$ is provided in Appendix A.

The next chapter gives a brief description about the design of full rank Cyclic codes. A novel scheme of Spatially Modulated Space Time Block Code (SM-NSTBC) is proposed, which utilizes the codewords derived from full rank Cyclic codes over $GF(q)$ where q is a prime. These derived full rank codewords are then translated into equivalent Space Time Block Codes by employing Gaussian Integer Map and Eisenstein Integer Map. These obtained non-binary codewords are then spatially modulated to select

active antenna combination. The performance of proposed scheme is compared with conventional SM, STBC-SM and SM-OSTBC schemes. An upper bound is derived to validate Monte-Carlo simulations. The computation complexity is evaluated for the proposed scheme. Later, a low complexity sphere decoding scheme is also provided. It is observed that proposed SM-NSTBC outperforms other competing schemes.

Chapter 3

Design and performance analysis of Spatially Modulated Non-Orthogonal Space Time Block Code

[1] A new class of non-binary Spatially Modulated Non-orthogonal Space Time Block Code designs (SM-NSTBCs) have been proposed. These designs employ full rank, length $n, (n|q^m - 1, m \leq n)$ Cyclic codes defined over $GF(q^m)$. The underlying Cyclic code constructions have the property that the codewords when viewed as $m \times n$ matrices over $GF(q)$ have rank equal to m (full rank). These codes are punctured to yield $m \times m$ full rank matrices over $GF(q)$. Rank preserving transformations have been employed to map the codewords of full rank codes over a finite field to full rank Space Time Block Codes. The proposed scheme can be generalized to handle any number of transmit antennas greater than two. Due to the characteristics of full rank Cyclic codes employed, a coding gain of approximately 1.5 dB to 5 dB is obtained over conventional STBC-SM and SM-OSTBC schemes. This is demonstrated for spectral efficiencies of 4,5,7 and 8 bpcu. Analytical as well as Monte-Carlo simulations show that the proposed SM-NSTBC outperforms STBC-SM and its variants. An upper bound on the average bit error rate has been derived and the computation complexity for ML detection has been estimated.

---

[1]Godkhindi Shrutkirthi S., et al. " Spatially Modulated Non Orthogonal Space Time Block Code: Construction and design from Cyclic codes over Galois Field". Physical Communication, 35, 100735., 2019

3.1 Introduction

It has been shown that the most effective and constructive way of increasing the performance of a wireless system is to use multiple antenna combinations at both transmitter and receiver terminals [Telatar (1999)]. This type of arrangement when combined with suitable signal processing techniques has the ability of being able to combat various signal fading effects. The two major limitations in wireless communication systems are power and the bandwidth. Multiple Input Multiple Output (MIMO) schemes have been deployed to improve the system throughput and reliability. MIMO systems have brought about significant improvements in the performance of wireless systems. These improvements are obtained at the cost of enhancement in the complexity at the transmitter and receiver. Thus, improvement in spectral efficiency, reliability of information transfer and throughput eventually increases the system complexity and power consumption (due to the use of more RF chains). Recently, there has been an active interest in designing novel wireless architectures that can yield some or all of the desirable goals with reduced complexity and power consumption [Mesleh et al. (2008)]. Developments in MIMO technology such as Spatial Multiplexing (SMX) and Space Time Block Codes (STBCs) have contributed to the improvement in spectral efficiencies and reliability of information transfer.

Space Time Block Codes were first introduced in [Tarokh et al. (1998)], which demonstrated the concept of Space-Time Codes for high data rate Wireless communications by employing the concept of transmit antenna diversity. The next generation 5G networks demand very high levels of reliability, high data rate and energy efficiency. Keeping these objectives in mind, researchers have developed intelligent and novel physical layer modulation techniques such as Spatial Modulation (SM) [Mesleh et al. (2008)] and STBC-SM schemes [Basar et al. (2011)]. In SM systems, the spatial domain is used as one of the information bearing dimensions to convey data bits. This has the effect of improving the spectral efficiency. This arrangement offers the dual benefits of reduction in energy consumption as well as decoding complexity by activating only one RF chain throughout the process of transmission. The requirement for having multiple RF chains is eliminated due to single antenna activation. However, it has to

be noted that single active antenna transmission will not improve the performance of the system in terms of transmit diversity. Transmit diversity plays a major role in optimizing the Bit Error Rate (BER) performance of a system evaluated over a deep fading environment. Orthogonal codes designed as STBCs have been employed in conjunction with SM systems to improve BER over uncorrelated Rayleigh fading channel. Such a scheme has been designed by [Basar et al. (2011)] and known as Space Time Block Coded Spatial Modulation (STBC-SM) system. This STBC-SM method represents information in the form of a STBC matrix, which is transmitted from different combinations of transmit antennas of a MIMO system. STBC-SM was first implemented with the Alamouti code. In this design, bits are divided into two parts, the information bearing bits and the antenna selection bits. The information bearing bits are used to set up two complex information symbols which are used to form Alamouti STBC, and the antenna selection bits (antenna indices) are used to determine the particular antenna which will radiate the information symbols for transmission.

Another transmit diversity scheme namely Space-Time Shift Keying (STSK) was proposed by Sugiura et.al [Sugiura et al. (2010)] in 2010. A number of high rate STBC-SM systems have been proposed in the recent past [Le et al. (2014), Wang and Chen (2014), Wang et al. (2014)]. Lie Wang in [Wang et al. (2014)] has proposed a STBC-SM with an embedded (n, k) Cyclic Error Correcting Code (ECC). This scheme provides a high spectral efficiency as a result of the large number of codewords employed. Another approach was designed to enhance the spectral efficiency of SM systems. This is designated as Space Time Block Coded Spatial Modulation with Cyclic structure (STBC-CSM), given by Xaiofeng Li et.al in [Li and Wang (2014)]. Spatially Modulated Orthogonal Space Time Block Codes (SM-OSTBC) which incorporated the concept of spatial constellation selection was proposed in [Le et al. (2014), Wang and Chen (2014)]. Helmy et.al. [Helmy et al. (2016)] had proposed STBC-TSM which utilizes the temporal modulation to further improve the performance of STBC-SM. In STBC-TSM, Cyclic spatially modulated rotated Alamouti STBCs are employed to obtain full transmit diversity over four consecutive time slots. The concept of utilizing the active antennas as layers was proposed in [Alkhawaldeh (2018)], which would ensure diversity

and coding gain at each antenna selection due to the use of multi-layer coding scheme.

A comprehensive study of the above literature has inspired us to explore the use of full rank codes. Full rank codes obtained from Cyclic codes are used in synthesizing designs for Spatially Modulated Non Orthogonal Space Time Block Codes (SM-NSTBC). We have derived $n-$length Cyclic codes over $GF(q^m)$ where $m \leq n$, has rank m when viewed as $m \times n$ matrices over $GF(q)$ [Sripati and Rajan (2003), Sripati et al. (2004)]. Using Rank preserving transformations, these full rank $m \times n$ matrices over $GF(q)$ are transformed into equivalent full rank matrices over the complex number field. This collection of all full rank matrices over the complex number field constitutes the SM-NSTBC design. The full rank property of the codeword contributes to the improvement in terms of bit error rate (BER) performance over SM, STBC-SM, SM-OSTBC, STBC-TSM and L-SM schemes.

The major contributions of this chapter are enumerated as follows:

- A new SM-MIMO transmission system, called SM-NSTBC, has been designed and presented. Following [Sripati et al. (2004)] we have constructed several full rank NSTBCs from Non-binary Cyclic codes over $GF(q^m)$.

- The proposed transmission scheme make use of Gaussian and Eisenstein integers as given by [Huber (1994b), Huber (1994a), Lusina et al. (2003)]. This mapping has been utilized to preserve the rank (i.e. to transform full rank codewords constructed over a finite field to full rank codewords in the complex number field). Further, unlike the standard STBC-SM system, the codewords are radiated using different transmit antenna combinations from the column vectors of the derived NSTBC matrix.

- A comprehensive framework for the SM-NSTBC is devised in the form of choosing and adapting the same procedure for different active antenna combinations. We have explored the use of $N_a = 2$ and $N_a = 4$ active antenna combinations.

- It is shown by computer simulations that the proposed SM-NSTBC scheme exhibits significant performance improvements over STBC-SM and other conven-

tional SMs described in the literature. A closed form expression for the union bound on the bit error rate of the SM-NSTBC scheme is derived to support our results. The derived upper bound is shown to become very tight with the increase in signal-to-noise (SNR) ratio. Finally, the computational complexity for the proposed SM-NSTBC scheme has been estimated.

The rest of the chapter is organized as follows. Section 3.2, describes the design and characterization of SM-NSTBC. In Section 3.3, we discuss the SM-NSTBC system model. Analytical performance is derived in Section 3.4. Section 3.5, gives the complexity analysis followed by simulation results in Section 3.6. Section 3.7 concludes the chapter with an emphasis on designing of new SM-NSTBC constructions.

Notation: In this chapter, vectors are represented by bold lowercase and matrices by bold uppercase letters, $\mathbf{X}^T$ represents the transpose of matrix $\mathbf{X}$, $\mathbf{X}^H$ represents the matrix Hermitian of $\mathbf{X}$, $\|\mathbf{X}\|_F^2$ denotes the Frobenius norm of the matrix. $E\{\cdot\}$ is the expectation of a matrix. $GF(q)$ represents the Galois Field of size q and $GF(q^m)$ is m^{th} Galois Field extension of $GF(q)$. Other notations and abbreviations are given below in Table 3.1.

Table 3.1 Abbreviations and Notations

STBC	Space Time Block Code			
SM	Spatial Modulation	N_t	Number of transmit antennas
STBC-SM	Space Time Block Coded Spatial Modulation	N_r	Number of receive antennas
SM-OSTBC	Spatially Modulated Orthogonal STBC	N_a	Number of active transmit antennas
STBC-TSM	Space Time Block Codes with temporal Modulation	$\mathscr{C}$	Cyclic code
GF	Galois Field	$\mathscr{Z}(i)$	Gaussian Map
GFFT	Galois Field Fourier Transform	$\zeta(i)$	Eisenstein Map
IGFFT	Inverse Galois Field Fourier Transform	$\mathbf{M}_{m\times m}$	Full rank codeword matrix
ML	Maximum Likelihood	$\mathbf{X}_{SM}$	Spatially modulated codeword matrix
SD	Sphere Decoding	n_s	Number of time slots
ABER	Average Bit Error Rate	η	Spectral Efficiency
PEP	Pairwise Error Probability	$\mathbf{Y}$	Received matrix
LSM	Layered Spatial Modulation	$\mathbf{H}$	Channel Matrix
CSI	Channel State Information		

3.2 Characterization of Cyclic codes derived from transform domain

The preliminary information required to understand the design of codewords of the proposed SM-NSTBC scheme is provided in this chapter 2. The codewords used for NSTBC scheme design are derived from full rank Cyclic codes by employing a Rank preserving map. Full rank Cyclic codes over $GF(q)$ are obtained by making use of the Galois Field Fourier Transform (GFFT) description. This technique of constructing full rank Cyclic codes can be used to synthesize binary as well as non-binary Cyclic codes [Sripati et al. (2004)]. We have used this technique to synthesize full rank codes over $GF(5), GF(7), GF(13)$ and $GF(17)$. The codewords are derived from $GF(q^m), m = 4$. These full rank codes have been used to derive suitable SM-NSTBC designs.

The full rank code with 4×4 matrices over $GF(q), q = \{5, 7, 13, 17\}$ are transformed into an equivalent collection of full rank codewords matrices over the complex number field by the using the rank-preserving maps, namely the Gaussian Integer map and the Eisenstein Integer map as described in literature. The Gaussian Integer map is applicable only for prime integers of the form $4K + 1$, where K is an integer. The Eisenstein map is applicable only for prime integers of the form $6K + 1$, where K is an integer.

Employing these two dimensional complex map of Gaussian mapping (for $GF(5)$, $GF(13)$, $GF(17)$) or Eisenstein map (for $GF(7)$) [Goutham Simha et al. (2017)] the full rank Cyclic codewords are constructed for the proposed SM-NSTBC. We now describe the system model of the proposed SM-NSTBC scheme.

Note: In general SM systems, the symbol zero indicates that antenna is inactive for given time slot. This creates an ambiguity with the conventional symbol zero of the codeword. To avoid this confusion of zero in codeword and zero which represents the inactive state of antenna, the convention is that zero symbol of the codeword is mapped to a equivalent non-zero prime number from Gaussian integers or Eisenstein integers. For the proposed scheme the symbol zero is represented by $\mathscr{Z}_{2+i}, \mathscr{Z}_{3+2i}, \mathscr{Z}_{4+i}$ for Gaussian map over $GF(5), GF(13)$ and $GF(17)$, $\zeta_{3+2\rho}$ for Eisenstein map over $GF(7)$.

3.3 SM-NSTBC System Model
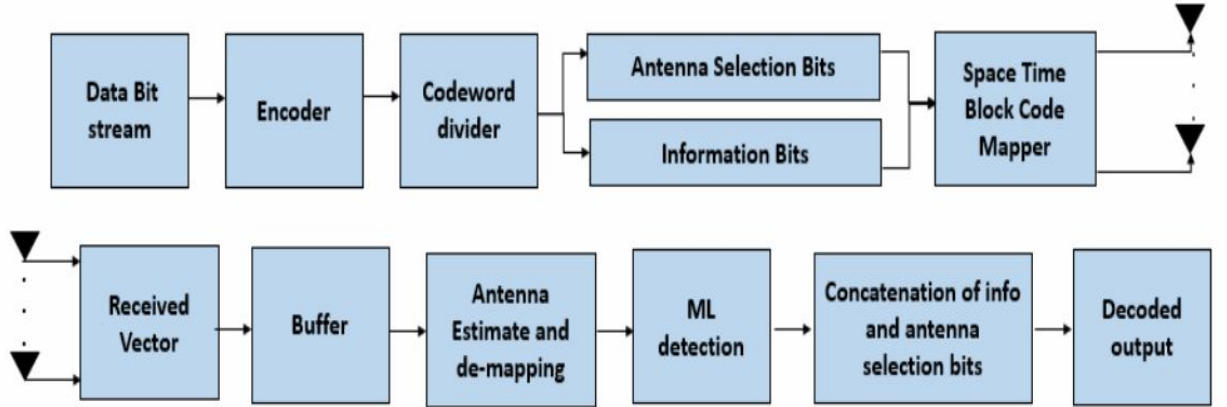
Figure 3.1 Block diagram of the proposed SM-NSTBC scheme

Figure 3.1, shows the block diagram of the proposed SM-NSTBC scheme. In the transmitter section, the information bits are encoded by a full rank n-length Cyclic code $\mathscr{C}$ over $GF(q^m)$ which yields full rank $m \times m$ codeword matrices after puncturing. Since, we assume that the incoming bit stream is binary, the number of bits that can be associated with a codeword is a power of 2. However, the number of codewords is a prime power q^m which is not necessarily a power of 2. Hence, we map $\lfloor \log_2(q^m) \rfloor$ bits to a single codeword of $\mathscr{C}$ over $GF(q)$.

In the following discussion, we have derived two SM-NSTBC schemes which differ in the number of active antennas in use over a given time slot. The number of active transmit antennas $(N_a) = 2, 4$ for case 1 and case 2 respectively. We have employed Cyclic codes over $GF(5^4), GF(7^4), GF(13^4)$ and $GF(17^4)$. Thus the codewords of all the codes are $4 \times n$ matrices over different values of $n, n | q^m - 1$. The various values of q, m and n employed in our constructions is specified in the Table 3.2.

Case 1: Two active antenna combination

The number of active antennas are 2 for a given time slot, so the minimum number of transmit antennas required is 3 or more. The elements of the codeword matrix are radiated column by column. The 4×4 matrix is viewed as a set of four 4×1 vectors.

Table 3.2 Values of q, m, n

q	m	n|q^m − 1
5	4	$13\|5^4 - 1$
7	4	$5\|7^4 - 1$
13	4	$5\|13^4 - 1$
17	4	$5\|17^4 - 1$

Each column is then divided into two parts, upper two symbols are used for antenna selection. These two symbols are responsible for selecting the two antennas which radiate during this time slot. The third and the fourth symbols of the column are now radiated using the selected antennas. These lower two symbols are transmitted after modulation using Gaussian or Eisenstein mapping from the activated transmit antennas. This process is then repeated for the remaining columns. Thus, $\lfloor \log_2 (q^m) \rfloor$ bits ($m = 4$) of information are transmitted by the use of one codeword over 4 time slots.

Here, every column of the codeword matrix selects the pair of active transmit antenna individually. Thus, each column of the codeword may be transmitted through a different set of active transmit antennas. One example of a possible transmitted codeword with $N_t = 4$ is illustrated in Equation (3.1). Here $\Im\{i\}$ represents the Gaussian ($\mathscr{Z}(i)$) or Eisenstein ($\zeta(i)$) map

$$\begin{bmatrix} 0 & 0 & \Im\{a_{2,2}\} & \Im\{a_{2,3}\} \\ \Im\{a_{2,0}\} & \Im\{a_{2,1}\} & 0 & 0 \\ \Im\{a_{3,0}\} & 0 & \Im\{a_{3,2}\} & 0 \\ 0 & \Im\{a_{3,1}\} & 0 & \Im\{a_{3,3}\} \end{bmatrix} \tag{3.1}$$

The 0s in each column of the matrix denote inactive antennas. Let us examine the first column of Equation (3.1). The first and the last entries are 0. This implies that antennas 1 and 4 are inactive during this time slot. The antenna selection bits have chosen

antennas 2 and 3 as the active antennas and the information symbols $a_{2,0}$ and $a_{3,0}$ are conveyed through these antennas after suitable Gaussian or Eisenstein mapping. The total number of ways in which two active antennas can be selected from N_t transmit antennas is $\binom{N_t}{2}$, while two symbols from $GF(q)$ can address as many as q^2 different combinations. For small values of N_t, this can represent a many to one mapping. To avoid ambiguity in antenna selection, we have constructed a look up table which maps all possible q^2 values to appropriate antenna pairs. Since, the number of transmit antennas is fixed, and the values of q^2 are relatively large, many two tuples of symbols from $GF(q)$ point to the same active transmit antenna pair. However, it must be kept in mind that at most $\left\lfloor q^2/\binom{N_t}{2} \right\rfloor + 1$ symbols are pointing to a given antenna pair. After an entire SM-NSTBC codeword is received, we employ ML decoding to identify the transmitted symbols as well as the antenna selection symbols.

The algorithm given below describes the encoding procedure for SM-NSTBC with $N_a = 2$. Here, $\mathbf{M}_{m \times m}$ are full rank $m \times m$ codeword matrices derived from Cyclic codes,

---

Algorithm 1 SM-NSTBC encoding algorithm for $N_a = 2$

1: Start
2: Consider $2^{\lfloor \log_2(q^m) \rfloor}$ bits
3: Step 1:Segregation into $\mathbf{M}_{m \times m}$ full rank matrices
4: Step 2: Obtain
5:   $\mathbf{M}_{m \times m} \to [\mathbf{M}_1]_{m/2 \times m}$ antenna selection symbols $+ [\mathbf{M}_2]_{m/2 \times m}$ information symbols
6: Step 3:for count=1:number of time slots for full codeword transmission
7: Step 4: Antenna selection
8:   $[\mathbf{M}_1]_{m/2 \times m} \to \mathbf{C}_1[a(1)a(2) \cdots a(2m)]$
9: Step 5: Mapping of Information symbols
10:   $\mathbf{C}_2[i(1)i(2) \cdots i(2m)]$
11:   Define map $\varphi : [\mathbf{M}_2]_{m/2 \times m} \to \Im(\mathbf{C}_2) * e^{j\theta}$
12:   Obtain suitable rank preserving map $X = \varphi(\mathbf{C}_2)$
13: end
14: Step 6: Obtain X_{SM}

$\mathbf{C}_1$ represents the antenna selection, and $\mathbf{C}_2$ represent information symbol mapping. The total number of transmit antenna considered here are $N_t = 4$ and $N_t = 6$.We have incorporated constellation rotation by θ in order to have two distinct constellations. The value of θ is selected to have maximum Euclidean distance between the two constella-

Table 3.3 Constellation points and rotation angle

Constellation points	Rotation angle θ
GF(5)	45
GF(7)	30
GF(13)	28
GF(17)	18

tion points. Example 1, gives a brief description of SM-NSTBC case 1 implementation.

Example 1: Consider $N_t = 4, N_a = 2$ and $N_r = 4$. The possible antenna pair combinations are $\binom{N_t}{2}$ in number. Let the codeword matrix over $GF(q)$ be represented as,

$$
\begin{bmatrix}
x_{0,0} & x_{0,1} & x_{0,2} & x_{0,3} \\
x_{1,0} & x_{1,1} & x_{1,2} & x_{1,3} \\
x_{2,0} & x_{2,1} & x_{2,2} & x_{2,3} \\
x_{3,0} & x_{3,1} & x_{3,2} & x_{3,3}
\end{bmatrix}
\tag{3.2}
$$

A brief description of the encoding procedure is presented. Consider the first column, $[x_{0,0} \ x_{1,0} \ x_{2,0} \ x_{3,0}]^T$. The first two symbols, $x_{0,0}$ and $x_{1,0}$ are used to select the transmit antenna pair and the remaining two symbols, $x_{2,0}$ and $x_{3,0}$ are mapped into suitable complex symbols by using the Gaussian or Eisenstein map. These symbols are then radiated by using the active antenna pair selected for that time slot. This process is repeated for the remaining three time slots as well. For a SM-NSTBC scheme with $N_a = 2$, the possible antenna pair combinations are $\binom{N_t}{2}$. While the possible combinations produced to by the two rows of codeword matrix is q^2, where $q = 5, 7, 13, 17$. So we have a situation of many to one mapping. This leads to an increase in the probability of error unless suitable steps are taken to mitigate the possibility of symbol

32
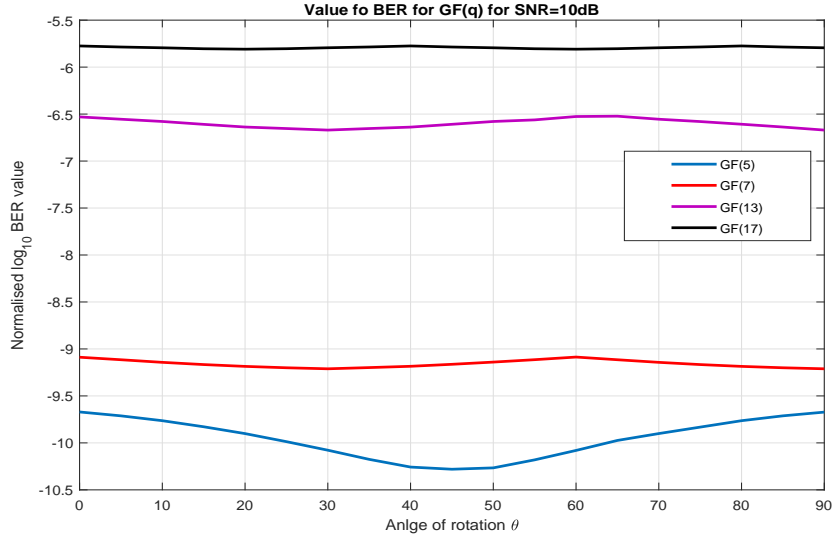
Figure 3.2 ABER performance for varying rotation angle for SNR value of 10 dB

being detected incorrectly. In order to improve the ABER performance we have introduced rotation angle. This has been achieved by rotating the original constellation by $\theta \in [0, \pi/2]$. Points from both the original and rotated constellations are judiciously employed according to the selection scheme to obtain optimum performance.

The angle of rotation is $e^{j\theta}$, the value of θ is 0 when original constellation points are selected. For the rotated case (constellation points) θ is chosen in order to have maximum Euclidean distance between the neighboring points of the constellation. Figure 3.2, gives the value of ABER for varying rotation angles for $GF(q)$ $(q = 5, 7, 13, 17)$. It is observed that the rotation angle decreases with increase in the number of points in the signal constellation. The obtained optimized rotation angles for each constellation point for different values of $GF(q)$ are listed in Table 3.3.

Example 2: Consider $GF(13)$, here for $N_t = 4, N_a = 2$ and $N_r = 4$ the possible antenna pair combinations are $\binom{4}{2} = 6$. While the possible combinations produced to by the two rows of codeword matrix is 13^2 i.e. 169. Let $(\mathscr{Z})\{x_i\}$ represent the Gaussian integer map of x_i defined as $\mathscr{Z}_{3+2i}$ for $GF(13)$. And $e^{j\theta}$ be then angle of rotation. The antenna selection bits and the codeword transmission bits are tabulated in Table 3.4.

Table 3.4 Antenna Selection and Transmission bits

x_0, x_1	Antenna Pair Selected	Constellation Points
$\{x_0 = 0; x_1 = 0, 1, ...12\}$		
$\{x_0 = 1; x_1 = 0\}$	1,2	$[(\mathscr{Z})\{x_2\}, (\mathscr{Z})\{x_3\}]$
$\{x_0 = 1; x_1 = 1, 2, ...12\}$		
$\{x_0 = 2; x_1 = 0, 1\}$	1,2	$[(\mathscr{Z})\{x_2\}, (\mathscr{Z})\{x_3\}] * e^{j\theta}$
$\{x_0 = 2; x_1 = 2, 3, ...12\}$		
$\{x_0 = 3; x_1 = 0, 1, 2\}$	1,3	$[(\mathscr{Z})\{x_2\}, (\mathscr{Z})\{x_3\}]$
$\{x_0 = 3; x_1 = 3, 4, ...12\}$		
$\{x_0 = 4; x_1 = 0, 1, ..3\}$	1,3	$[(\mathscr{Z})\{x_2\}, (\mathscr{Z})\{x_3\}] * e^{j\theta}$
$\{x_0 = 4; x_1 = 4, 5, ...12\}$		
$\{x_0 = 5; x_1 = 0, 1.., 4\}$	1,4	$[(\mathscr{Z})\{x_2\}, (\mathscr{Z})\{x_3\}]$
$\{x_0 = 5; x_1 = 5, 6, ...12\}$		
$\{x_0 = 6; x_1 = 0, 1.., 5\}$	1,4	$[(\mathscr{Z})\{x_2\}, (\mathscr{Z})\{x_3\}] * e^{j\theta}$
$\{x_0 = 6; x_1 = 6, 7, ...12\}$		
$\{x_0 = 7; x_1 = 0, 1.., 6\}$	2,3	$[(\mathscr{Z})\{x_2\}, (\mathscr{Z})\{x_3\}]$
$\{x_0 = 7; x_1 = 7, 8, ...12\}$		
$\{x_0 = 8; x_1 = 0, 1.., 7\}$	2,3	$[(\mathscr{Z})\{x_2\}, (\mathscr{Z})\{x_3\}] * e^{j\theta}$
$\{x_0 = 8; x_1 = 8, 9, ...12\}$		
$\{x_0 = 9; x_1 = 0, 1.., 8\}$	2,4	$[(\mathscr{Z})\{x_2\}, (\mathscr{Z})\{x_3\}]$
$\{x_0 = 9; x_1 = 9, 10, 11, 12\}$		
$\{x_0 = 10; x_1 = 0, 1.., 9\}$	2,4	$[(\mathscr{Z})\{x_2\}, (\mathscr{Z})\{x_3\}] * e^{j\theta}$
$\{x_0 = 10; x_1 = 10, 11, 12\}$		
$\{x_0 = 11; x_1 = 0, 1.., 10\}$	3,4	$[(\mathscr{Z})\{x_2\}, (\mathscr{Z})\{x_3\}]$
$\{x_0 = 11; x_1 = 11, 12\}$		
$\{x_0 = 12; x_1 = 0, 1.., 12\}$	3,4	$[(\mathscr{Z})\{x_2\}, (\mathscr{Z})\{x_3\}] * e^{j\theta}$

Case 2: Four active antenna combination

In case 2, we have turned our attention to systems possessing a large number transmit antennas in which four antennas (out of N_t) are active over any given time slot. We have designed SM-NSTBC schemes for six and eight transmit antennas. We employ the same codeword structure as given in Section 3.2. Here, a total of four transmit antennas are activated over every time slot. This essentially lead to transmission of four symbols in a single time slot. The codeword matrix is divided into set of two sub-matrices instead of four (as considered in case 1). Here a total of eight bits are transmitted in a single

time slot, where four bits are conveyed by antenna selection (as transmit antenna index) while other four bits are transmitted in the form of information bits. This is given in Equation (3.3).

The 4×4 full rank codeword matrix is interpreted as two sub-matrices, which is transmitted in each time slot. The total number of distinct antenna combinations is $\binom{N_t}{4}$, while four tuples of symbols over $GF(q)$ can address as many as q^4 different antenna combinations. In the first time slot the symbols $[x_{0,0}\ x_{1,0}\ x_{0,1}\ x_{1,1}\ x_{2,0}\ x_{3,0}\ x_{2,1}\ x_{3,1}]^T$ are employed with first four symbols $[x_{0,0}\ x_{1,0}\ x_{0,1}\ x_{1,1}]$ being used for antenna selection and the remaining four symbols $[x_{2,0}\ x_{3,0}\ x_{2,1}\ x_{3,1}]$ being radiated through the selected antennas.

$$\begin{bmatrix} x_{0,0} & x_{0,1} & x_{0,2} & x_{0,3} \\ x_{1,0} & x_{1,1} & x_{1,2} & x_{1,3} \\ x_{2,0} & x_{2,1} & x_{2,2} & x_{2,3} \\ x_{3,0} & x_{3,1} & x_{3,2} & x_{3,3} \end{bmatrix} \rightarrow \begin{bmatrix} x_{0,0} & x_{0,2} \\ x_{1,0} & x_{1,2} \\ x_{0,1} & x_{0,3} \\ x_{1,1} & x_{1,3} \\ x_{2,0} & x_{2,2} \\ x_{3,0} & x_{3,2} \\ x_{2,1} & x_{2,3} \\ x_{3,1} & x_{3,3} \end{bmatrix} \tag{3.3}$$

The transmission process employed in Case 2 is summarized by the algorithm 2.

Algorithm 2 SM-NSTBC encoding algorithm for $N_a = 4$

1: Start
2: Consider $2^{\lfloor \log_2(q^m) \rfloor}$ bits
3: Step 1:Segregation into $\mathbf{M}_{m \times m}$
4: Step 2:Obtain modified matrix:
5: $\quad \mathbf{M}_{m \times m} \rightarrow [\mathbf{M}]_{2m \times m/2}$
6: Step 3:Obtain Full rank matrix
7: $\quad [\mathbf{M}_1]_{2m \times m/2} \rightarrow [\mathbf{M}_1]_{m \times m/2}$ antenna selection symbols $+ [\mathbf{M}_2]_{m \times m/2}$ information symbols
8: Step 4:for count=1:number of time slots for full codeword transmission
9: Step 5:Antenna selection
10: $\quad [\mathbf{M}_1]_{m \times m/2} \rightarrow \mathbf{C}_1[a(1)a(2) \cdots a(2m)]$
11: Step 6:Mapping Information symbols
12: $\quad\quad [\mathbf{M}_2]_{m \times m/2} \rightarrow \mathbf{C}_2[i(1)i(2) \cdots i(2m)]$
13: $\quad$ Obtain suitable rank preserving map $X = \varphi(\mathbf{C}_2)$
14: end
15: Step 7: Obtain X_{SM}

3.3.1 Spectral Efficiency

The spectral efficiency is the maximum number of bits of data that can be transmitted for

a single time slot over the communication channel. The spectral efficiency calculation of proposed SM-NSTBC is evaluated as given below

1. The information bits are first encoded to respective codewords. The total number of codewords obtained from full rank n-length Cyclic code over $GF(q^m)$ is q^m.

2. The total number of binary information bits that can be assigned uniquely to q^m value is given by $\lfloor \log_2(q^m) \rfloor$

3. The total time slots required to transmit the whole codeword is denoted by n_s, in proposed SM-NSTBC scheme $n_s = 4$ for two active antenna and $n_s = 2$ for four active antenna system.

4. So the spectral efficiency (η) of proposed SM-NSTBC system is given by

$$\eta = \frac{\lfloor \log_2(q^m) \rfloor}{n_s} \tag{3.4}$$

here, the value of $n_s = 2m/N_a$, which corresponds to the time slots required to transmit the SM-NSTBC codeword, N_a represents the number of active antennas, q is a prime $(q = 5, 7, 13, 17)$, m is the order of the extension field $(m = 4)$.

The total of $2^{\lfloor \log_2(q^m) \rfloor}$ unique full rank codeword matrix are employed. It has to be noted that many to one mapping exists only for antenna selection, but the for any similar antenna combination activated, the radiated symbol are always different, in-turn achieving a unique one to one mapping of information bits to codeword matrix.

3.3.2 ML Decoding for SM-NSTBC

In this section, discussion about the Maximum likelihood (ML) detection strategy employed is outlined. Let the total number of time slots required to transmit a full codeword matrix be specified as n_s. At the receiver the information bits are buffered till the full codeword is obtained. The received $N_r \times n_s$ array is given by,

$$\mathbf{Y} = \mathbf{H}\mathbf{X}_{SM} + \mathbf{n} \tag{3.5}$$

Here, $\mathbf{Y}$ represents the received array, $\mathbf{X}_{SM}$ is the transmitted codeword matrix, $\mathbf{H}$ is the channel matrix and n is a realization of circularly symmetric complex independent and identically distributed Gaussian variable $C \mathcal{N}(0,1)$.

Once the full codeword is obtained, the active antenna index is extracted and the ML decoding of the received array is performed. This is given by

$$\hat{\mathbf{X}}_{SM} = argmin \left\| \mathbf{Y} - \mathbf{H}\tilde{\mathbf{X}}_{SM} \right\|_F^2 \tag{3.6}$$

Here, $\hat{\mathbf{X}}_{SM}$ is the estimated codeword.

Algorithm 3 Decoding Algorithm

1: Start
2: Input: $\mathbf{Y}$
3: Output: $\hat{\mathbf{M}}$
4: Step1: Obtain the count of Slot
5: Step 2:For count=1:length of slot
6: Step 3: Obtain the receiver array
7: Step 4:Compute $\hat{\mathbf{X}}_{SM} = argmin \left\| \mathbf{Y} - \mathbf{H}\tilde{\mathbf{X}}_{SM} \right\|_F^2 \forall \tilde{\mathbf{X}}_{SM} \in \mathbf{C}$
8: Step 5: Obtain $\hat{\mathbf{X}}_{SM}$

To enhance the overall performance of the proposed SM-NSTBC system, we have employed low complexity decoding technique (based on sphere decoding principle) as described in the following subsection.

3.3.3 Low complexity decoding scheme for SM-NSTBC

The ML decoding for a SM-NSTBC communication system is defined as follows,

$$\mathbf{Y} = \mathbf{H}\mathbf{X}_{SM} + \mathbf{n} \tag{3.7}$$

Here, $\mathbf{Y}$ represents the received array, $\mathbf{X}_{SM}$ is the transmitted codeword matrix, $\mathbf{H}$ is the channel matrix and n is a realization of circularly symmetric complex independent and identically distributed Gaussian variable $C \mathcal{N}(0,1)$.

Once the full codeword is obtained, the active antenna index is extracted and the ML decoding of the received array is performed. This procedure is summarized by Equation (3.8).

$$\hat{\mathbf{X}}_{SM} = argmin \left\| \mathbf{Y} - \mathbf{H}\mathbf{X}_{SM} \right\|_F^2 \tag{3.8}$$

Here, $\hat{\mathbf{X}}_{SM}$ is the estimated codeword. The Maximum Likelihood (ML) decoding gives

an optimal solution but involves very high computational complexity. It becomes very important to design an efficient decoding algorithm to reduce this complexity.

The concept of Sphere Decoding (SD) is commonly employed to avoid an exhaustive search by considering only those points which lie inside a sphere with a predefined radius R. The generalized Sphere decoding algorithm as given in [Viterbo and Boutros (1999)], is defined for a system with all antennas active. In SM-NSTBC scheme, as spatial modulation is adopted it becomes important to consider the active antenna combinations. As given in the Sphere decoding scheme, the search space is reduced by comparing the Euclidean distances for only those points that are present inside radius R and are centered around the received signal. In this scheme we first identify the active antenna combination. In the second step, the sphere decoding algorithm is applied for decoding the NSTBC codeword. Consider the real-valued equivalent of the complex-valued model of SM-NSTBC system as given below. Let $Re\{\cdot\}$ and $Im\{\cdot\}$ be the real and imaginary parts respectively.

$$\mathbf{Y} = \mathbf{H_e}\mathbf{X_{SMe}} + \mathbf{n} \tag{3.9}$$

here $\mathbf{H_e}$ is the equivalent channel matrix and $\mathbf{X_{SMe}}$ is the column matrix of symbols. The obtained complex valued model of SM-NSTBC as given below.

$$\mathbf{Y} = [Re\{Y^T\}, Im\{Y^T\}]^T \tag{3.10}$$

$$H_e = \begin{bmatrix} Re\{H_e\} & Im\{H_e\} \\ \\ -Im\{H_e\} & Re\{H_e\} \end{bmatrix} \tag{3.11}$$

$$\mathbf{X}_{SMe} = \begin{bmatrix} Re\{X_{SMe}^T\}, Im\{X_{SMe}^T\} \end{bmatrix}^T \tag{3.12}$$

$$\mathbf{n} = \begin{bmatrix} Re\{n^T\}, Im\{n^T\} \end{bmatrix}^T \tag{3.13}$$

Let us consider a SM-NSTBC system with four transmit and four receive antennas and two active transmit antennas. In SM-NSTBC scheme designed here, we work with 4×4 codeword matrices. Employing the $(13,1)$ Cyclic code for $GF(5)$, the codeword

matrices can be specified as,

$$
\mathbf{X} =
\begin{bmatrix}
a_0 & 3a_0 + a_1 + 2a_2 + 2a_3 & 2a_0 + 3a_1 + 2a_2 + 3a_3 & 3a_0 + 4a_1 + 4a_3 \\\\
a_1 & a_0 + 4a_1 + 3a_2 + 4a_3 & 2a_0 & a_0 + 2a_1 + 4a_2 + 4a_3 \\\\
a_2 & 4a_0 + 4a_1 + 4a_3 & 4a_0 + a_1 + a_2 + 4a_3 & 3a_1 + 2a_2 + a_3 \\\\
a_3 & 2a_0 + 4a_1 + 4a_2 & a_0 + 4a_1 + a_2 + a_3 & 3a_0 + 3a_2 + 2a_3
\end{bmatrix}
\tag{3.14}
$$

The upper two rows are used for antenna selection and the lower two rows are conventionally radiated as given in algorithm 1 and 2.

First we determine the active antenna combination for each time slot, and later the sphere decoding algorithm is applied. Let the $H_{eq(l,i)}$ represent the channel coefficient for l^{th} time slot and i^{th} active antenna index. So we determine the channel coefficients for values $i = 1, 2$. Now, $H_{eq(l,i)}$ is non zero only for $H_{eq(l,1)}$ and $H_{eq(l,2)}$ where $l = 1, 2, 3, 4$. $H_{eq} = 0$ for all other values of i. For instance, if second and third antennas are selected to be active for time slot $l = 1$, then the channel column elements are specified by $[0 \; H_{eq(1,1)} \; H_{eq(1,2)} \; 0]^T$. This procedure is followed for all the columns. Once the active antenna indices are obtained, then sphere decoding is applied to determine estimates of the radiated symbols.

$$
\mathbf{Y} = \mathbf{H_e X_{SMe}} + \mathbf{n}
\tag{3.15}
$$

Here $\mathbf{H_e}$ is the equivalent channel matrix. The values of $\mathbf{H_{eq}}$ are obtained by evaluating $\mathbf{H X_{SM}}$. Now the radiated symbols are:

$$
\begin{bmatrix}
a_2 & 4a_0 + 4a_1 + 4a_3 & 4a_0 + a_1 + a_2 + 4a_3 & 3a_1 + 2a_2 + a_3 \\\\
a_3 & 2a_0 + 4a_1 + 4a_2 & a_0 + 4a_1 + a_2 + a_3 & 3a_0 + 3a_2 + 2a_3
\end{bmatrix}
\tag{3.16}
$$

Processing this codeword through the rank preserving map yields,

$$
\begin{bmatrix}
\mathscr{L}(a_2) & -\mathscr{L}(a_0) - \mathscr{L}(a_1) - \mathscr{L}(a_3) & -\mathscr{L}(a_0) + \mathscr{L}(a_1) + \mathscr{L}(a_2) - \mathscr{L}(a_3) & -j\mathscr{L}(a_1) + j\mathscr{L}(a_2) + \mathscr{L}(a_3) \\\\
\mathscr{L}(a_3) & j\mathscr{L}(a_0) - \mathscr{L}(a_1) + -\mathscr{L}(a_2) & \mathscr{L}(a_0) - \mathscr{L}(a_1) + \mathscr{L}(a_2) + \mathscr{L}(a_3) & -j\mathscr{L}(a_0) + -j\mathscr{L}(a_2) + j\mathscr{L}(a_3)
\end{bmatrix}
\tag{3.17}
$$

An initial estimate of a_0 and a_1 is obtained by antenna selection, for further evaluation,

we now compute for a_2 and a_3.

$$
\begin{bmatrix}
0 & 0 & H_{eq(1,1)} & H_{eq(1,2)} \\
-(H_{eq(1,1)})+j(H_{eq(1,2)}) & -(H_{eq(1,1)})-(H_{eq(1,2)}) & -(H_{eq(1,2)}) & -(H_{eq(1,1)}) \\
-(H_{eq(1,1)})+(H_{eq(1,2)}) & (H_{eq(1,1)})-(H_{eq(1,2)}) & (H_{eq(1,1)})+(H_{eq(1,2)}) & -(H_{eq(1,1)})+(H_{eq(1,2)}) \\
-j(H_{eq(1,2)}) & -j(H_{eq(1,1)}) & j(H_{eq(1,1)})-j(H_{eq(1,2)}) & (H_{eq(1,1)})+j(H_{eq(1,2)}) \\
0 & 0 & H_{eq(2,1)} & H_{eq(2,2)} \\
-(H_{eq(2,1)})+j(H_{eq(2,2)}) & -(H_{eq(2,1)})-(H_{eq(2,2)}) & -(H_{eq(2,2)}) & -(H_{eq(2,1)}) \\
-(H_{eq(2,1)})+(H_{eq(2,2)}) & (H_{eq(2,1)})-(H_{eq(2,2)}) & (H_{eq(2,1)})+(H_{eq(2,2)}) & -(H_{eq(2,1)})+(H_{eq(2,2)}) \\
-j(H_{eq(2,2)}) & -j(H_{eq(2,1)}) & j(H_{eq(2,1)})-j(H_{eq(2,2)}) & (H_{eq(2,1)})+j(H_{eq(2,2)}) \\
0 & 0 & H_{eq(3,1)} & H_{eq(3,2)} \\
-(H_{eq(3,1)})+j(H_{eq(3,2)}) & -(H_{eq(3,1)})-(H_{eq(3,2)}) & -(H_{eq(3,2)}) & -(H_{eq(3,1)}) \\
-(H_{eq(3,1)})+(H_{eq(3,2)}) & (H_{eq(3,1)})-(H_{eq(3,2)}) & (H_{eq(3,1)})+(H_{eq(3,2)}) & -(H_{eq(3,1)})+(H_{eq(3,2)}) \\
-j(H_{eq(3,2)}) & -j(H_{eq(3,1)}) & j(H_{eq(3,1)})-j(H_{eq(3,2)}) & (H_{eq(3,1)})+j(H_{eq(3,2)}) \\
0 & 0 & H_{eq(4,1)} & H_{eq(4,2)} \\
-(H_{(eq4,1)})+j(H_{eq(4,2)}) & -(H_{eq(4,1)})-(H_{eq(4,2)}) & -(H_{eq(4,2)}) & -(H_{eq(4,1)}) \\
-(H_{eq(4,1)})+(H_{eq(4,2)}) & (H_{eq(4,1)})-(H_{eq(4,2)}) & (H_{eq(4,1)})+(H_{eq(4,2)}) & -(H_{eq(4,1)})+(H_{eq(4,2)}) \\
-j(H_{eq(4,2)}) & -j(H_{eq(4,1)}) & j(H_{eq(4,1)})-j(H_{eq(4,2)}) & (H_{eq(4,1)})+j(H_{eq(4,2)})
\end{bmatrix}
\tag{3.18}
$$

The matrix shown above gives the $\mathbf{H_{eq(l=1,i)}}$, similarly for $l = 2,3,4$ is obtained and full matrix of $\mathbf{H_e}$ is calculated. Considering the real value equivalent of complex valued model we obtain matrix $\mathbf{M}$ given by

$$
\mathbf{M} =
\begin{bmatrix}
Re\{H_e\} & Im\{H_e\} \\
\\
-Im\{H_e\} & Re\{H_e\}
\end{bmatrix}
\tag{3.19}
$$

Obtaining its Gram matrix we get $G_M = MM^*$. Let Cholesky factorisation of G_M be defined as $G_M = R^T R$. Let $[\mathscr{L}(a_0)\ \mathscr{L}(a_1)\ \mathscr{L}(a_2)\ \mathscr{L}(a_3)] = [a_0 + jb_0 : a_1 + jb_1 : a_2 + jb_2 : a_3 + jb_3]$

$$
[Re\{Y^T\}, Im\{Y^T\}]^T = [a_0\ a_1\ a_2\ a_3 : b_0\ b_1\ b_2\ b_3]M + n
\tag{3.20}
$$

Let $\rho = [Re\{Y^T\}, Im\{Y^T\}]^T M^{-1}$, ρ is the unconstrained solution and $z = n^{-1}$ Solving this for equation for 4-tuple of real numbers we obtain for radius value of R_i.

$$
\rho_4 - \sqrt{R_i/r_{44}} \le u_4 \le \rho_4 + \sqrt{R_i/r_{44}}
\tag{3.21}
$$

for next iteration

$$
\rho_3 + q_{34} - \sqrt{R_i/r_{44}} \le u_4 \le \rho_3 + \rho_4 + q_{34}\sqrt{R_i/r_{44}}
\tag{3.22}
$$

Once all the elements are obtained we re-evaluate for the new adjusted radius, and all steps are performed again until there is only one codeword in sphere with the modified radius. The performance comparison of sphere decoding over ML decoding scheme is presented in Figure 3.7.

3.4 Analytical Performance of the proposed Scheme

In this section, we give a detailed description about the error performance of the proposed SM-NSTBC system. An analytical upper bound on the Average Bit Error Rate (ABER) has been derived to verify the correctness of Monte Carlo simulations performed. A theoretical upper bound on ABER is given by [Proakis (1995), Simon and Alouini (2005), Basar et al. (2012), Goutham Simha (2018)].

$$ABER_{SM-NSTBC} \leq \frac{1}{2^{\lfloor \log_2 q^m \rfloor}} \sum_{i=1}^{2^{\lfloor \log_2 q^m \rfloor}} \sum_{j=1}^{2^{\lfloor \log_2 q^m \rfloor}} \frac{N(\mathbf{X}_{SM} - \hat{\mathbf{X}}_{SM})}{2\eta}(P(\mathbf{X}_{SM} \to \hat{\mathbf{X}}_{SM})) \quad (3.23)$$

Here, η is the spectral efficiency of the SM-NSTBC scheme, $N(\mathbf{X}_{SM} - \hat{\mathbf{X}}_{SM})$ is the number of non-zero elements of the difference matrix of $\mathbf{X}_{SM} - \hat{\mathbf{X}}_{SM}$, and $P(\mathbf{X}_{SM} \to \hat{\mathbf{X}}_{SM})$ is given below

$$P(\mathbf{X}_{SM} \to \hat{\mathbf{X}}_{SM}) = Pr\left(\|\mathbf{Y} - \mathbf{H}\mathbf{X}_{SM}\|_F^2 > \|\mathbf{Y} - \mathbf{H}\hat{\mathbf{X}}_{SM}\|_F^2 | \mathbf{H}\right) \quad (3.24)$$

here, for a given channel $\mathbf{H}$, $(P(\mathbf{X}_{SM} \to \hat{\mathbf{X}}_{SM}))$ is the pairwise error probability (PEP) of detecting $\hat{\mathbf{X}}_{SM}$, when $\mathbf{X}_{SM}$ is transmitted. The pairwise error probability is evaluated using [Simon and Alouini (2005), Basar et al. (2012), Goutham Simha (2018)]:

$$P(\mathbf{X}_{SM} \to \hat{\mathbf{X}}_{SM}) = Q\left(\sqrt{\frac{\rho}{2}}\|\mathbf{H}(\mathbf{X}_{SM} - \hat{\mathbf{X}}_{SM})\|\right) \quad (3.25)$$

Here $Q(x) = \frac{1}{\sqrt{2\pi}} \int_x^\infty \exp(-y^2/2)dy$. The unconditional PEP is obtained by the use of moment generating function [Simon and Alouini (2005)].

$$P(\mathbf{X}_{SM} \to \hat{\mathbf{X}}_{SM}) = \frac{1}{\pi} \int_0^{\frac{\pi}{2}} \prod_{l=1}^{L} \left(\frac{1}{1 + \frac{\rho \lambda_{i,j_l}}{4 \sin^2 \theta}}\right)^{N_r} d\theta \quad (3.26)$$

here, $L = 4$ and λ_{i,j_l} are the Eigen values of the distance matrix $(\mathbf{X}_{SM} - \hat{\mathbf{X}}_{SM})^H (\mathbf{X}_{SM} - \hat{\mathbf{X}}_{SM})$. Further PEP can be calculated as given in Equation (3.27)

$$P(\mathbf{X}_{SM} \to \hat{\mathbf{X}}_{SM}) =$$

$$\frac{1}{\pi} \int_0^{\frac{\pi}{2}} \left(\frac{1}{1 + \frac{\rho \lambda_{i,j_1}}{4 \sin^2 \theta}}\right)^{N_r} \left(\frac{1}{1 + \frac{\rho \lambda_{i,j_2}}{4 \sin^2 \theta}}\right)^{N_r} \left(\frac{1}{1 + \frac{\rho \lambda_{i,j_3}}{4 \sin^2 \theta}}\right)^{N_r} \left(\frac{1}{1 + \frac{\rho \lambda_{i,j_4}}{4 \sin^2 \theta}}\right)^{N_r} d\theta \quad (3.27)$$

Let $c_l = \frac{\rho \lambda_{i,j_l}}{4}$. The closed form solution of Equation (3.27) can be obtained from [Simon and Alouini (2005)], and is simplified as shown in Equation (3.28).

41

$$P(\mathbf{X}_{SM} \to \hat{\mathbf{X}}_{SM}) \leq \frac{1}{2} \prod_{l=1}^{L} \frac{1}{(1+c_l)^{N_r}} \tag{3.28}$$

Substituting Equation (3.28) in Equation (3.23), the analytical upper bound on the Average Bit Error Rate (ABER) is calculated as given in Equation (3.29).

$$ABER_{SM-NSTBC} \leq \frac{1}{2^{\lfloor \log_2 q^m \rfloor}} \sum_{i=1}^{2^{\lfloor \log_2 q^m \rfloor}} \sum_{j=1}^{2^{\lfloor \log_2 q^m \rfloor}} \frac{N(\mathbf{X}_{SM} - \hat{\mathbf{X}}_{SM})}{4\eta} \prod_{l=1}^{L} \frac{1}{(1+c_l)^{N_r}} \tag{3.29}$$

3.5   Complexity Analysis for the proposed SM-NSTBC

The computation complexity is given in terms of total complex multiplications and additions. Here, a computation is considered to be a real multiplication, real addition or real division.

All calculation are evaluated with following considerations.

- Consider matrix $\mathbf{M1} \in \mathbb{C}^{M \times N}$, and $\mathbf{M2} \in \mathbb{C}^{N \times L}$, then the matrix multiplication requires MNL number of complex multiplications and $ML(N-1)$ number of complex additions.

- To calculate $\|\mathbf{M1}\|_F^2$ requires MN number of complex multiplications and $(MN-1)$ number of complex additions.

Considering the above mentioned matrix multiplications and matrix addition, we now evaluate the computation complexity of ML decoding for the proposed SM-NSTBC system. For a single codeword matrix to be detected the number of complex multiplication required can be calculated by evaluating the total number of computation required to approximate $(\mathbf{Y} - \mathbf{H}\hat{\mathbf{X}}_{SM})^H (\mathbf{Y} - \mathbf{H}\,\hat{\mathbf{X}}_{SM})$. Here, $\mathbf{H}$ is a complex channel matrix, $\hat{\mathbf{X}}_{SM}$ is a transmitted matrix and $\mathbf{Y}$ is a complex receive matrix. The number of time slot required to transmit a full codeword matrix is given as n_s.

1. The total number of possible combination of activating N_a antennas out of N_t transmit antennas is $\binom{N_t}{N_a}$.

2. For an antenna selection decoding the total number of iterations (computations) required to identify active antenna combination is $\binom{N_t}{N_a} \frac{2m}{N_a}$.

3. The total number of complex multiplication required for estimating $\mathbf{H\tilde{X}}$ is given by $(N_r N_t n_s)$.

4. For estimating the Frobenius norm, the total number of complex multiplications required are $(N_r n_s)$.

So the total number of complex multiplications required for ML decoder is evaluated as follows:

$$2^{\lfloor \log_2 q^m \rfloor} \left(\binom{N_t}{N_a} n_s + (N_r N_t n_s) + (N_r n_s) \right) \qquad (3.30)$$

The total number of complex additions required are

$$2^{\lfloor \log_2 q^m \rfloor} \left((N_r n_s (N_t + 1)) + (N_r n_s - 1) \right) \qquad (3.31)$$

Example: Consider the proposed SM-NSTBC system with $N_t = 4$, $N_r = 4$, $N_a = 2$, with codewords derived over $GF(5)$.

Here, $q = 5$, $m = 4$ is incorporated. The total number of active antenna combination possible is $\binom{4}{2} = 6$. Total time slots required to transmit the whole codeword matrix is $n_s = \frac{2m}{N_a} = 4$. So by incorporating equation 3.30, we get the number of complex multiplications required to decode a single codeword is 5916.4 (computations/bit). Similarly, we the computations required for codeword matrix derived from $GF(7)$, $GF(13)$, $GF(17)$, is 19363 (computations/bit), 121710 (computations/bit), 425984 (computations/bit). Similarly the decoding complexity for each system is evaluated. For purpose of easy representation the values are normalized by base of log10 and presented in Figure 3.3.

Figure 3.3, shows the computational complexity of the proposed schemes which employ ML detection for two and four active antenna combinations. The computational complexity increases if the number of possible antenna combination increases or as the size of the constellation increases. Figure 3.4 gives the comparison of computational complexity of the proposed SM-NSTBC scheme, with other competing schemes namely SM-OSTBC [Le et al. (2014)], STBC-SM [Basar et al. (2011)], STBC-TSM [Helmy et al. (2016)] and L-SM [Alkhawaldeh (2018)] techniques. Here, the number of receive antenna for all the above schemes is considered as 1 and the spectral efficiency obtained is 4 bpcu. The computational complexity of proposed SM-NSTBC is
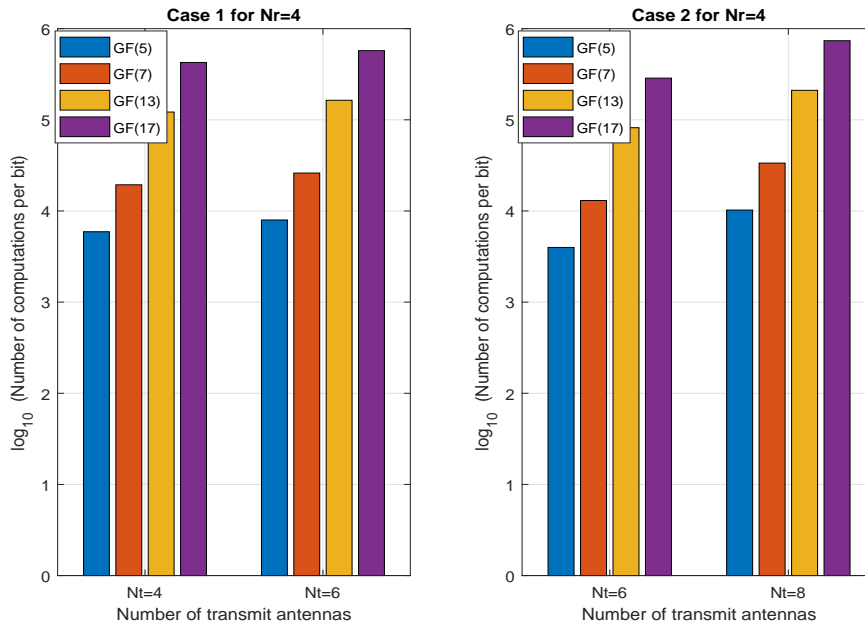
Figure 3.3 Computation complexity of ML decoder for different transmit antenna configurations.
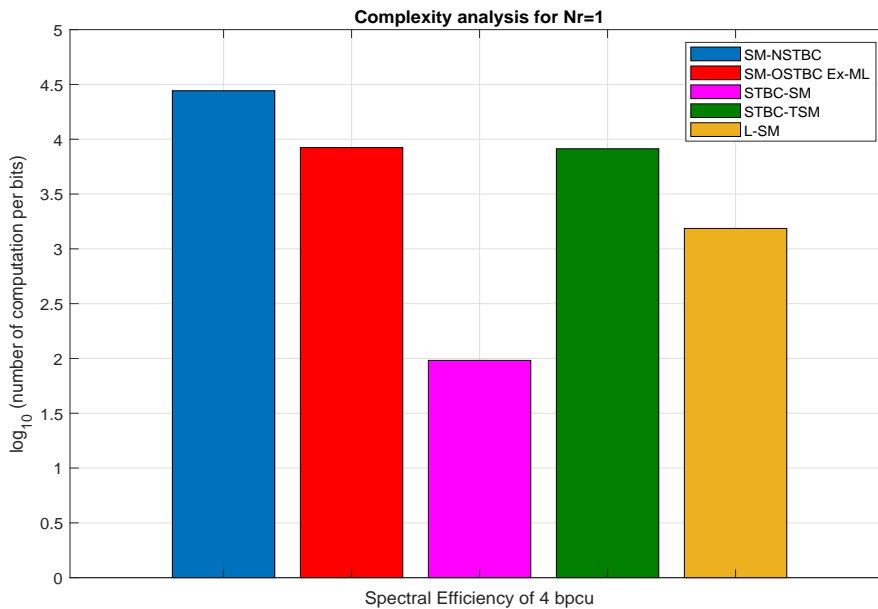
Figure 3.4 Comparison of the computation complexity of SM-NSTBC, SM-OSTBC, STBC-SM, STBC-TSM and L-SM.

51490 (computations/bit), for SM-OSTBC is 8396 (computations/bit), for STBC-SM is 961 (computations/bit), for STBC-TSM is 8192 (computations/bit), and L-SM is 1536 (computations/bit).

3.6   Simulation Results

This section demonstrates the simulation results of the proposed SM-NSTBC scheme for different values of N_t and N_a. The proposed SM-NSTBC is represented as $C(N_t, N_r, N_a)$ for all simulations. The proposed scheme has been compared with the variants of STBC-SM and SM systems. All performance comparison are carried out for a ABER value of 10^{-5}. It has been observed that for a given spectral efficiency the proposed SM-NSTBC scheme outperforms other STBC-SM scheme and SM schemes by ~ 1.5 dB to ~ 5 dB over Rayleigh fading channel.
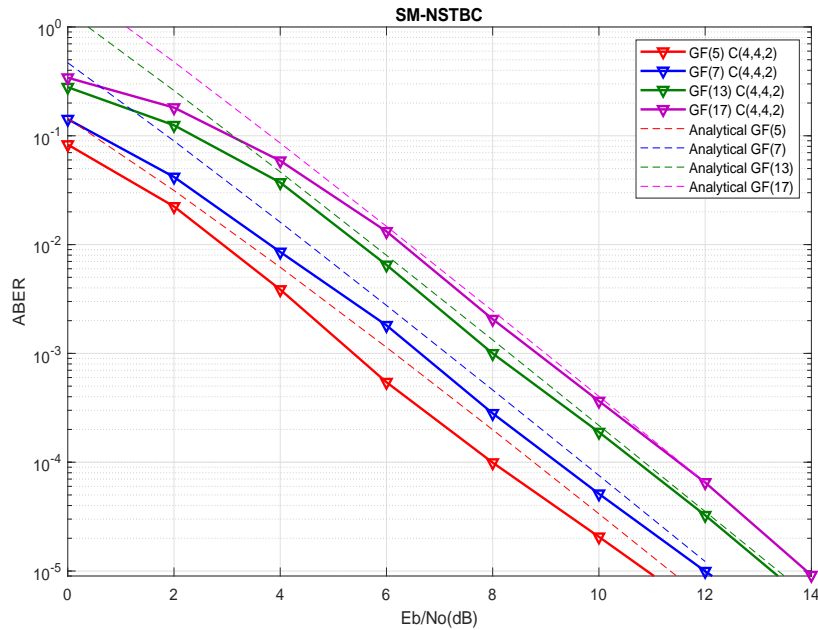
Figure 3.5 ABER performance of SM-NSTBC for $(N_t = 4, N_r = 4, N_a = 2)$ over $q = 5, 7, 13, 17$.

In Figure 3.5, the ABER curves of SM-NSTBC with $N_t = 4$, $N_r = 4$ and the active antennas are equal to 2 as specified in Case-1 are presented. A theoretical upper bound is shown in order to verify the correctness of the Monte-Carlo simulations. A close
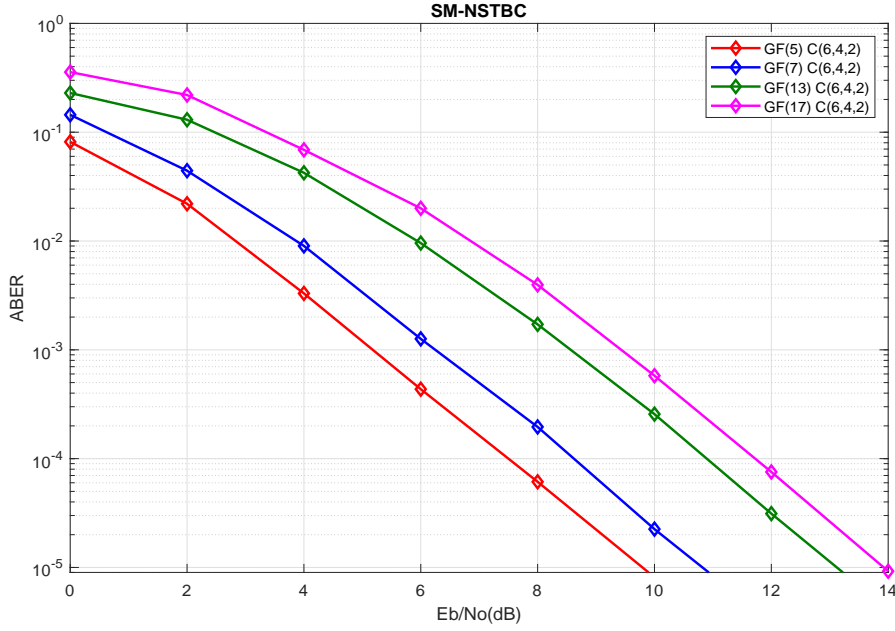
Figure 3.6 ABER performance of SM-NSTBC for $q = 5, 7, 13, 17$ for $(N_t = 6, N_r = 4, N_a = 2)$

correspondence between the analytical upper bound and simulation results is observed at higher SNR values. Simulation results are demonstrated for codewords obtained over $GF(5), GF(7), GF(13)$ and $GF(17)$. The spectral efficiency achieved for a system which utilizes $C(N_t = 4, N_r = 4, N_a = 2)$ is 2.322 bpcu for $q = 5$, 2.807 bpcu for $q = 7$, 3.701 bpcu for $q = 13$, and 4.087 bpcu is obtained for $q = 17$.

Figure 3.6, shows a SM-NSTBC system which employs 6 transmit antennas, 4 receive antennas and 2 active antenna combinations represented as $C(6, 4, 2)$. The simulation results demonstrate the ABER performance for $q = 5, 7, 13, 17$ with similar spectral efficiencies as indicated for $C(4, 4, 2)$ system.

Figure 3.7, shows the performance of SM-NSTBC system for $GF(5), GF(7), GF(13)$ with ML decoding and low complexity sphere decoding. There is a performance degradation of ~ 2dB with a significant reduction in complexity depending on the initial radius selection.
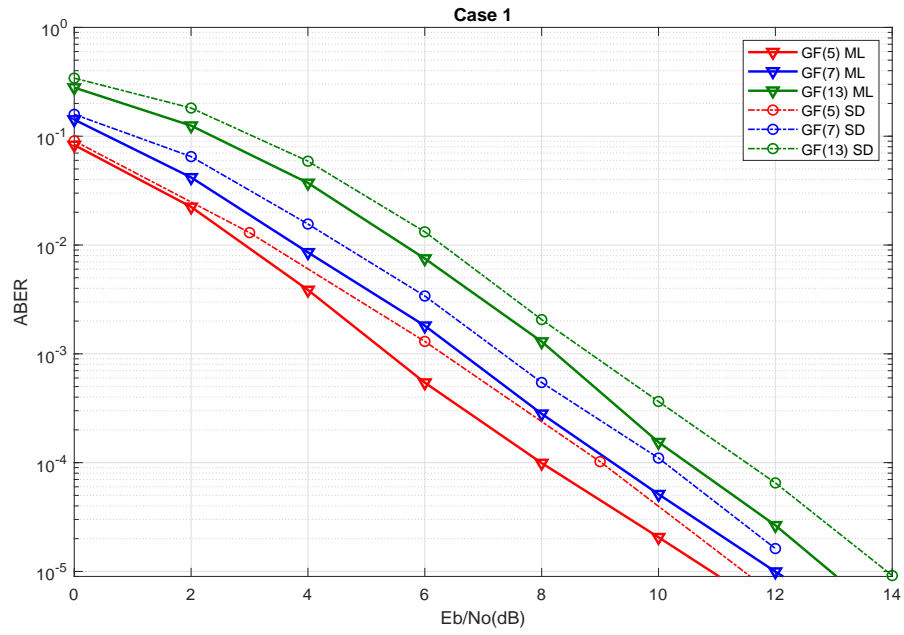
Figure 3.7 ABER performance of SM-NSTBC for Maximum likelihood and sphere decoding
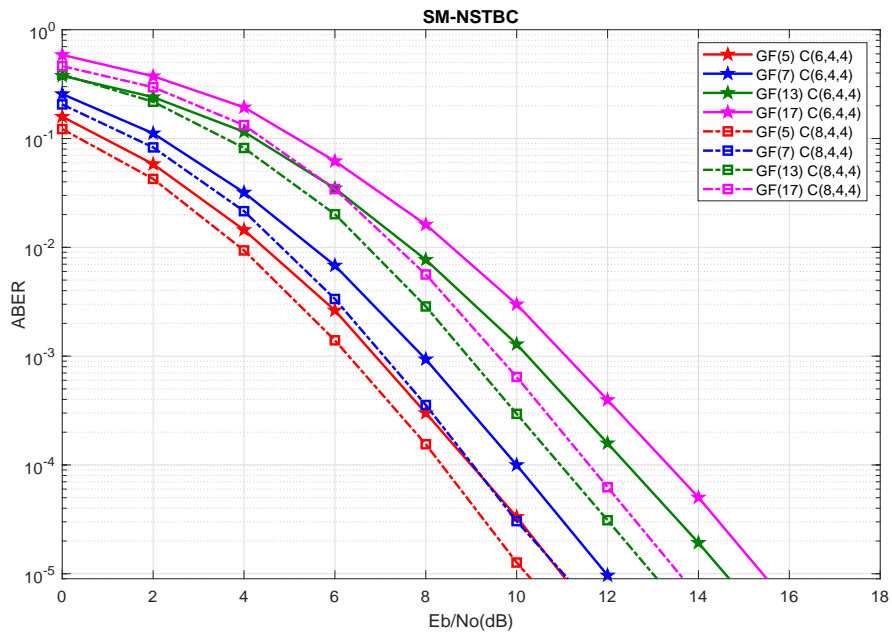
Figure 3.8 ABER performance of SM-NSTBC for $q = 5, 7, 13, 17$ for $(N_t = 6, N_r = 4, N_a = 4)$ and $(N_t = 8, N_r = 4, N_a = 4)$
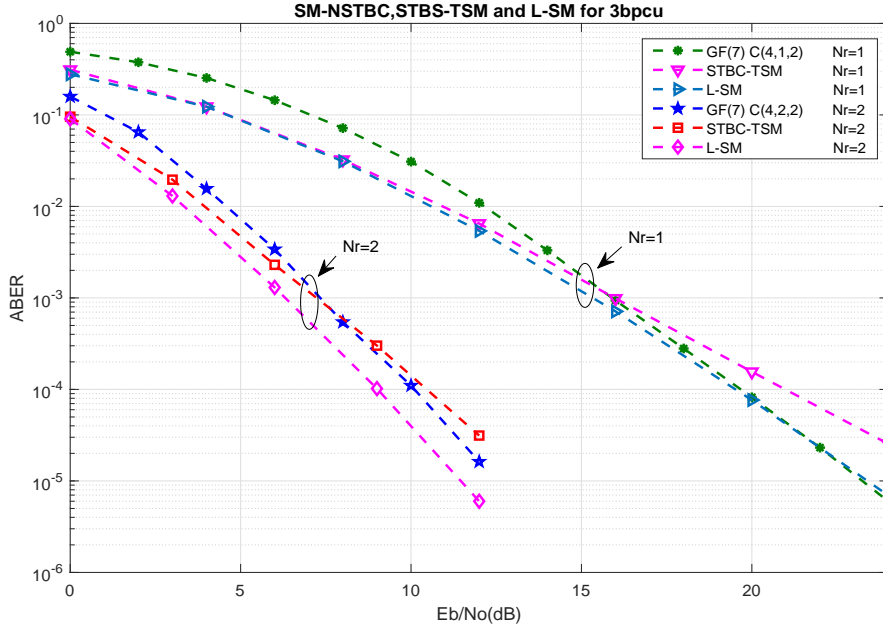
Figure 3.9 ABER performance comparison of SM-NSTBC, STBC-TSM and L-SM at 3 bpcu

Figure 3.8 demonstrates the simulation results for a system which employs $C(6,4,4)$ and $C(8,4,4)$ combinations as indicated in Case-2. These systems are evaluated over $GF(q)$. The corresponding values of $q = 5, 7, 13, 17$ yields a spectral efficiency of 4.643 bpcu, 5.614 bpcu, 7.4 bpcu and 8.175 bpcu respectively for a ABER of 10^{-5}.

In Figure 3.9 performance of the proposed SM-NSTBC is compared with STBC-TSM [Helmy et al. (2016)] and L-SM [Alkhawaldeh (2018)] schemes. All schemes employ four transmit antennas, two active antennas, and $N_r = 1$ and 2. By the use of these antenna configurations STBC-TSM and L-SM achieves a spectral efficiency of 3 bpcu, while SM-NSTBC has spectral efficiency of 2.8 bpcu. It is observed that for $N_r = 2$, at very low SNR values STBC-TSM and L-SM give a better performance compared to the proposed scheme. At higher values of SNR, SM-NSTBC outperforms STBC-TSM by ~ 1 dB, while L-SM gives better performance as compared to SM-NSTBC. However, for $N_r = 1$, at high values of SNR, SM-NSTBC outperforms both STBC-TSM and L-SM schemes as shown in Figure 3.9.

Figure 3.10, gives the comparison plot of SM-NSTBC with STBC-SM [Basar et al. (2011)] and SM [Mesleh et al. (2008)] systems. The proposed SM-NSTBC which uses

$C(4,4,2)$ with codewords derived from $GF(17)$ achieves a ABER performance improvement of ~ 1.5 dB over STBC-SM and ~ 3 dB over SM systems for a spectral efficiency of 4 bpcu. SM-NSTBC produces a fractional spectral efficiency of 4.087 bpcu.
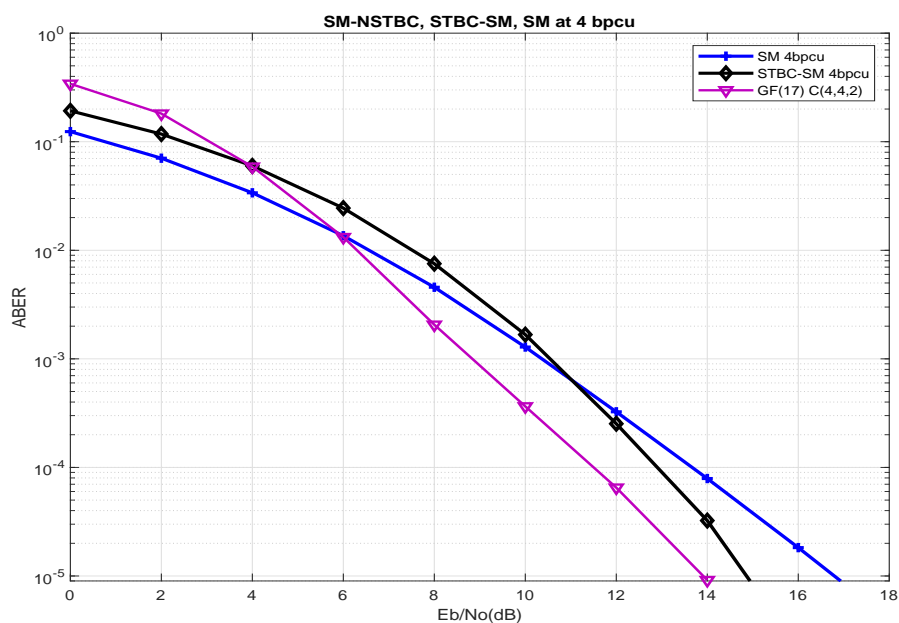
Figure 3.10 ABER performance comparison of SM-NSTBC, STBC-SM and SM at 4 bpcu

Figure 3.11, shows the ABER comparison of the SM-NSTBC, STBC-SM [Basar et al. (2011)] and SM [Mesleh et al. (2008)] schemes for a spectral efficiency of 5 bpcu. The proposed SM-NSTBC with codewords derived over $GF(7)$, $C(6,4,4)$ and $C(8,4,4)$ produces a spectral efficiency of 5.615. It is observed that the proposed scheme shows significant improvement of ~ 6 dB over STBC-SM and ~ 7.5 dB over SM systems.

Figure 3.12, delineates the simulation results of SM-NSTBC and SM-OSTBC [Wang and Chen (2014)] systems. The STBC-SM [Basar et al. (2011)] and SM [Mesleh et al. (2008)] systems cannot be compared with this plot, since, STBC-SM and SM systems will not provide four active antenna combinations. It is observed that the proposed SM-NSTBC scheme with $C(8,4,4)$ over $GF(13)$ (produces 7.4 bpcu) shows an im-
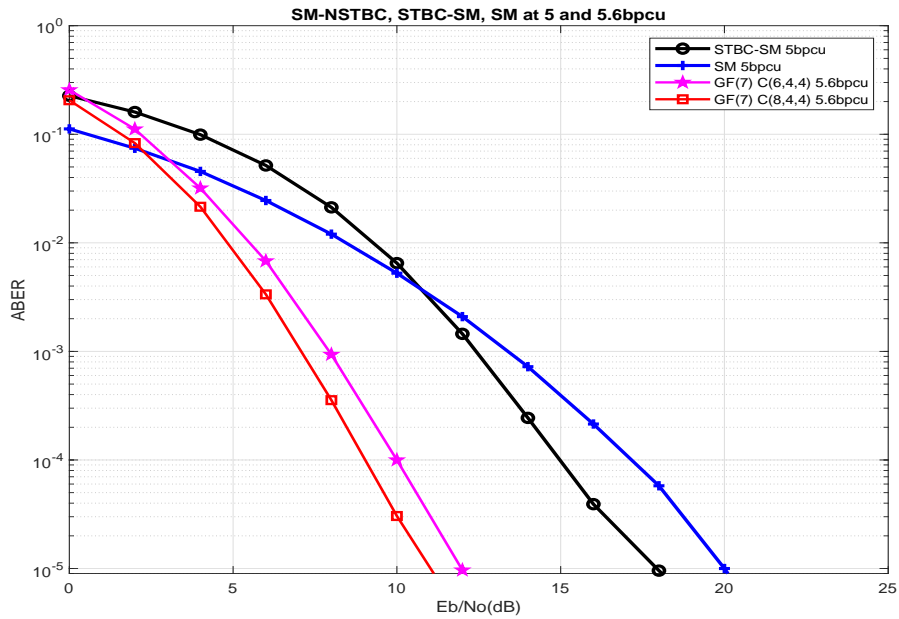
Figure 3.11 ABER performance comparison of SM-NSTBC, STBC-SM and SM at 5 bpcu. SM-NSTBC has a higher spectral efficiency of 5.6 bpcu
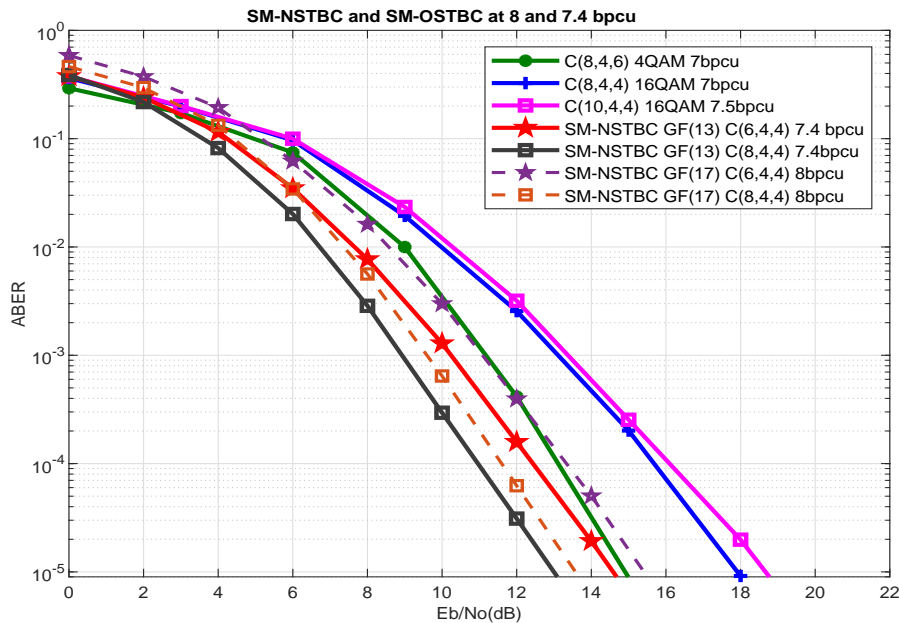
Figure 3.12 ABER performance comparison of SM-NSTBC, SM-OSTBC systems.

provement in the ABER performance of ~ 2 dB (Black Line), over SM-OSTBC system which uses $C(8,4,6)$ employing 4-QAM constellations to obtain a spectral efficiency of

7 bpcu (Green Line). Similarly, the proposed SM-NSTBC with $C(8,4,4)$ (Brown dotted line) over $GF(17)$ scheme (produces 8 bpcu) shows an improvement in the ABER performance of ~ 6 dB, over SM-OSTBC system which uses $C(10,4,4)$ employing 16-QAM constellations (magenta) to obtain a spectral efficiency of 7.5 bpcu.

3.7   Summary

A new SM-NSTBC scheme employing a full rank Cyclic code over $GF(q^m)$ has been proposed. These codes have codewords which can be viewed as full rank $m \times n, (m \leq n)$ matrices over $GF(q)$. By suitable puncturing, these $m \times m$ matrices are mapped into codewords of a SM-NSTBC using a suitable rank preserving map (Gaussian or Eisenstein map). The desired spectral efficiency can be achieved by selecting appropriate number of active antennas and order of Galois Field ($q = 5, 7, 13, 17$) over which codewords are constructed. An analytic upper bound on the ABER has been determined. Monte-Carlo simulations have been carried out to quantify the performance of these codes over Rayleigh fading channels. A close correspondence between the upper bound values and simulation results is observed. It is seen that proposed SM-NSTBC achieves an improvement of ~ 1.5 dB to ~ 5 dB over STBC-SM and SM-OSTBC schemes. The performance of the proposed SM-NSTBC scheme is compared with SM-OSTBC, STBC-SM, STBC-TSM and L-SM schemes. It is observed that proposed scheme outperforms other competing scheme, at the cost of marginal increase in computational complexity. The computational complexity of proposed SM-NSTBC is almost four times that of SM-OSTBC and STBC-TSM, while its above ten times that of STBC-SM and L-SM scheme

In this chapter, we have deduced the SM-NSTBC technique, where a selected subset of transmit antennas are activated and NSTBC is conveyed between transmitter and receiver. The study of SM-NSTBC has inspired us to explore Index Modulation scheme at the receiver terminal. We further explore the concept of activating a subset of receive antennas while allowing all transmit antennas to be active. In the next chapter, the concept of SM-NSTBC for Receive Spatial Modulation has been explored. In receive spatial modulation a part of information is conveyed by the active receive antenna

pattern. From the literature we have understood that SM schemes are vulnerable to correlated environments and the performance of SM schemes deteriorate over a completely dense correlated fading environment [Younis (2014), Goutham Simha (2018)]. We have studied the characteristics of uncorrelated and correlated channel conditions and proposed the aggrandized version of Precoded SM-NSTBC scheme for Receive Spatial Modulation. In this scheme the data to be transmitted is precoded in order to activate specific combination of receive antennas which in turn conveys a part of information. The performance of proposed precoded SM-NSTBC is compared with other precoded schemes which are available in the literature.

Chapter 4

Generalized designs for Precoded Receive Spatial Modulation derived from NSTBC

[1] In this chapter, a new MIMO scheme termed as Precoded Spatially Modulated Non-orthogonal Space Time Block Code (Precoded SM-NSTBC) is proposed. The primary concept of Precoded SM-NSTBC is to activate a subset of receive antennas in a pre-defined manner and choose specific activated patterns to represent information symbols. We have designed and synthesized schemes derived from full rank, length $n, (n|q^m - 1, m \leq n)$ Cyclic codes defined over Galois field $GF(q^m)$. Due to the characteristics of full rank Cyclic codes employed, a performance improvement of greater than 2 dB is observed. This advantage is realized when the performance of these schemes is compared with precoded SM-OSTBC, precoded STBC-SM and SM systems. Improvement due to the coding gain manifests in both uncorrelated as well as correlated Rayleigh fading environments. An upper bound on the average bit error rate (ABER) is derived. Close correspondence between Monte-Carlo simulations and analytic values are observed.

4.1 Introduction

The requirement of modern era communication is to provide uninterrupted and high-quality connectivity all the time. High throughput, widespread accessibility and relia-

---

[1]Godkhindi Shrutkirthi S. et.al," Generalized designs for Precoded Receive Spatial Modulation derived from Non-Orthogonal Space Time Block Codes" Telecommunication systems, Springer (under review)

bility are the significant aspects considered while designing a communication system. In light of these requirements, it becomes crucial for the forthcoming communication standards such as 5G and beyond to provide and a communication infrastructure which is energy as well as spectrally efficient at the same time provides enhances the reliability of communication. Multiple input-multiple output (MIMO) systems are capable of supporting the increasing demand for high-quality services of the wireless systems. Multiple antenna combinations can provide both multiplexing gain and also diversity gain [Foschini and Gans (1998)]. Spatial Multiplexing (SMX), Space Time Block Code (STBC), Spatial Modulation (SM), STBC-SM and their variants are the examples of MIMO techniques which provides higher multiplexing gains, improves reliability and enhances energy efficiency [Foschini (1996), Alamouti (1998), Mesleh et al. (2008), Basar et al. (2011)].

In the recent past, the concept of Precoding aided Spatial Modulation (PSM) was proposed in [Yang (2011), Stavridis et al. (2012)]. In contrast with SM techniques, Precoding aided Spatial Modulation techniques are designed to convey additional information bits by the use of active receive antenna indices instead of transmit antenna indices. This leads to the reduction in complexity and cost at the receiver terminal, so this technique is preferred for use on down-link communication. In order to select the receive antenna, it becomes necessary to precode the transmitted data suitably. Hence, it is generally assumed that Channel State Information is available at the transmitter side (CSIT). Rong Zhang et.al [Zhang et al. (2013)] proposed the concept of Generalised pre-coding aided spatial modulation (GPSM). In this work, a combination of multiple receive antennas were activated corresponding to the incoming information bits. This allowed the multi-stream of data to be parallelly detected at the receiver which further increases the spectral efficiency of the system. The precoding design ensures that the desired set of receive antennas are active and other receive antennas are in inactive state. In the recent past, several researchers have explored the use of generalized precoding aided spatial modulation schemes and its variants to achieve high data rate and low-complexity [Li et al. (2016), Luo et al. (2018)]. In any MIMO system, practical issues such as Spatial Correlation (SC) brought about by inadequate antenna separation have

to be taken into account because of size limitation of the hand held devices. Several researchers have devised techniques to minimize the effects of spatial correlation [Mesleh et al. (2010), Simha et al. (2017)]. So it becomes very crucial to consider the effect of spatial correlation between antennas at both transmitter as well as receiver end for any scheme that is to be deployed in practice.

A study of STBC, NSTBC literature has motivated us to explore the technique of precoding aided spatial modulation with non-orthogonal space time block codes (Precoded SM-NSTBC). To the best of our knowledge, there is no discussion of Precoded SM-NSTBC with receive antenna activation available in literature. We have proposed a precoded SM-NSTBC scheme and have compared its performance with precoded STBC-SM and precoded SM-OSTBC over spatially correlated and uncorrelated Rayleigh fading environments.

The major contributions of this chapter are described as follows:

- The concept of precoding aided spatial modulation employing non-orthogonal space time block codes to achieve receive spatial modulation, namely Precoded SM-NSTBC is proposed in this chapter. The information is conveyed by activating a subset of receive antennas in addition to the conventionally transmitted Non-orthogonal Space Time Block Codes (NSTBC). The NSTBC are designed from full-rank non-binary Cyclic codes over $GF(q^m)$, $q = 5, 7, 13, 17$ and $m = 4$ to achieve full-rank STBCs similar to the one presented in chapter 3.

- The proposed scheme is analyzed over both uncorrelated and spatially correlated Rayleigh fading environments. Performance of the proposed scheme is analyzed for the varying values of spatial correlation. The computational complexity of the proposed Precoded SM-NSTBC is also presented. Further, theoretical upper bound on average bit error rate has been derived. The close correspondence between analytically obtained upper bound and simulation results implies that the Monte-Carlo simulations carried out are accurate.

- ABER performance of the proposed Precoded SM-NSTBC is compared with precoded SM-OSTBC and precoded STBC-SM schemes over uncorrelated as well

as spatially correlated Rayleigh fading environments. We have obtained precoded SM-OSTBC by adopting OSTBC as described in [Le et al. (2014)] and incorporating suitable precoding technique. Similarly, precoded STBC-SM is designed by precoding the STBC obtained from [Basar et al. (2011)]. The proposed scheme outperforms competitive schemes by a minimum of 2 dB in both uncorrelated and correlated Rayleigh environment.

Notation: Throughout this paper, matrices and vectors are represented by bold uppercase and lowercase alphabets. $\mathbf{X}^T$, $\mathbf{X}^*$, $tr[\cdot]$ is the transpose, conjugate and trace of the matrix $\mathbf{X}$, $\lfloor \cdot \rfloor$ represents the floor operator, $||\cdot||_F^2$ is the Frobenius norm and $E\{\cdot\}$ is the expectation of a matrix. Other notations and abbreviations are given below in Table 4.1.

Table 4.1 Abbreviations and Notations

NSTBC	Non-orthogonal Space Time Block Code	N_t	Number of transmit antennas
SM	Spatial Modulation	N_r	Number of receive antennas
STBC-SM	Space Time Block Coded Spatial Modulation	N_a	Number of active receive antennas
GF	Galois Field	$\mathbb{M}_{m \times m}$	Full rank codeword matrix
GFFT	Galois Field Fourier Transform	$\mathbf{P}$	Precoding matrix
IGFFT	Inverse Galois Field Fourier Transform	$\mathbf{X}_{SM}$	Spatially modulated codeword matrix
PSM	Precoding aided Spatial Modulation	$\mathbf{X}$	Transmitted matrix
GPSM	Generalised pre-coding aided spatial modulation	n_s	Number of time slots
CSIT	Channel State Information at Transmitter	β	Normalization factor
SC	Spatial Correlation	η	Spectral Efficiency
SM-OSTBC	Spatially Modulated Orthogonal STBC	$\mathbf{Y}$	Received matrix
ML	Maximum Likelihood	$\mathbf{H}$	Channel Matrix
ABER	Average Bit Error Rate	$\mathbf{H}_c$	Spatially correlated channel matrix
PEP	Pairwise Error Probability	$\mathbf{R}_{Rx}$	Receiver correlation matrix
AWGN	Additive White Gaussian Noise	$\mathbf{R}_{Tx}$	Transmitter correlation matrix
		β_c	Coefficient of exponential decay

4.2   System Model

A Precoded-SM-NSTBC communication system consisting of N_t number of transmit antennas, N_r number of receive antennas (of which N_a receive antennas are active at

any given time) is considered. In this analysis, it is assumed that $N_t > N_r$. Knowledge of the channel matrix at the transmitter is employed to design a precoding scheme which enables the system to combat the effect of channel induced noise and distortion. This scheme differs from conventional SM schemes in the sense that a subset of receive antennas (rather than a subset of transmit antennas) are made active over any symbol interval (as given in [Zhang et al. (2013)]). The selection of active receive antennae depends upon the incoming information symbols. In order to ensure the appropriateness of precoder design for the channel over which communication is sought to be established, availability of perfect CSIT (Channel State Information at Transmitter) is essential. A detailed design and analysis of the proposed Precoded SM-NSTBC scheme is given below.

4.2.1 Design employed in Precoded SM-NSTBC

Overview of NSTBC Design: The NSTBC scheme makes use of full rank codewords which are obtained from Cyclic codes using a well defined procedure. In this design, we employ the Galois Field Fourier Transform (GFFT) approach in which codewords are initially specified in the transform domain and then converted to their time domain representations by employing the Inverse Galois Field Fourier Transform (IGFFT) representation as described in chapter 2. The brief overview is given by the example in following subsection.

4.2.2 Steps involved in NSTBC construction

To illustrate the steps involved in the code construction, consider the construction of a length $n = 13$, non binary Cyclic code over $GF(5^4)$. The Galois Field Fourier Transform (GFFT) of **a** is represented by $\mathbf{A} = (A_0, A_1, \ldots, A_{n-1})$. Let us choose A_1 as the free transform component and constrain all other transform components to zero to satisfy the conditions required to obtain full rank codewords. Hence, we allow A_1 to take on values successively from $\{0, 1, \ldots, \alpha^{5^4-2}\}$ in the field $GF(5^4)$ and constrain all other transform components to zero. Since $1 \in \{1, 5, 12, 8\}$, a cyclotomic coset of full size in $GF(5^4)$, all the non zero codewords will possess rank equal to four $(m = 4)$. This code has $q^m - 1$ (here, $5^4 - 1 = 624$) non zero codewords of full rank. Each codeword

is a $m \times n$ (4×13) matrix over $GF(5)$. These codes along with the all zero codeword matrix constitute all the 625 codewords of the Cyclic code. We now adopt the puncturing scheme in which the first four columns of each codeword are retained and the remaining nine columns are dropped. A list of twelve representative codewords chosen at random (after puncturing) is presented in Table 4.1.

Table 4.2 Some examples of $GF(5^4)$ NSTBC codewords corresponding to value of $A_1 = \alpha^x$

Value of A_1	Corresponding codeword	Value of A_1	Corresponding codeword	Value of A_1	Corresponding codeword
α^{40}	$\begin{bmatrix} 1 & 2 & 2 & 3 \\ 1 & 1 & 2 & 4 \\ 0 & 4 & 1 & 2 \\ 4 & 1 & 4 & 1 \end{bmatrix}$	α^{59}	$\begin{bmatrix} 0 & 1 & 1 & 0 \\ 1 & 2 & 0 & 1 \\ 2 & 1 & 0 & 1 \\ 3 & 2 & 4 & 4 \end{bmatrix}$	α^{93}	$\begin{bmatrix} 4 & 0 & 0 & 1 \\ 3 & 4 & 3 & 0 \\ 2 & 0 & 3 & 1 \\ 3 & 3 & 1 & 4 \end{bmatrix}$
α^{70}	$\begin{bmatrix} 2 & 1 & 1 & 3 \\ 4 & 1 & 4 & 2 \\ 4 & 0 & 2 & 4 \\ 4 & 1 & 1 & 1 \end{bmatrix}$	α^{272}	$\begin{bmatrix} 1 & 2 & 4 & 2 \\ 2 & 1 & 2 & 4 \\ 2 & 3 & 4 & 4 \\ 4 & 3 & 0 & 2 \end{bmatrix}$	α^{292}	$\begin{bmatrix} 1 & 1 & 2 & 4 \\ 3 & 4 & 2 & 2 \\ 4 & 0 & 0 & 3 \\ 1 & 0 & 3 & 2 \end{bmatrix}$
α^{397}	$\begin{bmatrix} 4 & 3 & 0 & 1 \\ 0 & 4 & 3 & 1 \\ 2 & 0 & 2 & 0 \\ 1 & 1 & 2 & 0 \end{bmatrix}$	α^{270}	$\begin{bmatrix} 3 & 3 & 4 & 1 \\ 1 & 1 & 1 & 1 \\ 2 & 4 & 3 & 4 \\ 2 & 3 & 1 & 4 \end{bmatrix}$	α^{285}	$\begin{bmatrix} 2 & 1 & 4 & 2 \\ 1 & 0 & 4 & 2 \\ 4 & 4 & 0 & 4 \\ 3 & 4 & 3 & 3 \end{bmatrix}$
α^{440}	$\begin{bmatrix} 3 & 3 & 0 & 0 \\ 1 & 2 & 1 & 1 \\ 1 & 3 & 1 & 3 \\ 3 & 4 & 1 & 3 \end{bmatrix}$	α^{492}	$\begin{bmatrix} 0 & 3 & 1 & 1 \\ 4 & 2 & 0 & 1 \\ 2 & 1 & 1 & 1 \\ 0 & 4 & 3 & 1 \end{bmatrix}$	α^{513}	$\begin{bmatrix} 0 & 0 & 3 & 4 \\ 2 & 4 & 0 & 0 \\ 0 & 4 & 3 & 0 \\ 4 & 3 & 2 & 3 \end{bmatrix}$

This procedure can be used to design Cyclic codes over both binary as well as

non-binary alphabets. Constructions over non-binary alphabets have the advantage of yielding higher spectral efficiencies. It is well known that rank preserving maps can be defined for prime numbers of the form $4K + 1$ (Gaussian integer map [Lusina et al. (2003)]) or $6K + 1$, (Eisenstein map [Huber (1994a)]) K is an integer. Hence, we use fields over these prime numbers as the base fields for code construction. The codewords of the proposed Precoded SM-NSTBC scheme are full rank matrices over a suitable non binary field. A detailed discussion of the proposed Precoded SM-NSTBC scheme and receive antenna selection procedure is described in the following section.

4.3   Proposed Precoded SM-NSTBC Scheme

In the proposed Precoded SM-NSTBC scheme, the first step is to assign sequences of information bits to the NSTBC codeword matrices. These codewords are then spatially modulated and transmitted. The concept of precoded SM-NSTBC is to activate N_a number of receive active antennas out of N_r antennas. N_r represents the total number of receive antennas. The novel concept of precoding explores the spatial modulation at receiver section. The combination of receive antennas to be activated is chosen depending on the incoming information bits.

In Precoded SM-NSTBC, N_a $(1 < N_a \leq N_r)$ number of receive antennas are active (out of the total number N_r of receive antennas). Hence, a total of N_a parallel data streams are received in every single time slot. When $N_a = N_r$ the proposed scheme degenerates into a conventional MIMO system. The total number of activation patterns possible when N_a number of antennas out of N_r receive antennas are activated is given by $k = \binom{N_r}{N_a}$. The procedure to select active antenna at the receiver depends on the information bits to be transmitted.

In this scheme, we have employed codewords obtained from full rank Cyclic codes over $GF(5^4)$, $GF(7^4)$, $GF(13^4)$ and $GF(17^4)$. These codes are punctured as described in subsection 4.2.1. and corresponding full rank 4×4 codewords are obtained. For convenience of mapping the available codewords are given by $q^m - 1$, out of which $2^{\lfloor \log_2(q^m) \rfloor}$ number of codewords are selected. In order to avoid fractional bit spectral efficiency the remaining codewords are not used.

The procedure for the proposed Precoded SM-NSTBC scheme is explained as given in Algorithm 4.

Algorithm 4 Precoded SM-NSTBC encoding algorithm

1: Start
2: Consider a block of $\lfloor \log_2(q^m) \rfloor$ bits over each time slot
3: Step 1:Acquire corresponding $\mathbb{M}_{m \times m} \in GF(q)$ full rank codeword matrix
4: Fix the possible active receive antenna patterns $k = \binom{N_r}{N_a}$; $\{A_1, A_2, \cdots, A_k\}$
5: Step 2: Extract from $\mathbb{M}_{m \times m}$, the antenna selection matrix $[\mathbb{M}_1]_{m/2 \times m}$ and the information symbol matrix $[\mathbb{M}_2]_{m/2 \times m}$ represented by $\mathbb{M}_{m \times m} \rightarrow [\mathbb{M}_1]_{m/2 \times m}$ (antenna selection symbols) ; $[\mathbb{M}_2]_{m/2 \times m}$ (information symbols)
6: Step 3:for count=1:number of time slots for full codeword transmission
7: Step 4: Select the active antenna pattern
8:   $[\mathbb{M}_1]_{m/2 \times m} \rightarrow A_j \in \{A_1, A_2, \cdots, A_k\}$ $(1 \le j \le k)$
9: Step 5: Mapping of Information symbols:$\mathbf{C}[i(1)i(2)\cdots i(2m)]$
10:   Define map $\varphi : [\mathbb{M}_2]_{m/2 \times} \rightarrow \Im(\mathbf{C})$
11:   Obtain suitable rank preserving map $\mathbf{S}_{SM} = \varphi(\mathbf{C}_2)$
12: end
13: Step 6: Get the full SM-NSTBC codeword $\mathbf{S}_{SM} \in \mathbb{C}^{N_r \times T}$
14: Step 7: Obtain precoding matrix with help of CSIT $\mathbf{P} \in \mathbb{C}^{N_t \times N_r}$
15: Step 8: Radiate the precoded SM-NSTBC signal $\mathbf{X} = \mathbf{P}\mathbf{S}_{SM} \in \mathbb{C}^{N_t \times T}$
    end

In the first step, the incoming binary bit-stream is divided into blocks of $\lfloor \log_2(q^m) \rfloor$ bits. Each information block is mapped into a suitable codeword depending upon the chosen Cyclic code. The obtained codeword (which is a full rank $m \times n$) matrix over $GF(q), q = \{5, 7, 13, 17\}$ depending upon the choice of the chosen Cyclic code is punctured to obtain a full rank $m \times m$ codeword. The antenna selection symbols and the radiated symbols are chosen from the encoded codeword. The process of selecting the active receiver antennas is performed column-wise. The elements of upper two rows of 4×4 codeword matrix are used to select one of the k antenna selection patterns, given by $\{A_1, A_2, \cdots, A_k\}$, here $A_i \in \mathbb{C}^{N_r \times 1}$. A_i is a vector with only N_a active elements. Once receive antenna selection is completed, the elements of lower two rows are modulated to obtain SM-NSTBC codeword $\mathbf{S}_{SM} \in \mathbb{C}^{N_r \times T}$. This concept of activation of receive antenna and design precoded SM-NSTBC is explained in the Algorithm 4.

In the Algorithm 4, let $\mathbf{S}_{SM}$ denote the SM-NSTBC codeword matrix and $\mathbf{P}$ denote the precoding matrix. Then the final radiated codeword is given in Equation (4.1).

60

$$\mathbf{X} = \mathbf{P}\mathbf{S}_{SM} \qquad (4.1)$$

Here $\mathbf{X} \in \mathbb{C}^{N_t \times T}$, T is the time slot required for transmission of whole codeword matrix, $\mathbf{P} \in \mathbb{C}^{N_t \times N_r}$ precoding matrix, $\mathbf{S}_{SM}$ is the SM-NSTBC codeword matrix.

Since the elements of codeword matrix $\mathbf{S}_{SM}$ are from $GF(q)$, the total number of possible patterns to be generated for $N_a = 2$ are q^2, while the total number of active antenna combinations are k. When $q^2 > k$, many to one mapping is executed. It has to be noted that all codeword matrices are unique and full rank. Even if the same activation pattern is selected by more than one codeword combination, the transmitted symbol would still be different. When $N_a = 4$, two columns are radiated in a single time slot. The performance of the proposed precoded SM-NSTBC scheme for $N_a = \{2, 4\}$ has been evaluated.

In order to ensure the correctness of active receive antenna combinations, channel state information (CSI) is assumed to be available at the transmitter where precoding has been performed. Let $\mathbf{P} \in \mathbb{C}^{N_t \times N_r}$ be the precoding matrix. The detailed description of the steps used to determine $\mathbf{P}$ is provided in the following sub-section.

4.3.1 Precoder Design

The precoding matrix $\mathbf{P} \in \mathbb{C}^{N_t \times N_r}$ must be designed in order to ensure the correct set of receive antennas activated over every time slot. As perfect CSIT is assumed, the value of $\mathbf{H}$ is well known at the transmitter. The precoder must be designed accordingly to combat channel effects and activate the predefined receiver subset. In the proposed precoded SM-NSTBC scheme, zero forcing precoder has been employed [Spencer et al., 2004]. Therefore, transmit precoding matrix corresponds to the pseudo-inverse of the channel matrix $\mathbf{H}^T$, ans is given in Equation (4.2) [Zhang et al. (2013)].

$$\mathbf{P} = \beta \mathbf{H}^* (\mathbf{H}^T \mathbf{H}^*)^{-1} \qquad (4.2)$$

here, $\mathbf{H} \in \mathbb{C}^{N_t \times N_r}$ is the channel matrix and β is the normalization factor used to normalize the power of the transmitted signal $\mathbf{X}$, defined in Equation (4.3) [Luo et al.

$$\beta = \sqrt{\frac{N_r}{N_a.tr[(\mathbf{H}^T\mathbf{H}^*)^{-1}]}} \tag{4.3}$$

Let $\mathbf{S}_{SM}$ be the spatially modulated codeword matrix such that $\mathbf{S}_{SM} \in \mathbb{C}^{N_r \times T}$. Here, T represents the time slot required to transmit the whole codeword matrix. Then the transmitted signal is described by $\mathbf{X} \in \mathbb{C}^{N_t \times T}$ as defined in Equation (4.1). The signal received at the receiver section is specified as

$$\mathbf{Y} = \mathbf{H}^T\mathbf{X} + \mathbf{N} \tag{4.4}$$

$$\mathbf{Y} = \mathbf{H}^T\mathbf{P}\mathbf{S}_{SM} + \mathbf{N} \tag{4.5}$$

Here $\mathbf{Y} \in \mathbb{C}^{N_r \times T}$ is the received signal and $\mathbf{N} \in \mathbb{C}^{N_r \times T}$ is the circularly symmetric complex independent and identically distributed Gaussian noise.

This process is further illustrated by example given below.

Example: Let $\mathbf{S}_{SM} \in \mathbb{C}^{N_r \times T}$ be the spatially modulated codeword matrix to be received at the receiver end. Consider a MIMO system with $N_t = 6, N_r = 4, N_a = 2$ number of transmit, receive and active antennas at receiver end respectively with $(1 < N_a < N_r)$.

Let,

$$\mathbf{S}_{SM} = \begin{bmatrix} 0 & 0 & \{a_{2,2}\} & \{a_{2,3}\} \\ \{a_{2,0}\} & \{a_{2,1}\} & 0 & 0 \\ \{a_{3,0}\} & 0 & \{a_{3,2}\} & 0 \\ 0 & \{a_{3,1}\} & 0 & \{a_{3,3}\} \end{bmatrix} \tag{4.6}$$

In order to assure that $\mathbf{S}_{SM}$ is received correctly at the receiver, zero forcing precoding technique is incorporated. The transmit codeword matrix $\mathbf{X}$ is obtained by multiplying the zero forcing precoder to the spatially modulated codeword matrix to be received. Hence the transmitting codeword obtained as shown in equation 4.7

$$\mathbf{X} = \mathbf{P}\mathbf{S}_{SM} \tag{4.7}$$

Here $\mathbf{X} \in \mathbb{C}^{N_t \times T}$, T is the time slot required for transmission of whole codeword

matrix, $\mathbf{P} \in \mathbb{C}^{N_t \times N_r}$ precoding matrix, $\mathbf{S}_{SM}$ is the SM-NSTBC codeword matrix.

Let $\mathbf{H} \in \mathbb{C}^{N_t \times N_r}$ is the channel matrix. Then by applying Zero forcing precoder technique the corresponding to the pseudo-inverse of the channel matrix $\mathbf{H}^T$ is given in Equation (4.2). The channel matrix $\mathbf{H}$ is given below .

$$\mathbf{H} = \begin{bmatrix} h_{0,0} & h_{0,1} & \cdots & h_{0,(N_r-1)} \\ h_{1,0} & h_{1,1} & \cdots & h_{1,(N_r-1)} \\ \vdots & \vdots & \cdots & \vdots \\ h_{(N_t-1),0} & h_{(N_t-1),1} & \cdots & h_{(N_t-1),(N_r-1)} \end{bmatrix} \tag{4.8}$$

The precoding matrix obtained by $\mathbf{P} = \beta \mathbf{H}^*(\mathbf{H}^T\mathbf{H}^*)^{-1} \in \mathbb{C}^{N_t \times N_r}$. Let $\mathbf{Y} \in \mathbb{C}^{N_r \times T}$ be the received codeword matrix and $\mathbf{N} \in \mathbb{C}^{N_r \times T}$ is the circularly symmetric complex independent and identically distributed Gaussian noise.

The received codeword matrix as shown in equation (4.13) is given below

$$\mathbf{Y} = \mathbf{H}^T\mathbf{X} + \mathbf{N} \tag{4.9}$$

$$\mathbf{Y} = \mathbf{H}^T\mathbf{P}\mathbf{S}_{SM} + \mathbf{N} \tag{4.10}$$

$$\begin{bmatrix} y_{0,0} & y_{0,1} & y_{0,2} & y_{0,3} \\ y_{1,0} & y_{1,1} & y_{1,2} & y_{1,3} \\ y_{2,0} & y_{2,1} & y_{2,2} & y_{2,3} \\ y_{3,0} & y_{3,1} & y_{3,2} & y_{3,3} \end{bmatrix} = \begin{bmatrix} \beta & 0 & 0 & 0 \\ 0 & \beta & 0 & 0 \\ 0 & 0 & \beta & 0 \\ 0 & 0 & 0 & \beta \end{bmatrix} \begin{bmatrix} 0 & 0 & \{a_{2,2}\} & \{a_{2,3}\} \\ \{a_{2,0}\} & \{a_{2,1}\} & 0 & 0 \\ \{a_{3,0}\} & 0 & \{a_{3,2}\} & 0 \\ 0 & \{a_{3,1}\} & 0 & \{a_{3,3}\} \end{bmatrix} + \mathbf{N}$$

$$\tag{4.11}$$

Hence, the receive spatial modulation is accomplished.

Detection: At the receiver end, detection becomes simpler in terms of complexity

as the zero forcing precoder is applied. Once, all the elements of codeword matrix are obtained then the ML detection for full codeword matrix is performed as given in Equation (4.12).

$$\hat{\mathbf{S}}_{SM} = argmin||\mathbf{Y} - \mathbf{H}^{\mathbf{T}}\tilde{\mathbf{X}}||_F^2 \tag{4.12}$$

Here, $\hat{\mathbf{S}}_{SM}$ is the estimated codeword and $\tilde{\mathbf{X}}$ is the set of all possible values of codewords. From Equation (4.5) the received signal can be written as given in Equation (4.13)

$$\mathbf{Y} = \beta\mathbf{S}_{SM} + \mathbf{N} \tag{4.13}$$

Therefore, the ML detection reduces to

$$\hat{\mathbf{S}}_{SM} = argmin||\mathbf{Y} - \beta\tilde{\mathbf{S}}_{SM}||_F^2 \tag{4.14}$$

here, β is the normalization factor defined in Equation (4.3) and $\tilde{\mathbf{S}}_{SM}$ is the set of all possible codeword matrix of the system.

Spectral Efficiency calculation: The spectral efficiency of the Precoded SM-NSTBC scheme is given by η.

$$\eta = \lfloor log_2(q^m) \rfloor / n_s \tag{4.15}$$

where $n_s = T$ is the total number of time slots required for transmission of whole codeword matrix, $q \in \{5, 7, 13, 17\}$ and $m = 4$ is the order of the extension field.

Spatially Correlated Channel Model: For any MIMO system, the spacing (correlation) between receive and/or transmit antenna elements has to be taken into account in the process of decoding. When the spacing between these array elements is not sufficient, spatial correlation is created and correlated channel paths are generated. In this work, Kronecker channel model is incorporated to obtain the correlated channel matrix [Younis (2014), Simha et al. (2017)].

$$\mathbf{H}_c = \mathbf{R}_{Rx}^{1/2}\mathbf{H}\mathbf{R}_{Tx}^{1/2} \tag{4.16}$$

Here, $\mathbf{R}_{Rx}$ and $\mathbf{R}_{Tx}$ represent the receiver and transmitter correlation matrix respectively. These $\mathbf{R}_{Tx}$ and $\mathbf{R}_{Rx}$ are modeled using exponential decay model [Younis (2014)].

$$\mathbf{R} = \begin{bmatrix} 1 & \rho & \rho^2 & \cdots & \rho^{n-1} \\ \rho & 1 & \rho & \cdots & \rho^{n-2} \\ \rho^2 & \rho & 1 & \cdots & \rho^{n-3} \\ \vdots & \ddots & \ddots & \ddots & \vdots \\ \rho^{n-1} & \cdots & \rho^2 & \rho & 1 \end{bmatrix} \tag{4.17}$$

In this matrix, $\rho = exp(\beta_c)$, where β_c is the coefficient of exponential decay. For transmit correlation matrix $\mathbf{R}_{Tx}$, $n = N_t$ and for receiver correlation matrix $\mathbf{R}_{Rx}$, $n = N_r$. The

value of ρ equals ρ_t for transmit correlation matrix, similarly for receive correlation matrix the value of ρ equals ρ_r. The value of correlation coefficient ρ varies from 0 to 0.9 with 0 representing uncorrelated scenario and 0.9 for dense spatial correlation environment. In the following section, performance investigation and mathematical analysis of the proposed precoded SM-NSTBC scheme has been presented.

4.4 Mathematical treatment for Precoded SM-NSTBC

In this section, a detailed description about the analytical upper bound for the proposed Precoded QM-NSTBC system has been derived. An analytical upper bound on the Average Bit Error Rate (ABER) is presented by following the approach outlined in [Simon and Alouini (2005)].

$$ABER_{SM} \leq \frac{1}{2^{\lfloor \log_2 q^m \rfloor} 2\eta} \sum_{i=1}^{2^{\lfloor \log_2 q^m \rfloor}} \sum_{j=1}^{2^{\lfloor \log_2 q^m \rfloor}} d(\mathbf{S}_{SM}, \hat{\mathbf{S}}_{SM}) E\{P(\mathbf{S}_{SM} \to \hat{\mathbf{S}}_{SM})\} \qquad (4.18)$$

Here, η is the spectral efficiency, $d(\mathbf{S}_{SM}, \hat{\mathbf{S}}_{SM})$ is the number of non-zero elements of the difference matrix of $\mathbf{S}_{SM} - \hat{\mathbf{S}}_{SM}$. $(P(\mathbf{S}_{SM} \to \hat{\mathbf{S}}_{SM}))$ is the pairwise error probability (PEP) of detecting $\hat{\mathbf{S}}_{SM}$ when $\mathbf{S}_{SM}$ is transmitted for a given channel $\mathbf{H}$. This is described by,

$$P(\mathbf{S}_{SM} \to \hat{\mathbf{S}}_{SM}) = Pr\left(\left|\left| \mathbf{Y} - \mathbf{H}^T \mathbf{X} \right|\right|_F^2 > \left|\left| \mathbf{Y} - \mathbf{H}^T \hat{\mathbf{X}} \right|\right|_F^2 | \mathbf{H} \right) \qquad (4.19)$$

here, $\mathbf{X} = \mathbf{P}\mathbf{S}_{SM}$ and $\hat{\mathbf{X}} = \mathbf{P}\hat{\mathbf{S}}_{SM}$

From Equations (4.13) and (4.19), we get

$$P(\mathbf{S}_{SM} \to \hat{\mathbf{S}}_{SM}) = Pr\left(\left|\left| \mathbf{Y} - \beta \mathbf{S}_{SM} \right|\right|_F^2 > \left|\left| \mathbf{Y} - \beta \hat{\mathbf{S}}_{SM} \right|\right|_F^2 \right) \qquad (4.20)$$

The pairwise error probability is evaluated using [Luo et al. (2018), Simon and Alouini (2005)]:

$$P(\mathbf{S}_{SM} \to \hat{\mathbf{S}}_{SM}) = Q\left(\sqrt{\frac{\rho}{2}} \beta \left|\left| (\mathbf{S}_{SM} - \hat{\mathbf{S}}_{SM}) \right|\right| \right) \qquad (4.21)$$

Here $Q(\cdot) = \frac{1}{\sqrt{2\pi}} \int_x^\infty \exp(-y^2/2) dy$. β is defined as given in Equation (4.3) and ρ represents the Signal to Noise Ratio (SNR) of the signal. Using Gamma approximation as given in [Luo et al. (2018)], the PEP can be written as below.

$$P(\mathbf{S}_{SM} \to \hat{\mathbf{S}}_{SM}) = Q\left(\sqrt{\frac{\rho}{2}}\gamma\sqrt{\delta}\right) \tag{4.22}$$

Here $\delta = \frac{N_r}{N_a}||\mathbf{S}_{SM} - \hat{\mathbf{S}}_{SM}||^2$ and $\gamma = \sqrt{(\frac{N_a}{N_r})}\beta$. The expectation of pairwise error probability is given by 4.23. This is obtained by the use of Craig representation of the Q function and moment generating function.

$$E\left\{Q\left(\sqrt{\frac{\rho}{2}}\gamma\sqrt{\delta}\right)\right\} = \frac{1}{\pi}\int_0^{\frac{\pi}{2}} M_\alpha\left(\frac{-\delta\rho}{4sin^2\theta}\right)d\theta \tag{4.23}$$

Here M_α is the moment generating function of α, the gamma distribution is used to approximate the argument of α. Let $\alpha = \gamma^2$. Then the probability density function (PDF) of α is specified as given by Equation (4.24) [Luo et al. (2018)].

$$f_{(\alpha)}(\alpha) = \frac{\alpha^{a-1}}{b^a\Gamma(a)}e^{\frac{-\alpha}{b}}; \alpha > 0 \tag{4.24}$$

Here a is the shaping parameter and b is the scaling parameter. Using Equation (4.24), the expectation of PEP is obtained by the use of moment generating function [Simon and Alouini (2005)].

$$E\{P(\mathbf{S}_{SM} \to \hat{\mathbf{S}}_{SM})\} \leq \frac{1}{\pi}\int_0^{\frac{\pi}{2}}\prod_{l=1}^{L}\left(\frac{1}{1+\frac{b\rho\lambda_{i,j_l}}{4sin^2\theta}}\right)^{N_r}d\theta \tag{4.25}$$

here, $L = 4$ and λ_{i,j_l} are the Eigen values of the distance matrix $(\mathbf{S}_{SM} - \hat{\mathbf{S}}_{SM})^H(\mathbf{S}_{SM} - \hat{\mathbf{S}}_{SM})$. The closed form solution for PEP can be obtained from [Simon and Alouini (2005)] is given below

$$E_H\{P(\mathbf{S}_{SM} \to \hat{\mathbf{S}}_{SM})\} \leq \frac{1}{2}\prod_{l=1}^{L}\frac{1}{\left(1+\frac{b\rho\lambda_{i,j_l}}{4}\right)^{N_r}} \tag{4.26}$$

Thus the analytical upper bound on the Average Bit Error Rate (ABER) is calculated as given in Equation (4.27).

$$ABER_{SM} \leq \frac{1}{2^{\lfloor\log_2 q^m\rfloor}4\eta}\sum_{i=1}^{2^{\lfloor\log_2 q^m\rfloor}}\sum_{j=1}^{2^{\lfloor\log_2 q^m\rfloor}}d(\mathbf{S}_{SM}-\hat{\mathbf{S}}_{SM})\prod_{l=1}^{L}\frac{1}{\left(1+\frac{b\rho\lambda_{i,j_l}}{4}\right)^{N_r}} \tag{4.27}$$

In the following section the computational complexity of the proposed scheme is determined.

4.5   Decoding Complexity of the Precoded SM-NSTBC

The computation complexity is given in terms of total complex multiplications and additions. All calculation are evaluated with following considerations.

- Consider matrix $\mathbf{M1} \in \mathbb{C}^{M \times N}$, and $\mathbf{M2} \in \mathbb{C}^{N \times L}$, then the matrix multiplication requires MNL number of complex multiplications and $ML(N-1)$ number of complex additions.

- To calculate $\|\mathbf{M1}\|_F^2$ requires MN number of complex multiplications and $(MN-1)$ number of complex additions.

The computational complexity for the proposed system is defined in terms of complex multiplications required for decoding one codeword. The ML detection is defined as $\|\mathbf{Y} - \beta \tilde{\mathbf{S}}_{SM}\|_F^2 \in C$. The total number of codewords possible are given by $2^{\lfloor log_2(q^m) \rfloor}$, number of receive activation pattern possible is $\binom{N_r}{N_a}$. The number of complex multiplications required for computing the Frobenius norm is $(N_r T)$ where $T = n_s$ i.e. the time slots required to transmit whole codeword. So the total complexity of ML detection for the proposed scheme can be quantified as

$$2^{\lfloor log_2(q^m) \rfloor} \left(\binom{N_r}{N_a} + N_r T \right) \tag{4.28}$$

Figure 4.1 gives the complexity comparison of ML detection for the proposed Precoded SM-NSTBC scheme, precoded SM-OSTBC scheme with spectral efficiency of 5.5 bpcu and precoded STBC-SM achieves a spectral efficiency of 5 bpcu. The proposed Precoded SM-NSTBC scheme employs ($N_t = 8$, $N_r = 6$, $N_a = 4$) antenna configuration, with the codeword derived over $GF(7)$, while precoded SM-OSTBC scheme employs ($N_t = 8$, $N_r = 6$, $N_a = 4$) antenna configuration, and precoded STBC-SM employs ($N_t = 4$, $N_r = 4$, $N_a = 2$) antenna configuration. The decoding computational complexity of above configurations is 7820 (computations/bit) for Precoded SM-NSTBC scheme, 63500 (computations/bit) for precoded SM-OSTBC scheme and 3840 (computations/bit) for precoded STBC-SM scheme.
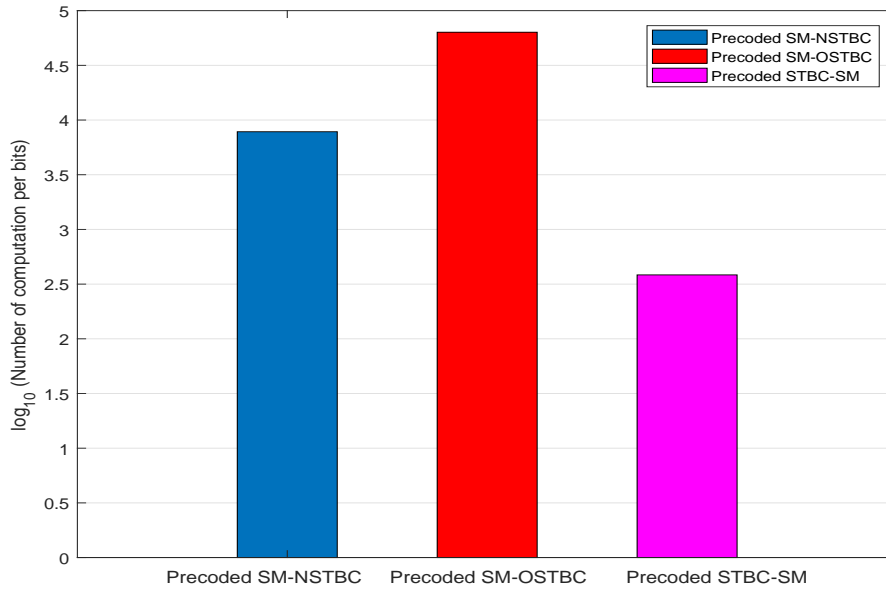
Figure 4.1 Computational Complexity of precoded SM-NSTBC for 5.5 bpcu, precoded SM-OSTBC for 5.5 bpcu and precoded STBC-SM for 5 bpcu

The complexity of proposed Precoded SM-NSTBC is higher than precoded STBC-SM. However, this increase in complexity is a trade off for improvement in ABER performance. The Precoded SM-NSTBC schemes provides a performance improvement of more than 2 dB as compared to precoded STBC-SM as shown in figure 4.6.

4.6 Simulation Results

In this chapter, the proposed Precoded SM-NSTBC system is denoted as $C(N_t, N_r, N_a)$ where N_t and N_r represent the number of transmit antennas and receive antennas respectively. N_a represents the number of active antennas at the receiver over a given time slot. A total of 10^6 random channel realizations are employed to determine the performance using Monte-Carlo simulations. The correlated fading environment is obtained by the use of Kronecker channel model description given in [Mesleh et al. (2008)]. The correlation matrices for the transmitter and receiver are generated using the exponential decay model [Simha et al. (2017)]. The performance of Precoded SM-NSTBC has been analyzed for both uncorrelated as well as correlated Rayleigh fading environment. The

performance in correlated fading environments is obtained by incorporating the spatial correlation coefficient with $\rho = \{0, 0.5, 0.9\}$. In order to obtain accurate precoding, perfect CSIT availability is assumed.
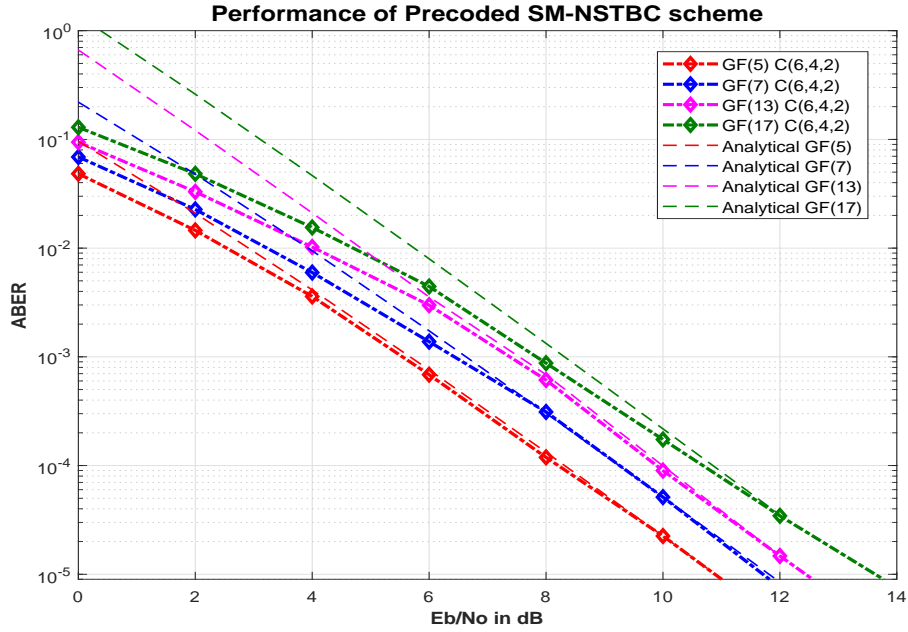
Figure 4.2 Performance of Precoded SM-NSTBC for $GF(q); q = \{5, 7, 13, 17\}$

The performance of proposed Precoded SM-NSTBC scheme over $GF(q)$ for $q = \{5, 7, 13, 17\}$ employing antenna configuration of $C(N_t = 6, N_r = 4, N_a = 2)$ is given in Figure 4.2. A spectral efficiency obtained is 2.25 bpcu, 2.75 bpcu, 3.5 bpcu and 4 bpcu for value of $q = \{5, 7, 13, 17\}$ respectively. The analytical upper bound is also presented in Figure 4.2. The close correspondence between simulation results and plot of the upper bound testifies to the tightness of the analytical upper bound derived. As the signal to noise ratio (SNR) value increases, the upper bound becomes more tight.

In figure 4.3, the ABER performance of the proposed Precoded SM-NSTBC scheme over $GF(5)$, $GF(7)$, $GF(13)$ and $GF(17)$ is shown with antenna configuration of $C(6, 4, 2)$ for correlated and uncorrelated Rayleigh fading environment. The spectral efficiency (η) achieved is 2.25 bpcu, 2.75 bpcu, 3.5 bpcu and 4 bpcu respectively. The analysis is given for uncorrelated ($\rho = 0$), medium correlated ($\rho = 0.5$) and highly dense corre-
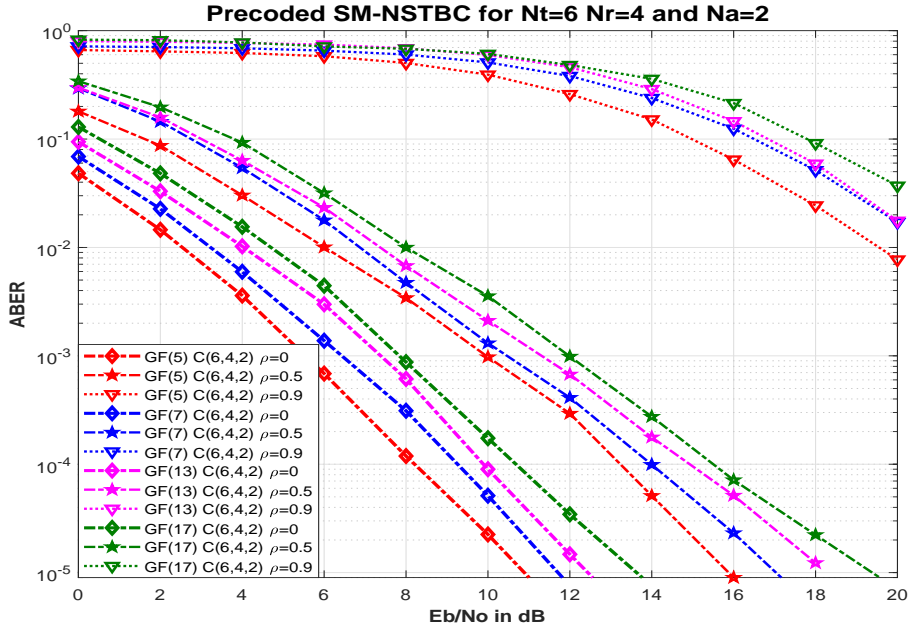
Figure 4.3 Performance of Precoded SM-NSTBC for $GF(5), GF(7), GF(13), GF(17)$ for uncorrelated and correlated Rayleigh fading conditions

lated ($\rho = 0.9$) Rayleigh fading environment. As expected, there exists a performance degradation as the spatial correlation increases.

Figure 4.4 illustrates the performance of proposed Precoded SM-NSTBC schemes over $GF(5)$, $GF(7)$, $GF(13)$ and $GF(17)$ with higher (applicable to eight or more) transmit antennas. We have evaluated the performance with eight transmit antennas. The number of active receive antennas considered here is four. In Figure 4.4 performance over uncorrelated and correlated Rayleigh fading channels with antenna configurations of $C(8,6,4)$ has been evaluated. Spectral efficiencies of 4.5 bpcu, 5.5 bpcu, 7 bpcu and 8 bpcu have been attained for $q = \{5,7,13,17\}$ respectively. The values of spatial correlation coefficient chosen in our evaluation are $\rho = 0, 0.5, 0.9$. This data is used for determining transmit and receive correlation matrices.

In figure 4.5, performance of the proposed scheme is compared with precoded STBC-SM schemes for $N_r = 4, N_a = 2$ and $N_t = 4$ antennas. Precoded STBC-SM is obtained by activating receive antennas, the STBC-SM adopted from [Basar et al. (2011)] in which active transmit antennas are used instead of receive antennas. Precoded STBC-
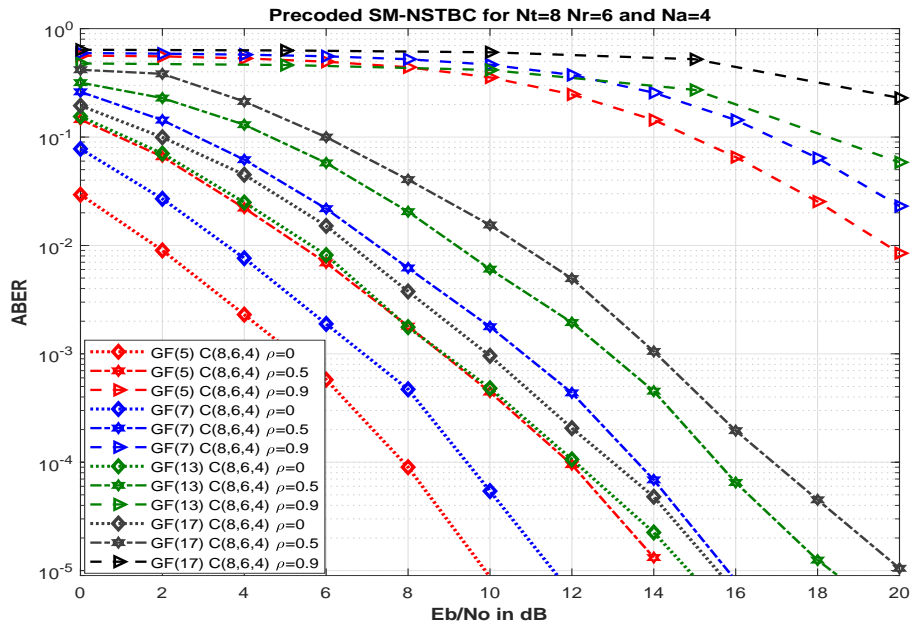
Figure 4.4 Performance of Precoded SM-NSTBC for $GF(5), GF(7), GF(13), GF(17)$ for $C(8,6,4)$
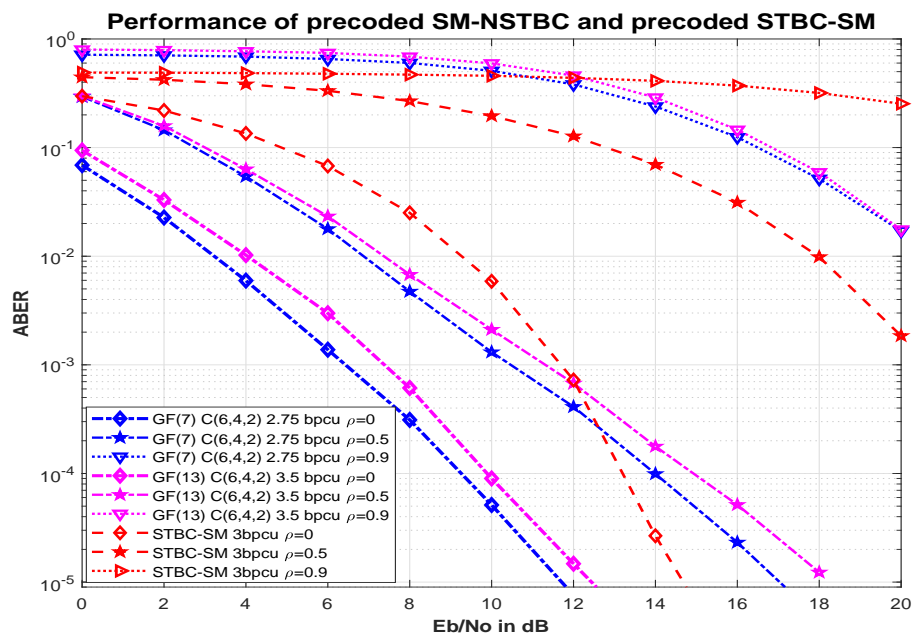

Figure 4.5 Comparison of Precoded SM-NSTBC scheme with $\eta = 2.5, 3.5$ bpcu and precoded STBC-SM scheme with $\eta = 3$ bpcu

SM achieves the spectral efficiency of $\eta = 3$ bpcu, while proposed scheme shown has spectral efficiency of $\eta = 2.75, 3.5$ bpcu respectively for $GF(7), GF(13)$. It is shown that the proposed scheme achieves a superior performance of approximately 2 dB in uncorrelated environment and ~ 6 dB as the channel exhibits greater correlation. It is important to note that for a medium correlation scenario, that is ($\rho = 0.5$), the proposed scheme outperforms precoded STBC-SM with very high margin of about 6 dB. Hence it can be employed as an alternative to precoded STBC-SM in generalized scenarios.

In figure 4.6, a comparison of the proposed scheme with precoded SM-OSTBC and precoded STBC-SM is given. Precoded SM-OSTBC designed with 8-PSK achieves $\eta = 5.5$ bpcu with an antenna configuration specified by $C(8,6,4)$. This scheme of precoded SM-OSTBC is designed by incorporating concept of SM-OSTBC as given in [Le et al. (2014)] and adding a suitable precoding structure. Precoded STBC-SM achieves a spectral efficiency of 5 bpcu for $N_r = 4, N_a = 2, N_t = 4$ for 32-QAM system designed from [Basar et al. (2011)]. The proposed Precoded SM-NSTBC outperforms both precoded SM-OSTBC by ~ 3 dB and ~ 2dB over uncorrelated and correlated Rayleigh scenario. The proposed scheme outperforms precoded STBC-SM by a large value of ~ 6 dB in uncorrelated environment and ~ 8 dB in correlated Rayleigh environments. The performance of proposed scheme in medium correlation ($\rho = 0.5$) environment outperforms precoded STBC-SM in uncorrelated ($\rho = 0$) fading condition. Thus, we conclude that the performance of Precoded SM-NSTBC is vastly superior to precoded STBC-SM.

Fig. 4.7 shows the performance of the proposed scheme of Precoded SM-NSTBC scheme over $GF(7)$ with $C(8,6,4)$ configuration. The spectral efficiency obtained is $\eta = 5.5$ bpcu. The performance has been analyzed for varying values of SNR along with different spatial correlation values. Here the value of spatial correlation coefficient ρ is considered same for both transmit and receiver correlation matrix that is $\rho_t = \rho_r = \rho$. Performance degradation is observed with increase in the value of spatial correlation. For a value of $\rho = 0$, it can be observed that the ABER reaches the value of 10^{-9} for a observed SNR value of 20 dB. At the same value of SNR with a higher
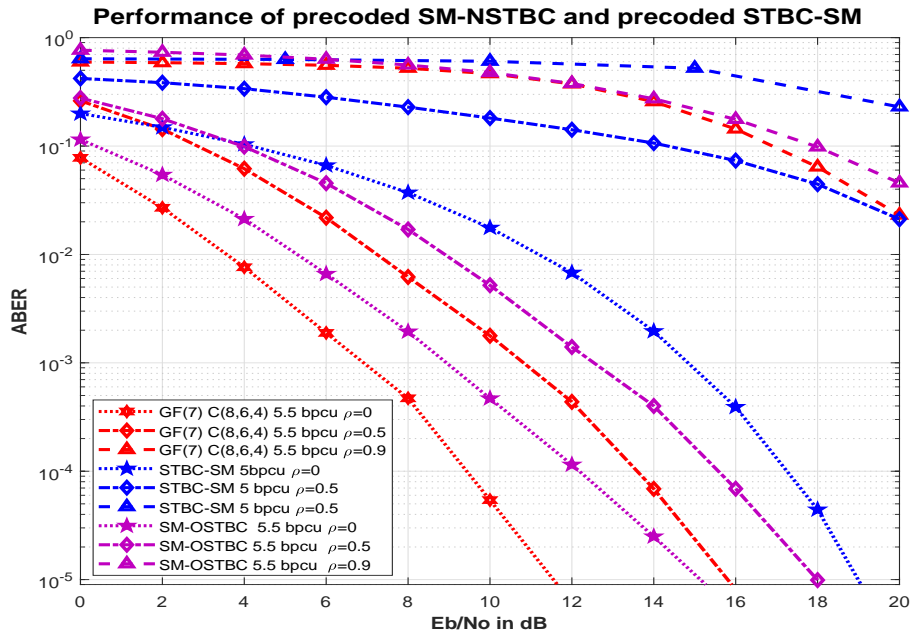
Figure 4.6 Performance of Precoded SM-NSTBC for $GF(7)$ $C(8,6,4)$ and precoded SM-OSTBC $(N_t = 8, N_r = 6, N_a = 4)$ for $\eta = 5.5$ bpcu and precoded STBC-SM for 5bpcu
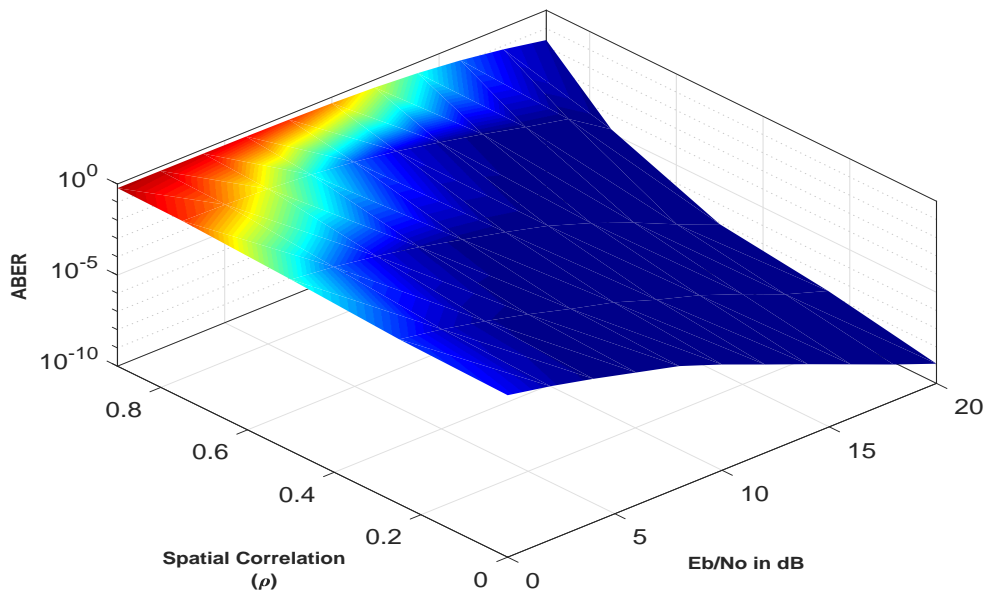
Figure 4.7 Performance of Precoded SM-NSTBC for $GF(7)$ $C(8,6,4)$ for $\eta = 5.5$ bpcu over varying SNR in the presence of spatial correlation.
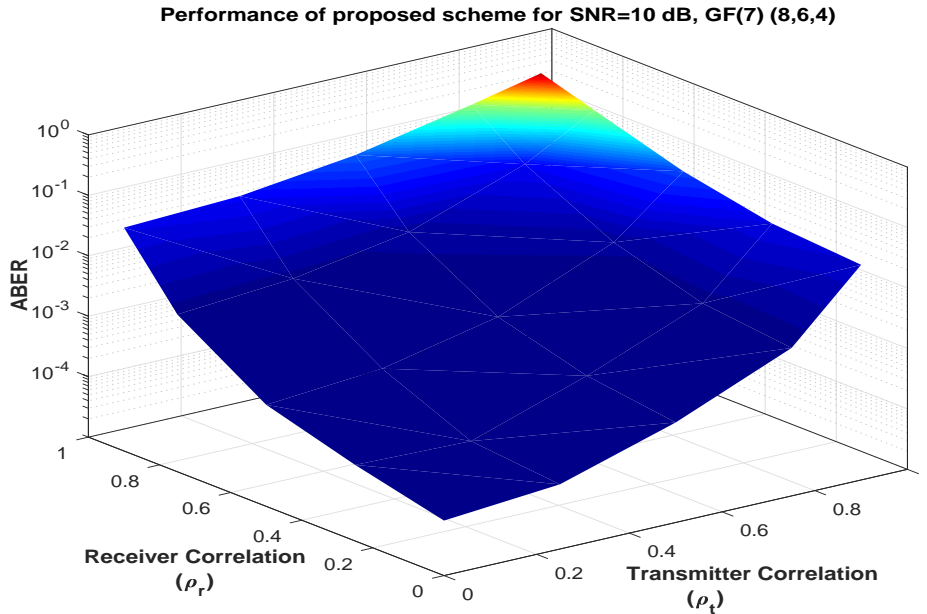
Figure 4.8 Performance of Precoded SM-NSTBC for $GF(7)$ $C(8,6,4)$, $\eta = 5.5$ bpcu at SNR value of 10 dB for varying values of transmit and receive spatial correlation.

value of ρ, ($\rho = 0.4$), the ABER increases to the order of 10^{-8}. This variation is expected as performance improves with increase in SNR and a decrease in the value of the correlation coefficient ρ.

Fig. 4.8 demonstrates the effect of spatial correlation coefficients on the ABER performance of the proposed precoded SM-NSTBC scheme over $GF(7)$ with $C(8,6,4)$ configuration. In this plot, the SNR is kept fixed at 10 dB and the variation of ABER with ρ is observed. As anticipated, the performance degradation is noted with the increased values of spatial correlation coefficient. The performance of proposed scheme for varying values of transmit as well as receive spatial correlation is demonstrated. Similar performance plots have been obtained for other configurations of transmit-receive antenna and codes defined over other Galois fields. A close perusal of these plots reveal very similar variation of ABER as a function of receiver and transmitter spatial correlation.

4.7 Summary

In this chapter, a new class of Precoded SM-NSTBC schemes suitable for use over both uncorrelated and correlated Rayleigh fading environments have been proposed. In this scheme, a subset of receive antennas are activated, and the selection depends upon incoming information bits. Further the decoding complexity of the proposed Precoded SM-NSTBC scheme is computed and an analytical upper bound on the Average Bit Error Rate (ABER) is determined. Monte-Carlo simulations have been carried out to quantify the performance of these codes. It is observed that proposed scheme outperforms precoded SM-OSTBC and precoded STBC-SM schemes by ~ 2 dB and ~ 3 dB respectively over uncorrelated environment. For correlated Rayleigh fading, an improvement of ~ 3 dB and ~ 7 dB is observed over precoded SM-OSTBC and precoded STBC-SM respectively. From the simulation results, it can be inferred that the proposed Precoded SM-NSTBC can be used as a promising alternative to the existing state-of-art MIMO systems. Because of the improved ABER performance in both uncorrelated and correlated Rayleigh fading environments, the proposed scheme is well suited for deployment in spatially correlated channels (especially in 5G MIMO systems), where the restrictions of physical space in the transmitter/receiver can lead to spatial correlation.

In the preceding chapters, we have explored the concepts of spatial modulation at transmitter and receiver ends, the next contributory chapter describes a cooperative communication system. The concept of cooperative communication utilizes relays to convey information from source to destination with high reliability. It also provides the advantage of diversity gain by establishing a virtual MIMO scenario. In the following chapter, system model and channel model of an Amplify and Forward relay based cooperative communication system is analyzed and studied. Finally, the performance analysis of SM-NSTBC and other competitive schemes has been given. An analytical upper bound is evaluated for Amplify and Forward based SM-NSTBC scheme.

Chapter 5

Design and performance analysis of cooperative SM-NSTBC with amplify and forward relaying

[1] In this chapter, the design and analysis of a cooperative communication system is explored. The performance of SM-NSTBC for amplify and forward (AF) MIMO system has been presented. We have proposed a technique in which an amplify and forward cooperative communication link and a direct link are suitably combined to yield superior performance over state of the art SM scheme. The performance of the proposed scheme is quantified by deriving the closed-form expression for average bit error rate (ABER) of this composite link over Rayleigh fading environment. There is a close correspondence between the derived analytical result and the simulation values obtained. Furthermore, an expression for the outage probability has been derived for the proposed system. The analytic and the simulation results show that the proposed composite SM-NSTBC scheme with amplify and forward relaying achieves a performance improvement of ~ 2 dB when compared to conventional SM-NSTBC scheme and a performance improvement of ~ 3 dB over cooperative STBC-SM scheme.

5.1   Introduction

As the science and technology of wireless communication evolves beyond 5G, many communication strategies including peer to peer communication would have to be de-

---

[1]Godkhindi Shrutkirthi S., et al., Design and performance analysis of cooperative SM-NSTBC with amplify and forward relaying, IEEE Transactions on Wireless Communications (Under Review)

signed and deployed. Applications such as video streaming, navigation, emergency communication have led to a tremendous increase in the demand for higher data rates, increased integrity of information transfer, spectral and power efficiency in wireless communication systems. This requirement in turn has motivated researchers to propose a number of innovative schemes which can yield higher data rates with enhanced data integrity at the same time without compromising on the need to conserve spectrum and transmit energy [Laneman and Wornell (2000), Kramer et al. (2005)]. Future beyond-5G technologies will involve communication strategies such as cooperative communications in which the nodes cooperate with each other to convey information from source to the desired destination with high levels of information integrity. Communication between two distant points on the globe will invariably require the use of multiple nodes. There exists a need to develop strategies which can work in a network involving multiple nodes and deliver enhanced quality of service from source to destination. Cooperative communication with antenna indexing is one novel strategy, in which one or more relays are utilized effectively to enhance the signal quality at the destination node. Such systems offer advantage of high diversity gain due to the ability of forming virtual multiple-input multiple-output (MIMO) transmit and receive systems [Öztoprak et al. (2017)]. The relay nodes present in the geographical locations between the transmit and receive nodes assist the source in communicating effectively with the destination. This is due to the fact that multiple replicas of signal are received at the destination and hence the reliability of communication process is enhanced [Laneman and Wornell (2000), Nosratinia et al. (2004)]. The advantages of cooperative communication and MIMO techniques have motivated researchers to explore the field of cooperative MIMO systems to achieve increased network coverage and higher spectral efficiency for wireless systems of the future. The setup of multiple antennas at transmitter and/or receiver is not always attainable in all applications due to the limitation of hardware size and cost. For such scenarios, multiple relays can be employed to form a virtual MIMO system.

This concept of cooperative relay based communication has attracted the attention of many researchers, as it has the potential to provide higher reliability, greater net-

work coverage, higher data rates and reduced bit error rates (BER) over fading channels [Varshney et al. (2016)]. Two of the most widely employed relay cooperative techniques are amplify-and-forward (AF) which is non-regenerative and decode-and-forward (DF) which is regenerative. In the DF relaying technique the decoded signal at the relay node is re-transmitted without any verification from the source, leading to higher probability of degradation of overall ABER due to decoding inaccuracy under poor channel conditions.

A dual hop strategy involving SM combined with DF was presented by Serafimovski et al. in [Serafimovski et al. (2011)]. In this work the spatial domain of dual-hop has been utilized to transmit additional information bits. DF relaying for Space Shift Keying was presented with coherent and non-coherent relay selection in [Sugiura et al. (2011)], where, the authors utilize matrix dispersion method to activate one of the relays in the system. In [Yang et al. (2011)], the concept of cooperative space-time Space Shift Keying with AF relaying was demonstrated with large number of transmit antennas and a single relay. A scenario in which the source sends information to relay as well as to the destination in single time phase has been proposed by Mesleh et al.[Mesleh et al. (2012)]. Further, Mesleh et.al have determined and analyzed the performance of SM with multiple decode and forward relaying. In this scheme, the decoded signal at relay is forwarded to destination by use of predetermined orthogonal channels [Mesleh and Ikki (2013)]. A system with multiple transmit antennas, a single antenna at the relay node and destination for dual-hop SSK was presented in [Mesleh et al. (2011)]. This approach employs amplify and forward relaying. A mathematical analysis resulting in the determination of exact ABER for a SSK system with DF relaying and multiple antenna configuration at source, relay nodes and destination was provided in [Som and Chockalingam (2013)]. A comparative study of both AF and DF relaying for SM system with multiple antenna configuration at source, multiple relays and destination was discussed in [Altın et al. (2017)]. The performance of a cooperative communication scheme through a direct link between the source and destination in addition to the AF link is analyzed and a new low complexity relay selection is presented in [Öztoprak et al. (2017)].

Varshney et al. in [Varshney et al. (2015)] have presented a cooperative communication scheme with a single/multiple relay employing a MIMO Space Time Block Code with decode-and-forward technique. The performance of both single and multiple relay configuration has been evaluated in the above paper. In addition, the concept of STBC-SM cooperative communication with selective decode-and-forward technique over spatially correlated environment has also been studied. Optimal power allocation between source and relay was also explored in [Varshney et al. (2016)]. The concept of spectrum sharing technique for SM and STBC-SM has been presented in [Babaei et al. (2016)]. The analysis of capacity and the outage probability of a cooperative SM scheme for both DF and AF relaying scheme is provided in [Altın et al. (2016)].

An extensive study of cooperative communication over SM and STBC has inspired us to conceptualize an arrangement of cooperative communication operating along with Spatially Modulated Non-orthogonal Space Time Block Codes (SM-NSTBC). To the best of author's knowledge, the concept of relaying working in conjunction with Non-orthogonal designs has not been investigated so far. We have proposed a novel transmission system of a cooperative SM-NSTBC amplify and forward scheme comprising of a single relay working in tandem with the direct link. We have named it as Spatially Modulated Non-Orthogonal Space Time Block Code with Amplify and Forward relaying (SM-NSTBC-AF). The outage probability of the proposed scheme is evaluated. An upper bound on the ABER has been derived and the performance of the scheme has been compared with that of conventional SM-NSTBC and cooperative STBC-SM in Rayleigh fading environment.

The remaining part of the chapter is organized as follows: Section 5.2, presents the description of the system and channel model of the proposed cooperative SM-NSTBC scheme. Section 5.3, describes the design of the proposed Cooperative Spatially Modulated Non-orthogonal Space Time Block Code scheme with amplify and forward relaying (SM-NSTBC-AF) technique. In Section 5.4, a detailed analysis of the analytical upper bound on the average bit error rate (ABER) has been presented. In Section 5.5 the outage probability of the SM-NSTBC-AF scheme is presented. In Section 5.6, Monte-Carlo simulation results which present the variation of ABER as a function of SNR

has been presented. The chapter is concluded in Section 5.7 with a discussion on the significance of the results presented with other standard SM techniques.

Notation: Throughout this paper, matrices and vectors are represented by bold uppercase and lowercase alphabets. Here, $\mathbf{X}^T$ is the transpose of the matrix $\mathbf{X}$, $\lfloor \cdot \rfloor$ represents the floor operator, $||\cdot||_F^2$ is the Frobenius norm and $E\{\cdot\}$ is the expectation of a matrix. Other notations and abbreviations are given below in Table 5.1.

Table 5.1 Abbreviations and Notations

		N_s	Number of source antennas
SM	Spatial Modulation	N_a	Number of active transmit antennas
NSTBC	Non-orthogonal Space Time Block Code	N_re	Number of relay antennas
AF	Amplify and Forward	N_d	Number of destination antennas
GF	Galois Field	$\mathbb{C}_{m\times m}$	Full rank codeword matrix
ABER	Average Bit Error Rate	$\mathbf{X}$	Spatially modulated codeword matrix
DF	Decode and Forward	$\mathbf{H}$	Channel Matrix
SMX	Spatial Multiplexing	$\mathbf{H}_{SR}$	Source to relay channel matrix
SSK	Space Shift Keying	$\mathbf{H}_{SD}$	Source to destination channel matrix
GFFT	Galois Field Fourier Transform	$\mathbf{H}_{RD}$	Relay to destination channel matrix
IGFFT	Inverse Galois Field Fourier Transform	$\mathbf{Y}_{SR}$	Received vector from source to relay
CSI	Channel State Information	$\mathbf{Y}_{SD}$	Received vector from source to destination channel matrix
ML	Maximum Likelihood	$\mathbf{Y}_{RD}$	Received vector from relay to destination
PEP	Pairwise Error Probability	P_{out}	Outage Probability
		η	Spectral Efficiency

5.2   System Model

A cooperative SM-NSTBC amplify-and forward relaying technique (SM-NSTBC-AF) employing a single relay with multiple antennas is considered in this work. The proposed system consists of multiple transmit antennas at the source and relay, as well as multiple receive antennas at relay and the destination. Here the number of transmits antenna at the source is denoted as N_s, the number of antennas at relay is represented by N_{re} and N_d denotes the number of antennas at the destination.

In the proposed scheme, antenna indexing is considered at the source node. The number of active transmit antennas at the source is N_a such that $(1 \leq N_a \leq N_s)$. The

81

transmission of information signal occurs in two steps. In the first step, a spatially modulated full rank NSTBC codeword is broadcasted from the source to relay and source to destination. In the second step, the information received at the relay is amplified and further transmitted to the destination. The design of SM-NSTBC employed was described in chapter 3. In section 5.3 the concept and design of cooperative SM-NSTBC with amplify-and-forward relaying technique has been demonstrated.

5.3 Proposed Cooperative SM-NSTBC with Amplify and Forward relaying Scheme
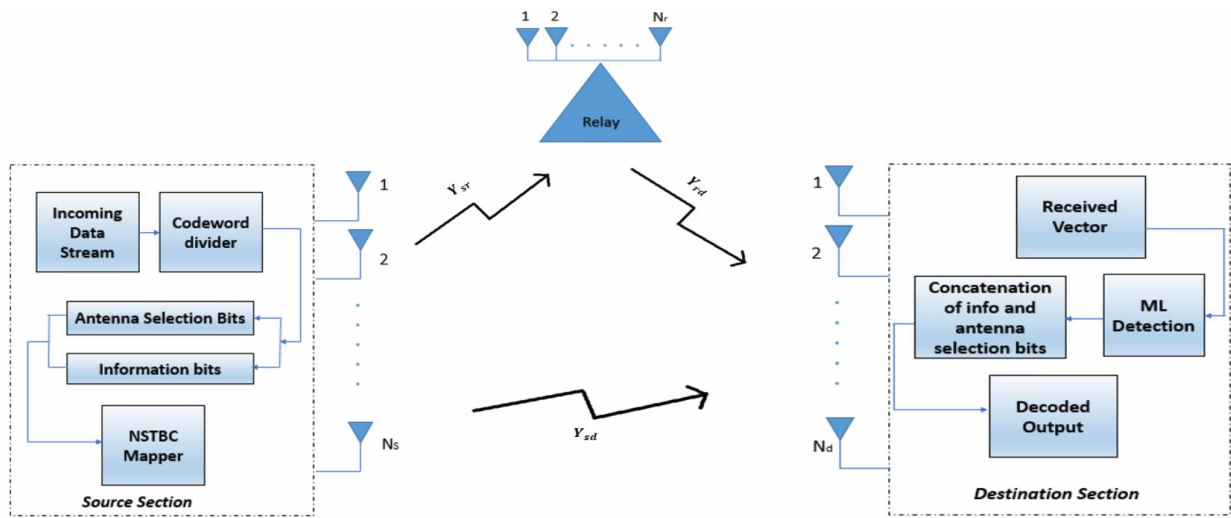
Figure 5.1 Block diagram of the proposed cooperative SM-NSTBC-AF scheme.

Figure 5.1 gives the block description of the proposed cooperative Spatially Modulated Non-orthogonal Space Time Block Code with amplify and forward relaying (SM-NSTBC-AF). In the proposed scheme, the total transmission of information from source to destination occurs in two phases. The process begins with a sequences of information bits being mapped to a specific full rank NSTBC codeword matrix. This codeword is spatially modulated and transmitted from the source. As we are employing an SM-NSTBC scheme, antenna selection indexing has been incorporated. A set of symbols determine the selection of N_a number of transmit active antennas out of N_s total number of source antennas. The remaining symbols are conventionally radiated using the active antennas. In the first phase, the SM-NSTBC codeword matrix is transmitted by

the source to both relay node and to the destination node. This results in the creation of a cooperative link through the relay and a direct link from source to destination.

In the second phase, the received signal at the relay is amplified and radiated towards the destination. The entire series of steps involved in the proposed SM-NSTBC-AF technique is described in the following algorithm 5. In our constructions, the maximum number of active antennas employed is 4. This scheme can be generalized for any number of active transmit antennas.

Algorithm 5 Cooperative SM-NSTBC-AF technique

1: Start
2: Step 1: Compute the set of q^m full rank SM-NSTBC Codewords
3:     Group the information bits into block of $\lfloor \log_2(q^m) \rfloor$ bits
4:     Map each $\lfloor \log_2(q^m) \rfloor$ length bit sequence to a corresponding full rank codeword matrix $\mathbb{C}_{m \times m} \in GF(q)$
5: Consider column-wise selection of $m \times m$ codeword matrix to obtain antenna selection symbols and symbols to be radiated.
6: Acquire antenna selection matrix $[\mathbb{C}_1]_{m/2 \times m}$ and the symbol radiation matrix $[\mathbb{C}_2]_{m/2 \times m}$.
7: Step 2: for count=1:number of time slots for full codeword transmission
8: Step 3: Select the active antenna pattern
9:     $[\mathbb{C}_1]_{m/2 \times m} \rightarrow T_i \in \{T_1, T_2, \cdots, T_k\}$ $(1 \le i \le k)$
10: Step 4: Mapping of Information symbols: $\mathbf{C}[i(1)i(2) \cdots i(2m)]$
11:     Define map $\varphi : [\mathbb{C}_2]_{m/2 \times m} \rightarrow \Im(\mathbf{C})$
12:     Obtain suitable rank preserving map $\mathbf{S} = \varphi(\mathbf{C}_2)$
13: Step 5: Get the full SM-NSTBC codeword $\mathbf{X} \in \mathbb{C}^{N_s \times T}$
14: Step 6: Phase 1:
15: The information is radiated from source
16:     $\mathbf{Y}_{sr} = \sqrt{E_s/N_a}\mathbf{H}_{SR}\mathbf{X} + \mathbf{N}_{sr}$; $\mathbf{Y}_{sr}$: vector of received symbol at relay, $\mathbf{H}_{SR}$ is the channel matrix from source to relay
17:     $\mathbf{Y}_{sd} = \sqrt{E_s/N_a}\mathbf{H}_{SD}\mathbf{X} + \mathbf{N}_{sd}$; $\mathbf{Y}_{sd}$: vector of received symbol at destination, $\mathbf{H}_{SD}$ is the channel matrix from source to destination
18: Step 7: Phase 2:
19: Step 8: The amplified information is transmitted by the relay and received at destination.
20: $\mathbf{Y}_{rd} = G\sqrt{E_r/N_{re}}\mathbf{H}_{RD}\mathbf{Y}_{sr} + \mathbf{N}_{rd}$; $\mathbf{Y}_{rd}$ vector of received symbol at destination from relay, $\mathbf{H}_{RD}$ is the channel matrix from relay to destination
21: Step 9: At destination ML detection is applied to estimate information
22: end

In cooperative SM-NSTBC-AF, the total number of active transmit antenna is N_a such that $(1 < N_a \le N_s)$. The total number of activation patterns possible when N_a

number of antennas out of N_s source antennas are activated is given by $k = \binom{N_s}{N_a}$. The procedure to select active antenna depends on the information bits to be transmitted. This process has been described in chapter 3. There are two modes of antenna selection employed for SM-NSTBC as descried below.

- If the number of active antennas is 2, each column is selected one by one over individual time slots. The elements $A_{0,j}$ and $A_{1,j}$ are used to select the active antennas while the symbols $A_{2,j}, A_{3,j}$, are radiated conventionally.

- If the number of active antennas is equal to 4, two columns are selected one by one over one time slot. The elements $A_{0,j}, A_{0,j+1}$ and $A_{1,j}, A_{1,j+1}$ are used to select the active antennas while the symbols $A_{2,j}, A_{2,j+1}, \cdots, A_{3,j}, A_{3,j+1}$, ($j$ is an odd integer ranging from 0 to $(m-1)$) are radiated conventionally.

The working procedure of the proposed SM-NSTBC-AF scheme has been given in Algorithm 5. At the source, a block of $\lfloor \log_2(q^m) \rfloor$ incoming binary bit-stream is considered for processing at a time. This block of information bits is mapped to a specific full rank codeword matrix from the chosen Cyclic code. The obtained codeword which is a $m \times n$ matrix is then punctured by dropping dependent columns to obtain a full rank $m \times m$ codeword matrices. The antenna selection symbols and the radiated symbols are then selected from the codeword matrix. The process of selecting the active antennas is performed column-wise. The elements of upper two rows of 4×4 codeword matrix are used to select one of the k antenna selection patterns, given by $\{T_1, T_2, \cdots, T_k\}$, where k represents the total number of antenna activation patterns. Once antenna selection is completed, the elements of lower two rows are modulated using suitable rank-preserving maps to obtain SM-NSTBC codeword $\mathbf{X} \in \mathbb{C}^{N_s \times T}$.

Let $\mathbf{X}$ be the spatially modulated codeword matrix such that $\mathbf{X} \in \mathbb{C}^{N_s \times T}$. Here, T represents the number of time slots required to transmit the whole codeword matrix. In the first phase, the spatially modulated full rank NSTBC is radiated from source to relay and the destination. The signal received in the relay node and the destination at the end of first phase are described in Equations (5.1) and (5.2) respectively.

$$\mathbf{Y}_{sr} = \sqrt{\frac{E_s}{N_a}} \mathbf{H}_{SR} \mathbf{X} + \mathbf{N}_{sr} \qquad (5.1)$$

$$\mathbf{Y}_{sd} = \sqrt{\frac{E_s}{N_a}} \mathbf{H}_{SD} \mathbf{X} + \mathbf{N}_{sd} \qquad (5.2)$$

Here, E_s is the symbol energy, N_a is the total number of active antennas, $\mathbf{H}_{SR} \in \mathbb{C}^{N_{re} \times N_s}$ is the channel matrix from source to relay and $\mathbf{H}_{SD} \in \mathbb{C}^{N_d \times N_s}$ is the channel matrix from source to destination respectively. $\mathbf{N}_{sr} \in \mathbb{C}^{N_{re} \times T}$ and $\mathbf{N}_{sd} \in \mathbb{C}^{N_d \times T}$ are independent identically distributed (i.i.d) additive white Gaussian Noise (AWGN) given as $C \mathcal{N}(0, N_0)$, $\mathbf{Y}_{sr} \in \mathbb{C}^{N_{re} \times T}$ is the received signal at the relay and $\mathbf{Y}_{sd} \in \mathbb{C}^{N_d \times T}$ is the received signal at destination in first time phase.

In the second phase, the signal received at the relay is amplified and transmitted to the final destination.

$$\mathbf{Y}_{rd} = G \sqrt{\frac{E_r}{N_{re}}} \mathbf{H}_{RD} \mathbf{Y}_{sr} + \mathbf{N}_{rd} \qquad (5.3)$$

Here $\mathbf{Y}_{rd} \in \mathbb{C}^{N_{re} \times T}$ is the received signal and $\mathbf{N}_{rd} \in \mathbb{C}^{N_{re} \times T}$ is the circularly symmetric complex independent and identically distributed additive white Gaussian noise (i.i.d AWGN). Here $G = \sqrt{1/(N_{re}(E_s + N_0))}$ is the amplification factor at the relay, where $\sqrt{1/N_{re}}$ in G is the scaling factor for transmit energy normalization. Substituting the value of $\mathbf{Y}_{sr}$ we get,

$$\mathbf{Y}_{rd} = G \sqrt{\frac{E_r}{N_{re}}} \mathbf{H}_{RD} (\sqrt{\frac{E_s}{N_a}} \mathbf{H}_{SR} \mathbf{X} + \mathbf{N}_{sr}) + \mathbf{N}_{rd} \qquad (5.4)$$

$$\mathbf{Y}_{rd} = G \sqrt{\frac{E_s E_r}{N_a N_{re}}} \mathbf{H}_{RD} \mathbf{H}_{SR} \mathbf{X} + \mathbf{H}_{RD} \mathbf{N}_{sr} + \mathbf{N}_{rd} \qquad (5.5)$$

Here N_r is Gaussian noise value from the first phase, after noise normalization, the total noise is considered as $\tilde{\mathbf{N}} = \mathbf{H}_{RD} \mathbf{N}_{sr} + \mathbf{N}_{rd}$. $\tilde{\mathbf{N}}$ is the complex value Gaussian variable given by $C \mathcal{N}(0, N_0)$. Perfect channel state information (CSI) is assumed to be available at the destination. Considering noise normalization at destination as given in [Öztoprak et al. (2017)], the composite signal received at the destination is given by the Equation (5.6).

$$\mathbf{Y}_{rd} = \mathscr{A} \mathbf{H}_{RD} \mathbf{H}_{SR} \mathbf{X} + \tilde{\mathbf{N}} \qquad (5.6)$$

where $\mathscr{A} = \sqrt{\frac{E_s E_r G^2}{N_a N_{re} E_r ||g||^2 + 1}}$, and g is the complex channel path gain between relay

85

and the destination.

Detection: At the destination, the signal received from source as direct link in first phase and signal received from relay in second phase both are compared as given in Equation (5.7).

$$\hat{\mathbf{X}} = argmin\{||(\mathbf{Y}_{rd} - \mathscr{A}\mathbf{H}_{RD}\mathbf{H}_{SR}\tilde{\mathbf{X}})||_F^2 + ||(\mathbf{Y}_{sd} - \sqrt{E_s/N_a}\mathbf{H}_{SD}\tilde{\mathbf{X}})||_F^2\} \qquad (5.7)$$

Here, $\hat{\mathbf{X}}$ is the estimated codeword and $\tilde{\mathbf{X}}$ is the set of all possible values codewords.

In the following section the performance analysis of proposed cooperative SM-NSTBC-AF scheme is provided.

5.4 Analytical ABER Evaluation

A detailed description of closed-form ABER expression corresponding to the proposed SM-NSTBC-AF is given in this section. Analytical upper bound is derived following the outline provided in [Simon and Alouini (2005)].

$$ABER_{SM} \leq \frac{1}{2^{\lfloor \log_2 q^m \rfloor} 2\eta} \sum_{i=1}^{2^{\lfloor \log_2 q^m \rfloor}} \sum_{j=1}^{2^{\lfloor \log_2 q^m \rfloor}} d(\mathbf{X}, \hat{\mathbf{X}}) E\{P(\mathbf{X} \to \hat{\mathbf{X}})\} \qquad (5.8)$$

Here, η is the spectral efficiency of the proposed scheme, $d(\mathbf{X}, \hat{\mathbf{X}})$ is the number of non-zero elements of the difference matrix of $\mathbf{X} - \hat{\mathbf{X}}$. $(P(\mathbf{X} \to \hat{\mathbf{X}}))$ is the pairwise error probability (PEP) of detecting $\hat{\mathbf{X}}$ when $\mathbf{X}$ is transmitted for a given channel.

As there are two signal components received at the destination, the process of maximum likelihood (ML) detection has been employed as shown in Equation (5.8). The pairwise error probability is specified in Equation (5.9). It follows that,

$$P(\mathbf{X} \to \hat{\mathbf{X}}|H_{SR}, H_{SD}, H_{RD}) = Pr\left(||(\mathbf{Y}_{rd} - \mathscr{A}\mathbf{H}_{RD}\mathbf{H}_{SR}\mathbf{X})||_F^2 + ||(\mathbf{Y}_{sd} - \sqrt{E_s/N_a}\mathbf{H}_{SD}\mathbf{X})||_F^2 \right.$$
$$\left. > ||(\mathbf{Y}_{rd} - \mathscr{A}\mathbf{H}_{RD}\mathbf{H}_{SR}\hat{\mathbf{X}})||_F^2 + ||(\mathbf{Y}_{sd} - \sqrt{E_s/N_a}\mathbf{H}_{SD}\hat{\mathbf{X}})||_F^2 \right)$$
$$(5.9)$$

$$P(\mathbf{X} \to \hat{\mathbf{X}}|H_{SR}, H_{SD}, H_{RD}) =$$
$$Pr\left(||((\mathscr{A}\mathbf{H}_{RD}\mathbf{H}_{SR}\mathbf{X} + \tilde{\mathbf{N}}) - \mathscr{A}\mathbf{H}_{RD}\mathbf{H}_{SR}\mathbf{X})||_F^2 + ||((\sqrt{E_s/N_0}\mathbf{H}_{SD}\mathbf{X} + \mathbf{N}_{sd}) - \sqrt{E_s/N_a}\mathbf{H}_{SD}\mathbf{X})||_F^2 \right.$$
$$\left. > ||((\mathscr{A}\mathbf{H}_{RD}\mathbf{H}_{SR}\mathbf{X} + \tilde{\mathbf{N}}) - \mathscr{A}\mathbf{H}_{RD}\mathbf{H}_{SR}\hat{\mathbf{X}})||_F^2 + ||((\sqrt{E_s/N_0}\mathbf{H}_{SD}\mathbf{X} + \mathbf{N}_{sd}) - \sqrt{E_s/N_a}\mathbf{H}_{SD}\hat{\mathbf{X}})||_F^2 \right)$$
$$(5.10)$$

For simplicity, consider $\gamma^{SD} \triangleq \sqrt{\frac{\rho}{2}}||\mathbf{H}_{SD}(\mathbf{X} - \hat{\mathbf{X}})||_F^2$, here ρ is the signal to noise ratio. Similarly let γ^{SRD} be the Frobenius norm value of the cooperative path from source to relay and then forwarded to destination.

The pairwise error probability is evaluated using [Altın et al. (2017), Öztoprak et al. (2017)]:

$$P(\mathbf{X} \to \hat{\mathbf{X}}) = Q\left(\sqrt{\gamma^{SD} + \gamma^{SRD}}\right) \qquad (5.11)$$

Here $Q(\cdot) = \frac{1}{\sqrt{2\pi}} \int_x^\infty \exp(-y^2/2)dy$. Using the approach given in [Öztoprak et al. (2017)], and averaging the value of $\mathbf{H}_{SD}, \mathbf{H}_{SR}, \mathbf{H}_{RD}$, and following the moment generating function as described in [Simon and Alouini (2005)], the unconditional PEP upper bound can be described as presented in Equation (5.12). This is obtained by the use of Craig representation of the Q function and moment generating function.

$$P(\mathbf{X} \to \hat{\mathbf{X}}) \leq E\left\{ Q\left(\sqrt{\gamma^{SD} + \gamma^{SRD}}\right) \right\} = \frac{1}{\pi} \int_0^{\frac{\pi}{2}} M_{\gamma^{SD}}\left(\frac{\rho}{4sin^2\theta}\right) M_{\gamma^{SRD}}\left(\frac{\rho}{4sin^2\theta}\right) d\theta$$
$$(5.12)$$

Here M_x is the moment generating function of x and the gamma distribution is used to approximate the argument of x. The probability density function (PDF) of x is given by Equation (5.13) [Öztoprak et al. (2017), Simon and Alouini (2005)].

$$f_{\gamma^{SD}}(x) = \frac{x^{N_{re}N_d - 1}}{(E_S/N_0)^{N_{re}N_d}\Gamma(N_{re}N_d)} e^{\frac{-x}{(E_S/N_0)}} \qquad (5.13)$$

Using Equation (5.13), the expectation of PEP is obtained by the use of moment generating function [Simon and Alouini (2005)].

$$E\{P(\mathbf{X} \to \hat{\mathbf{X}})\} \leq \frac{1}{\pi} \int_0^{\frac{\pi}{2}} \prod_{l=1}^{L} \left(\frac{1}{1 + \frac{\rho\lambda_{i,j_l}}{4sin^2\theta}}\right)^{N_d} \prod_{l=1}^{L} \left(\frac{1}{1 + \frac{\rho\lambda_{m,n_l}}{4sin^2\theta}}\right)^{N_{min}} d\theta \qquad (5.14)$$

here, $L = 4$ and λ_{i,j_l} are the Eigenvalues of the distance matrix $(\mathbf{X} - \hat{\mathbf{X}})^H (\mathbf{X} - \hat{\mathbf{X}})$ of direct link from source to destination, λ_{m,n_l} are the Eigenvalues of the distance matrix obtained by the cooperative link from source to relay and forwarded to destination and $N_{min} = N_{re}$ if $N_{re} < N_d$ otherwise $N_{min} = N_d$. Let $c_l = \frac{\rho\lambda_{i,j_l}}{4}$ and $k_l = \frac{\rho\lambda_{m,n_l}}{4}$. The closed form solution for PEP can be obtained from [Simon and Alouini (2005)] is given below

$$E_H\{P(\mathbf{X} \to \hat{\mathbf{X}})\} \leq \frac{1}{2} \prod_{l=1}^{L} \frac{1}{(1+c_l)^{N_d}} \prod_{l=1}^{L} \frac{1}{(1+k_l)^{N_{min}}} \tag{5.15}$$

Thus the analytical upper bound on the Average Bit Error Rate (ABER) is calculated as given in Equation (5.16).

$$ABER_{SM} \leq \frac{1}{2^{\lfloor \log_2 q^m \rfloor} 4\eta} \sum_{i=1}^{2^{\lfloor \log_2 q^m \rfloor}} \sum_{j=1}^{2^{\lfloor \log_2 q^m \rfloor}} d(\mathbf{X} - \hat{\mathbf{X}}) \prod_{l=1}^{L} \frac{1}{(1+c_l)^{N_d}} \prod_{l=1}^{L} \frac{1}{(1+k_l)^{N_{min}}} \tag{5.16}$$

In the following section the outage probability for the proposed system is evaluated.

5.5 Outage Probability

The amplify and forward relaying generates a total of two complex Gaussian noise distributions at the destination each with varying noise levels [Laneman et al. (2004)]. The fading coefficient from source to relay, relay to destination and source to destination is given by $h_{min}^{SR}, h_{min}^{RD}$ and h_{min}^{SD} respectively. The outage probability in terms of fading coefficients are given by

$$P_{out} = Pr\{|h_{min}^{SD}|^2 + \frac{1}{\rho} f\left(\rho|h_{min}^{SR}|^2, \rho|h_{min}^{RD}|^2\right) \leq \gamma_{th}\} \tag{5.17}$$

Here γ_{th} is the threshold SNR, $f(x,y) = \frac{xy}{x+y+C_s}$ and C_s is a constant, when $C_s = 1$ the noise variance is considered to be available at the relay node and when $C_s = 0$, indicates no noise variance at the relay [Yeoh et al. (2011)]. The moment generating function of the direct link is given as:

$$M_{\gamma^{SD}}(s) = (1 + s(E_s/N_0))^{-N_d} \tag{5.18}$$

For the dual hop link, the cumulative distribution function (CDF) for source to relay is defined as

$$F_{\gamma^{SR}}(x) = 1 - e^{-\frac{kx}{P_s}} \tag{5.19}$$

Here $k = \binom{N_s}{N_a}$ and $P_s = E_s/N_0$. From [Öztoprak et al. (2017)], the complete CDF of dual hop link from source to relay and relay to destination is given by

$$F_{\gamma^{SRD}}(x) = \int_0^\infty F_{\gamma^{SR}}\left(\frac{x+y+C_s}{xy}\right) f_{\gamma^{RD}}(y)dy \tag{5.20}$$

Here $f_{\gamma^{RD}}(y)$ is the PDF of γ^{RD}, and γ^{RD} is the chi-square random variable. The final

outage probability is denoted by $Pr\{z \leq \gamma_{th}\} = F_{\gamma^{SRD}}(\gamma_{th})$, where $z = P_s|h_{min}^{SD}|^2 + P_r|h_{min}^{RD}|^2$ and P_s, P_r represents the power from source to destination and from relay to destination respectively. Substituting Equations (5.19) and (5.13) in (5.20), the outage probability for the proposed system is calculated as shown in Equation (5.21)

$$Pr\{z \leq \gamma_{th}\} = \frac{1}{(2P_s)^{N_{re}N_d}\Gamma(N_{re}N_d)}$$
$$\left[\int_0^\infty y^{N_{re}N_d-1} e^{-\left(\frac{y}{2P_r}\right)} dy - \int_0^\infty e^{-\frac{k}{P_s}\left(\frac{1}{y}+\frac{1}{\gamma_{th}}+\frac{C_s}{\gamma_{th}y}\right)} y^{N_{re}N_d-1} e^{-\frac{k}{\gamma_{th}P_s}} dy \right] \quad (5.21)$$

Using (Equation 3.471.9 of [Gradshteyn et al. (2007)]) the final outage probability is given by,

$$Pr\{z \leq \gamma_{th}\} = 1 - \frac{2e^{-\frac{k}{P_s\gamma_{th}}}}{(2P_s)^{N_{re}N_d}\Gamma(N_{re}N_d)} \left(\frac{2P_s k\left(1+\frac{C_s}{\gamma_{th}}\right)}{P_s} \right)^{\frac{N_{re}N_d}{2}} K_{N_{re}N_d}\left(\sqrt{\frac{2k\left(1+\frac{C_s}{\gamma_{th}}\right)}{P_r P_s}} \right)$$
$$(5.22)$$

Here, $K_x(\cdot)$ is the modified Bessel function of second kind and x^{th} order.
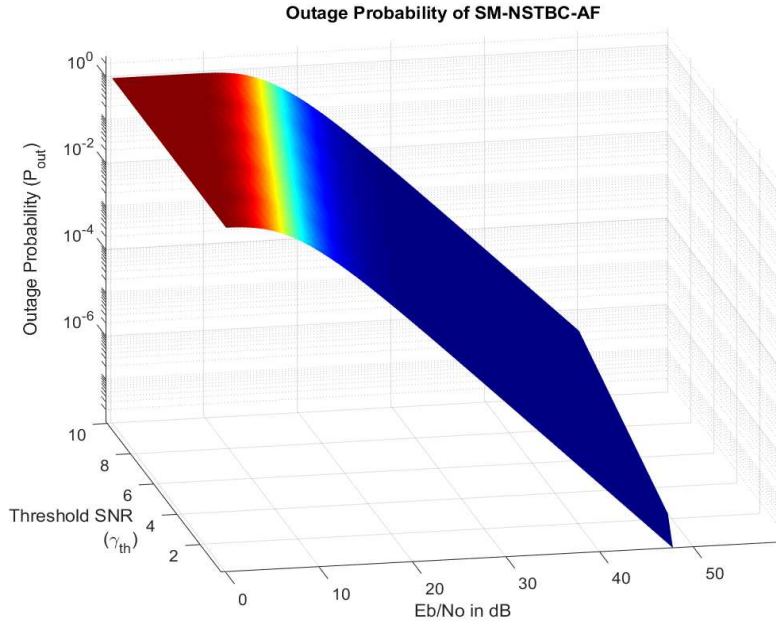

Figure 5.2 Outage Probability of the proposed SM-NSTBC-AF scheme

Figure 5.2 gives the 3D plot of outage probability for the proposed SM-NSTBC-

AF scheme. Where, X-axis represents the average signal to noise ratio (SNR), Y-axis portrays the threshold SNR and Z-axis shows the outage probability of the system. The value of γ_{th} varies from 0 dB to 10 dB. The antenna selection error at higher values of SNR is less, hence the outage probability performance is improved.

5.6 Simulation Results
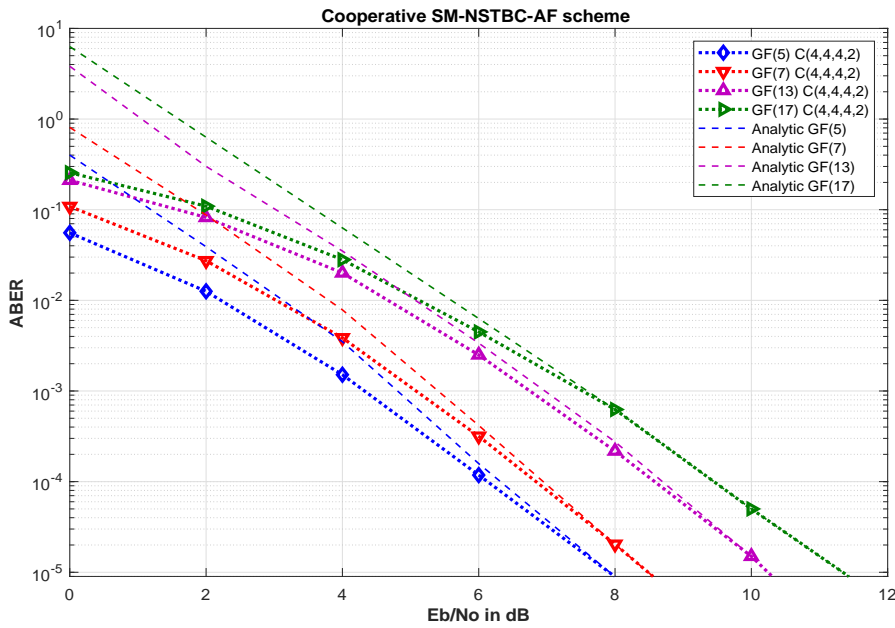
Figure 5.3 ABER performance of cooperative SM-NSTBC-AF scheme for $(N_s = 4, N_d = 4, N_{re} = 4, N_a = 2)$ over $q = 5, 7, 13, 17$.

This section demonstrates the Monte-Carlo simulation results of the proposed SM-NSTBC-AF scheme for different values of N_s and N_a. All performance comparison are carried out for a ABER value of 10^{-5}. Monte Carlo simulations reveal that for a Rayleigh fading channel and at a given value of spectral efficiency, the proposed cooperative SM-NSTBC scheme outperforms cooperative STBC-SM schemes, cooperative SM and conventional SM-NSTBC schemes by ~ 3 dB, ~ 5 dB and ~ 2 dB respectively. The notation of $C(N_s, N_d, N_{re}, N_a)$ is used throughout the chapter to represent a proposed SM-NSTBC-AF scheme where N_s represents the number of source antenna, N_d denotes the number of destination antenna, N_{re} denotes the number of relay antenna

and N_a represents the number of active antenna at source.

In Figure 5.3, the ABER plots of cooperative SM-NSTBC with $N_s = 4$, $N_d = 4$ and $N_a = 2$ configuration and $N_{re} = 4$ has been depicted. A theoretical upper bound is shown in order to verify the correctness of the Monte-Carlo simulations. A close correspondence between the Analytical upper bound and simulation results is observed for SNR value of 6 dB and above. Simulation results are demonstrated for codewords obtained over $GF(5), GF(7), GF(13)$ and $GF(17)$. The spectral efficiency achieved for a system which utilizes $C(N_s = 4, N_d = 4, N_{re} = 4, N_a = 2)$ is 2.25 bpcu for $q = 5$, 2.75 bpcu for $q = 7$, 3.5 bpcu for $q = 13$, and 4.0 bpcu is obtained for $q = 17$.
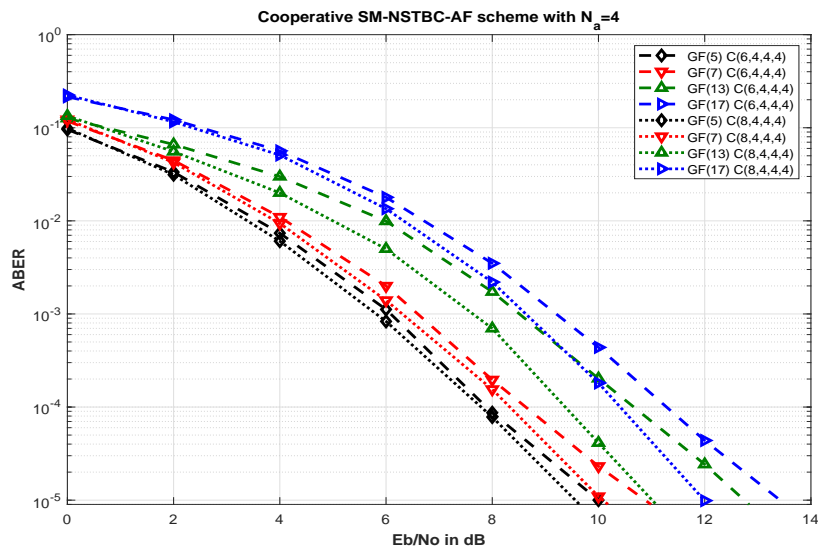
Figure 5.4 ABER performance of cooperative SM-NSTBC-AF for $q = 5, 7, 13, 17$ for $(N_s = 6, N_d = 4, N_{re} = 4, N_a = 4)$ and $(N_s = 8, N_d = 4, N_{re} = 4, N_a = 4)$.

Figure 5.4, demonstrates the simulation results for a proposed cooperative SM-NSTBC-AF system which employs $C(6, 4, 4, 4)$ and $C(8, 4, 4, 4)$ antenna configurations. The codes derived from extension fields $GF(q), q = 5, 7, 13, 17$ which yields a spectral efficiencies of 4.5 bpcu, 5.5 bpcu, 7 bpcu and 8.0 bpcu respectively. When the constellation is dense, the additional diversity provided by the increased number of transmit antennas in the $C(8, 4, 4, 4)$ scheme over the $C(6, 4, 4, 4)$ scheme yields a significant improvement in ABER performance.
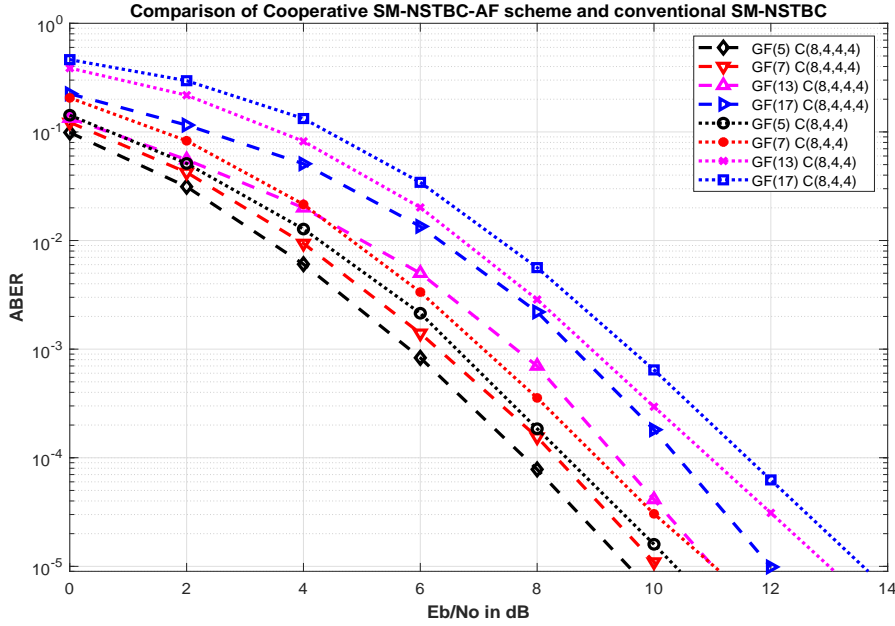
Figure 5.5 ABER performance comparison of SM-NSTBC $(N_s = 8, N_d = 4, N_a = 4)$ and cooperative SM-NSTBC-AF scheme with $(N_s = 8, N_d = 4, N_{re} = 4, N_a = 4)$ for $q = 5, 7, 13, 17$.

In Figure 5.5, the comparison of conventional SM-NSTBC scheme with the proposed SM-NSTBC-AF is shown. The simulation results demonstrate that the proposed SM-NSTBC-AF scheme achieves a performance improvement of approximately 1 dB with codewords derived over $GF(5)$, $GF(7)$ and a performance improvement of ~ 2 dB over $GF(13)$ and $GF(17)$. The spectral efficiency achieved by both the schemes is same for codewords over $GF(q)$ for $q = \{5, 7, 13, 17\}$ i.e., 4.5 bpcu, 5.5 bpcu, 7 bpcu and 8 bpcu respectively.

Figure 5.6, shows the ABER comparison of the cooperative SM-NSTBC-AF with cooperative SM and cooperative STBC-SM with AF relaying. This scheme of cooperative STBC-SM is designed by incorporating STBC-SM as given in [Basar et al. (2011)] and by adding suitable cooperative AF relaying technique. Similarly cooperative SM is designed as given in [Mesleh et al. (2008)]. The cooperative STBC-SM scheme and cooperative SM scheme achieves a spectral efficiency of 5 bpcu. The spectral efficiency of the proposed scheme achieves 5.5 bpcu for the codewords derived over $GF(7)$. It is
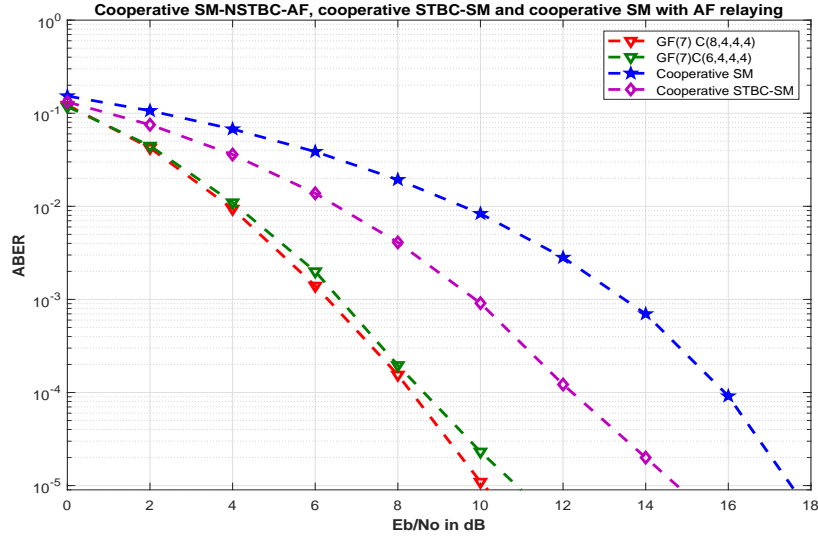
Figure 5.6 ABER performance comparison of cooperative STBC-SM, cooperative SM at 5 bpcu and proposed SM-NSTBC-AF with spectral efficiency of 5.5 bpcu.

observed that the proposed cooperative SM-NSTBC scheme achieves a significant improvement of approximately 3 dB and 5 dB over cooperative STBC-SM and cooperative SM schemes respectively.

5.7 Summary

In this chapter, the concept of cooperative amplify-and-forward communication for a class of SM-NSTBC schemes and their performance over Rayleigh fading environment has been designed and studied. The cooperative amplify-and-forward technique which we have considered possess single relay with N_{re} nodes. In addition to the relayed dual-hop link, a direct link between source and destination is also considered. The performance of two SM-NSTBC-AF setups, namely $C(N_s, 4, 4, 4)$ $(N_s = 6, 8)$ and $C(4, 4, 4, 2)$ has been studied. The outage probability for the proposed scheme is also evaluated. An analytical upper bound on the Average Bit Error Rate (ABER) under conditions of Rayleigh fading has been determined. Monte-Carlo simulations have been carried out to quantify the performance of these codes. It is observed that proposed scheme outperforms cooperative STBC-SM schemes by ~ 3 dB and show a performance improvement of ~ 2 dB over conventional SM-NSTBC scheme. From the simulation results, it can

be inferred that the proposed cooperative SM-NSTBC can be used as an alternative to existing non orthogonal systems. The proposed schemes could be employed to ensure integrity of information transfer in technologies such as communication links based on unmanned aerial vehicle (UAV), high altitude platforms (HAP) and any communication application involving a relay based MIMO scheme.

The next chapter discusses, the implementation of proposed SM-NSTBC scheme in practical scenarios. High Altitude Platforms have recently gained attention because they can be conveniently located and deployed to enable high data rates and reliable communication. The propagation channel of HAP differs from traditional cellular environment. In the next chapter the channel parameters and system model of HAP communication link has been discussed. Further the performance of the proposed scheme is analyzed for a spatially correlated scenario with Imperfect Channel State Information (Imp-CSI).

Chapter 6

Performance of SM-NSTBC and variants for High Altitude Platform environment

[1], [2] In this chapter, the design and model of a High Altitude Platform (HAP) communication system is presented. High Altitude platforms can support systems that can provide quick deployment with the convenience of relocation, quick service and can provide high quality of service. The performance of SM-NSTBC scheme for High Altitude Platform (HAP) communication systems is designed and analyzed. In order to obtain higher spectral efficiencies in terms of data rate, NSTBC schemes have been devised. SM-NSTBC gives an improvement in the ABER performance of ~ 3 dB as compared to other conventional STBC-SM schemes given in literature. Monte Carlo simulations have been performed to validate the results. Furthermore, the performance is analyzed for a correlated High Altitude Platform (HAP) MIMO system in the presence of Perfect and Imperfect Channel State Information (Imp-CSI) availability. It is observed that the proposed SM-NSTBC scheme has a higher BER performance in comparison to conventionally existing STBC-SM and SM-OSTBC schemes. Monte-Carlo simulations have been performed to validate the claims.

---

[1]Godkhindi Shrutkirthi S., et al., A MIMO SM-NSTBC scheme for High Altitude Platform communication systems: Study and Analysis.". 6th International Conference on Signal Processing and Integrated Networks (SPIN-2019), IEEE

[2]Godkhindi Shrutkirthi S., et al.,"Performance of SM-NSTBC for correlated HAP fading channels with Imperfect-CSI. ", International Conference on Optical and Wireless Technologies (OWT-2019), Springer proceedings

6.1 Introduction

The primary objective of mobile communication systems is to provide uninterrupted services over a large coverage area. With the proliferation of smart phone usage in every section of society, there is a huge demand for very high data rates along with high quality of service (QoS) even at every corner/edge of the cell boundary. Meeting this demand for high data transfer speeds is a challenging task as there are severe constraints on the bandwidth that is available to a service provider. Providing QoS along with high data transfer rates in areas such as remote localities, highly crowded gatherings, regions characterized by shadowing due to natural or man made obstructions, locations where people gather temporarily (like stadiums) is highly challenging. Deploying an additional temporary base station in these areas is not a cost effective or a practical choice. One of the easiest means to overcome these challenges is to employ High altitude platforms (HAPs), as it has been determined that repeaters mounted on HAPs are an effective solution to the problem of assuring high data rates with appropriate QoS values [Mohammed et al. (2011)]. Due to the quick restoration feature of HAPs, they have been proven to be one of the most effective makeshift frameworks for next generation wireless systems. The use of HAPs as Air to Ground (A-to-G) communication link has the potential to provide extensive support for wide applications such as intelligent transport systems, provision of high rate data transfer in moving trains (high speed platforms), navigation applications, military use, provision of relief in emergency conditions such as earth-quake or floods and temporary arrangements in stadiums where a huge crowd is expected for a very limited amount of time [Zajic (2012)]. HAPs allow quick deployment as base stations and also as "airborne cellular links". Some of the examples of existing HAPs are "Google balloon" from Google and "Internet from sky" of Facebook.

Accurate characterization of the channel model is one of the key features in establishing a reliable and high speed communication link. The statistical attributes of a HAP channel plays an indispensable role in achieving high data rates. The propagation medium of a HAP link differs from conventional terrestrial cellular communication systems. To design the appropriate architecture for high speed and reliable communication,

(a)　　　　　　　　　　　　　　(b)
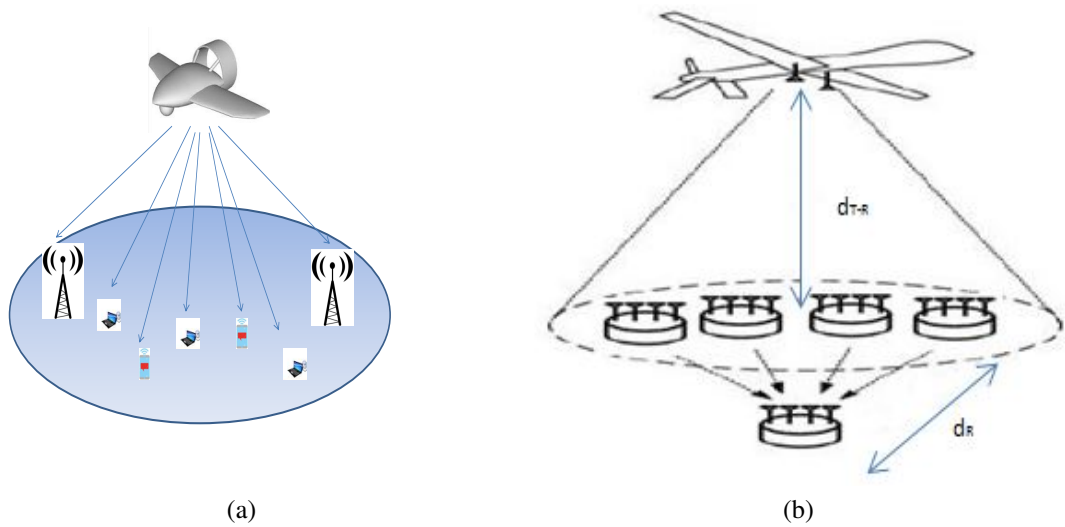
Figure 6.1 HAP-MIMO communication link

an in-depth understanding of channel parameters influencing the HAP link is desired. The HAP communication link is mainly affected by three effects, namely, reflection, diffraction and scattering. These disruptions are created by the presence of tall buildings, mountains, trees and other environmental factors [Zajic (2012)]. This leads the transmitted signal to undergo different delays, rapid variations in terms of amplitudes and phase, causing a composite multipath signal to be received at the receiving end.

HAP-MIMO has wide range of advantages since it allows elevated connectivity in regions where conventional mobile connections may not provide high efficiency and reliability. HAP communication is a cost effective technique which possesses the advantages of easy installation and fast access [Mozaffari et al. (2019)]. Incorporating MIMO techniques enhances the usage of HAP in terms of both capacity and coding gain. Another important benefit that exists by employing SM-MIMO system is energy efficiency. Therefore, the design and synthesis of energy efficient schemes that can provide useful BERs under conditions of severe channel fading is an important requirement expected of modern wireless (5G) communication systems.

In this chapter the Spatially modulated Non-orthogonal Space Time Block Codes derived from full rank Cyclic codes is designed and evaluated for the HAP-MIMO

environments. The major contribution of this chapter is as follows:

- The design of a HAP environment is explored. The HAP channel is composed of both Line-of-Sight (LoS) and Non-Line-of-Sight (NLoS) components. The channel parameters also depend on the distance of HAP from the ground surface, the angle of departure and arrival of the signal.

- The BER performance of full rank SM-NSTBC is analyzed and compared with STBC-SM and SM-OSTBC.

- Further the scenario of Imperfect Channel State Information in considered. It is observed that the proposed SM-NSTBC out performs SM-OSTBC and STBC-SM systems in both Perfect as well as Imperfect CSI environments.

Notation: Throughout this paper, matrices and vectors are represented by bold uppercase and lowercase alphabets. Table 6.1 provides the list of all abbreviations and notations used in this chapter.

Table 6.1 Abbreviations and Notations

		$\mathbf{X}$	Transmitted matrix
UAV	Unmanned Ariel Vehicle	$\mathbf{Y}$	Received matrix
HAP	High Altitude Platform	$\mathbf{H}$	Channel Matrix
LoS	Line of Sight	K	Rician factor
NLoS	Non-line of Sight	θ_A	Angle of Arrival
SM	Spatial Modulation	θ_D	Angle of Departure
NSTBC	Non-orthogonal Space Time Block Code	λ	Wavelength of signal
GF	Galois Field	d_R	Antenna spacing in the receiver array
CSI	Channel State Information	d_{T-R}	Antenna spacing between Tx and Rx antenna
Imp-CSI	Imperfect Channel State Information	η	Spectral Efficiency
ABER	Average Bit Error Rate	$\mathbf{R}_{Rx}$	Receiver correlation matrix
ML	Maximum Likelihood	$\mathbf{R}_{Tx}$	Transmitter correlation matrix
PEP	Pairwise Error Probability	$\tilde{\mathbf{H}}$	Estimated channel matrix
		$\mathbf{e}$	Channel estimation error matrix

6.2   System Model

A HAP-MIMO communication system with N_t transmit antennas, N_a active transmit antennas and N_r receive antennas is considered in our analysis. The main difference in HAP-MIMO communication and conventional terrestrial communication is the existence of line of sight (LoS) communication path. A slow varying, flat fading scenario is used to model the LoS component of HAP-MIMO communication system. The received signal has the form as given in Equation (6.1).

$$\mathbf{Y} = \mathbf{HX} + \mathbf{n} \tag{6.1}$$

where, $\mathbf{X}$ represents the transmitted vector such that $\mathbf{X} \in \mathscr{C}^{N_t \times T}$, the received signal is given by $\mathbf{Y}$ such that $\mathbf{Y} \in \mathscr{C}^{N_r \times T}$, $\mathbf{H}$ is the channel matrix of HAP-MIMO communication and $\mathbf{n}$ is the circularly symmetric complex independent and identically distributed Gaussian noise with zero mean and unit variance $C\mathscr{N}(0,1)$. The channel matrix $\mathbf{H}$ is described in the following sub-section.

6.2.1   Channel Model

The signal obtained at the receiver is the envelope created by the superposition of both line of sight (LoS) and non-line of sight (NLoS) components. The near optimum estimate of HAP channel obtained by approximating its CDF and PDF resembles the Rician distribution [Zajic (2012)]. The channel matrix of the HAP-MIMO system is given by [Cho et al. (2010), Sudheesh et al. (2018)].

$$\mathbf{H} = \sqrt{\frac{K}{1+K}}\mathbf{H}_{LoS} + \sqrt{\frac{1}{1+K}}\mathbf{H}_{NLoS} \tag{6.2}$$

where $\mathbf{H}$ is a $N_r \times N_t$ channel matrix, with $\mathbf{H}_{LoS}$ representing the line of sight component (free space propagation loss). $\mathbf{H}_{NLoS}$ represents the non-line of sight paths and K represents the Rician factor which is given by Equation (6.3).

$$K = \frac{\sigma^2_{LoS}}{\sigma^2_{NLoS}} \tag{6.3}$$

here, σ_{LoS}^2 is the power of LoS and σ_{NLoS}^2 is the power of NLoS components. The $\mathbf{H}_{NLoS}$ matrix possesses channel coefficients due to the existence of non-line of sight components, the effects of scattering, diffraction and reflections make the channel Rayleigh distributed. While $\mathbf{H}_{LoS}$ describes the line of sight component which depends on several parameters such as Angle-of-Arrival (AoA) of the signal at receiving end, Angle-of-Departure (AoD) at the transmitter. Considering the above statistical parameters the $\mathbf{H}_{LoS}$ matrix is defined as follows [Sudheesh et al. (2018)].

$$
H_{LoS} = \begin{bmatrix} 1 \\ e^{j2\pi\frac{d_R}{\lambda}\sin(\theta_A)} \\ \vdots \\ e^{j2\pi\frac{d_R}{\lambda}(M-1)\sin(\theta_A)} \end{bmatrix} \begin{bmatrix} 1 \\ e^{j2\pi\frac{d_{T-R}}{\lambda}\sin(\theta_D)} \\ \vdots \\ e^{j2\pi\frac{d_{T-R}}{\lambda}(N-1)\sin(\theta_D)} \end{bmatrix}^T \tag{6.4}
$$

where, λ is the wavelength of the signal, d_R is the antenna spacing in the receiver array, d_{T-R} represents the antenna spacing in the transmit and receive antenna, $M = N_r$, $N = N_t$, θ_A gives the Angle-of-Arrival and θ_D is the Angle-of-Departure.

6.2.2 Signal Model

The signal model received at the receiver is given by

$$
\mathbf{Y} = \left(\sqrt{\frac{K}{1+K}} \mathbf{H}_{LoS} + \sqrt{\frac{1}{1+K}} \mathbf{H}_{NLoS} \right) \mathbf{X} + \mathbf{n} \tag{6.5}
$$

here K is the Rician factor as defined in Equation (6.3). In case of transmit and receive correlation the channel matrix is considered as defined in Equation (6.5).

Spatial correlation: The mathematical analysis of spatial correlation can be given by Kronecker channel model [Younis (2014)]. The spatially correlated channel matrix $\mathbf{H}_c$ is given below.

$$\mathbf{H}_c = R_{Rx}^{1/2} \mathbf{H} R_{Tx}^{1/2} \qquad (6.6)$$

here R_{Tx} and R_{Rx} are transmitter correlation matrix and receiver correlation matrix, $\mathbf{H}$ represents the HAP uncorrelated channel matrix. This correlated channel matrix can also be obtained as $\mathbf{H}_c = vec(\mathbf{H})R_s^{1/2}$, here $vec(\mathbf{H})$ is vectorization of $\mathbf{H}$ and $Rs = R_{Rx} \otimes R_{Tx}$, where $\otimes$ Kronecker product [Simha et al. (2017)]. The spatial correlation between any two distinct antenna pairs depends on the product of corresponding transmit and receive correlation elements. The detailed explanation of the spatial correlation model which is being employed is described in Chapter 4.

6.2.3 Imperfect Channel Scenario

In practical scenarios, the channel conditions are not available at the receiver. Here we have considered complete imperfect channel scenario [Alsmadi et al. (2018), Mesleh and Ikki (2012)]

$$\mathbf{H} = \tilde{\mathbf{H}} + \mathbf{e} \qquad (6.7)$$

here, $\tilde{\mathbf{H}}$ is the estimated channel matrix at the receiver and $\mathbf{e}$ is the channel estimation error matrix. The coefficient $e_{i,j} \sim C\mathcal{N}(0, \sigma_e^2)$, is the channel estimation error between j^{th} transmit antenna and i^{th} receiver antenna.

The performance of SM-NSTBC is compared with STBC-SM and SM-OSTBC over HAP-MIMO environment is demonstrated and is shown in section 6.3. The brief description of conventional STBC-SM and SM-OSTBC system models are as follows.

STBC-SM: The basic idea of Space time block coded spatial modulation was presented by [Basar et al. (2011)]. In STBC-SM, Alamouti's STBC is incorporated in the spatial domain. The on/off status of antenna carries information as a key property of Spatial Modulation (SM) and information is transmitted through STBC. It is further generalized for any number of transmit antennas. The performance improvement is achieved by utilizing the diversity advantage and improvement in the spectral efficiency is achieved by the additional information bits that are conveyed by the antenna selection pattern.

SM-OSTBC: The codewords employed in Spatially Modulated Orthogonal Space Time Block Codes (SM-OSTBC) are obtained by multiplying orthogonal space time block codes with spatial constellations [Le et al. (2014)]. This allows the SM-OSTBC to fulfill the property of non-vanishing determinant which adds up in achieving a transmit diversity of second order.

The following section gives the performance of SM-NSTBC, STBC-SM and SM-OSTBC for uncorrelated and correlated HAP-MIMO environment.

6.3 Simulation results

In this section, HAP-MIMO system performance is evaluated through Monte-Carlo simulations. The results presented in this section are for a frequency of 48 GHz. As the distance of HAP is very high from the ground node ($\sim$17 to 22 km) for communication, the value of Angle-of-Arrival and Angle-of-Departure are considered to be in between $10° - 30°$ as mentioned in [Sudheesh et al. (2018)]. In our simulations, the performance analysis of SM-NSTBC, STBC-SM and SM-OSTBC schemes are compared for an effective BER of 10^{-5}. Further, the system representation of SM-NSTBC is given in the form $C(N_t, N_r, N_a)$. Where N_t, N_r, N_a are the number of transmit, receive and active antennas respectively in the same order.

Figure 6.2 shows the performance of SM-NSTBC, with $C(N_t = 4, N_r = 4, N_a = 2)$. The codewords obtained over $GF(q), q = 5, 7, 13, 17$ yields a spectral efficiency (η) of 2.322 bpcu, 2.807 bpcu, 3.701 bpcu and 4.087 bpcu respectively. Here, perfect channel state information is assumed (CSIR) and the channel considered is quasi-static flat uncorrelated HAP environment. Similarly in Figure 6.3, the spectral efficiency can be increased by increasing the number of active antennas. The antenna configuration shown in figure 6.3 is denoted by $C(N_t = 6; N_r = 4; N_a = 4)$ over $GF(q), q = 5; 7; 13; 17$. which yields a spectral efficiency of $\eta = 4.643$ bpcu, 5.614 bpcu, 7.4 bpcu and 8.17 bpcu respectively.

The ABER analysis for SM-NSTBC over $GF(7)$, employing $C(6, 4, 4)$ and $C(8, 4, 4)$ yields a spectral efficiency of $\eta = 5.6$ bpcu. The conventional SM-OSTBC [Le et al.
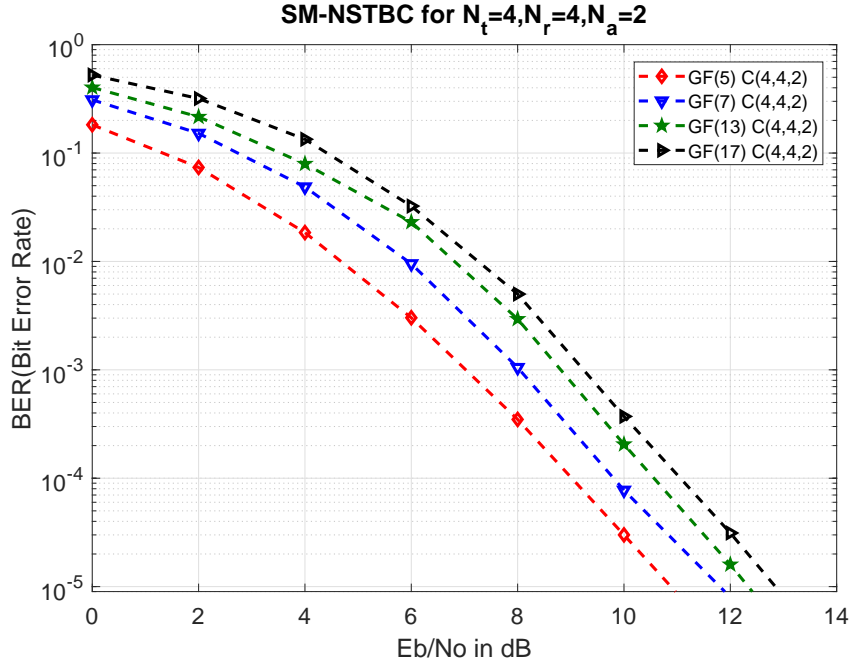
Figure 6.2 BER performance of SM-NSTBC for HAP-MIMO, with $(N_t = 4; N_r = 4; N_a = 2)$ with $\eta = 2.322$ bpcu, 2.807 bpcu, 3.701 bpcu and 4.087 bpcu respectively.

(2014)] scheme with $N_t = 16$, $N_r = 4$ and $N_a = 4$ produces a spectral efficiency of $\eta = 6$ bpcu and STBC-SM with the configurations of $N_t = 4$, $N_r = 4$ and $N_a = 2$ employing 16-QAM produces a spectral efficiency of $\eta = 5$ bpcu have been compared in Figure 6.4. It is observed that SM-OSTBC achieves $\eta = 6$ bpcu but the total number of transmit antennas required to achieve this spectral efficiency is 16, which is very large as compared to SM-NSTBC which requires only 6 transmit antennas to achieve a total of 5.6 bpcu. A BER performance improvement of ~ 3 dB over SM-OSTBC and ~ 5 dB in comparison to STBC-SM systems is achieved over a HAP-MIMO environment.

In Figure 6.5, the ABER performance of SM-NSTBC and SM-OSTBC schemes have been compared. The proposed scheme uses $C(6, 4, 4)$ and $C(8, 4, 4)$ antenna configurations to produce a spectral efficiency of $\eta = 7.4$ bpcu (using $GF(13)$ Gaussian map). On the contrary to obtain a spectral efficiency of 7.5 bpcu the SM-OSTBC scheme utilizes $C(10, 4, 4)$ configurations. It can be clearly observed that our proposed SM-NSTBC scheme has a higher coding gain of ~ 4.5 to 5 dB in comparison to SM-OSTBC scheme over a HAP-MIMO environment.
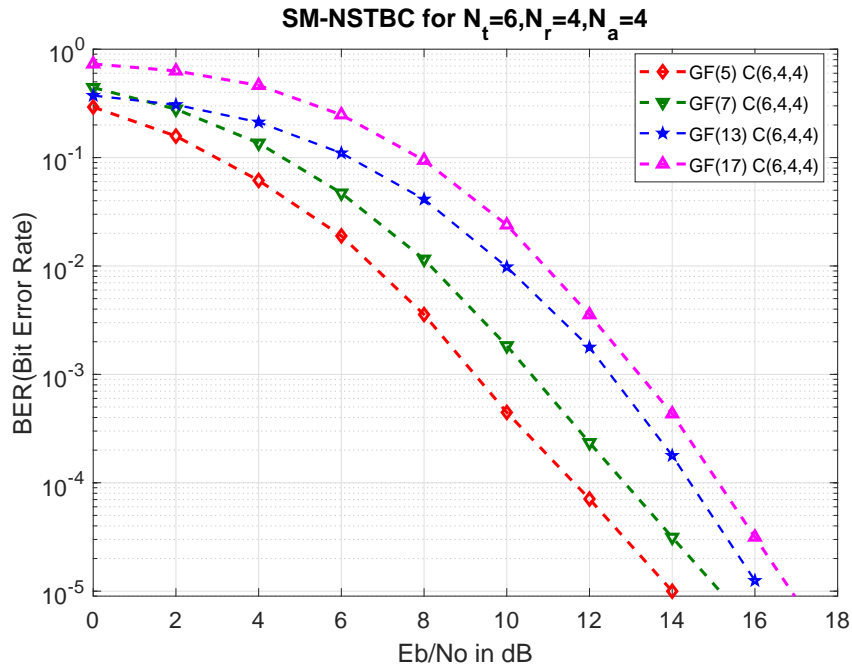
Figure 6.3 BER performance of SM-NSTBC for HAP-MIMO, with $(N_t = 6; N_r = 4; N_a = 4)$ with $\eta = 4.643$ bpcu, 5.614 bpcu, 7.4 bpcu and 8.17 bpcu respectively.
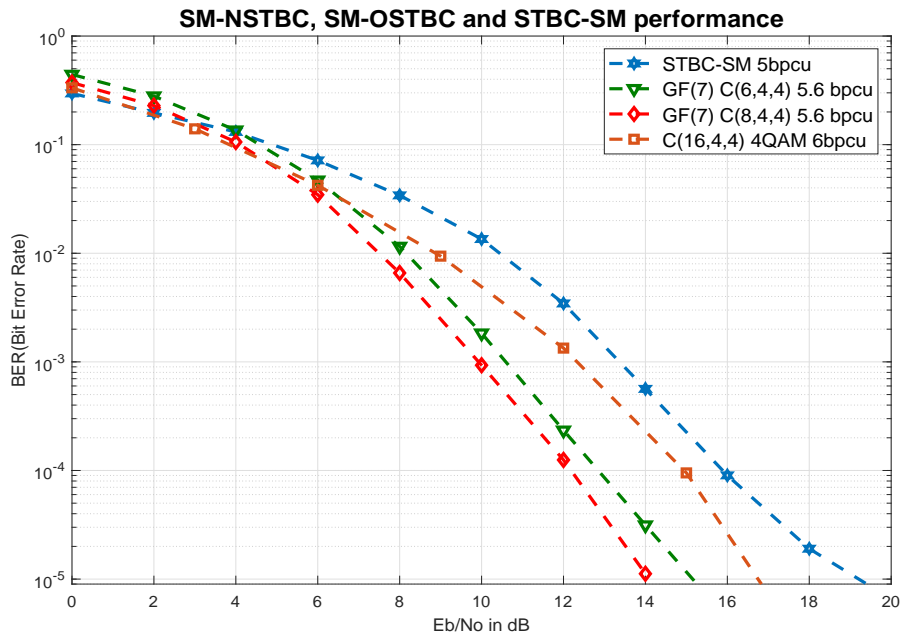

Figure 6.4 BER performance of SM-NSTBC, STBC-SM and SM-OSTBC for a spectral efficiency of 5.6 bpcu, 5 bpcu and 6 bpcu respectively.
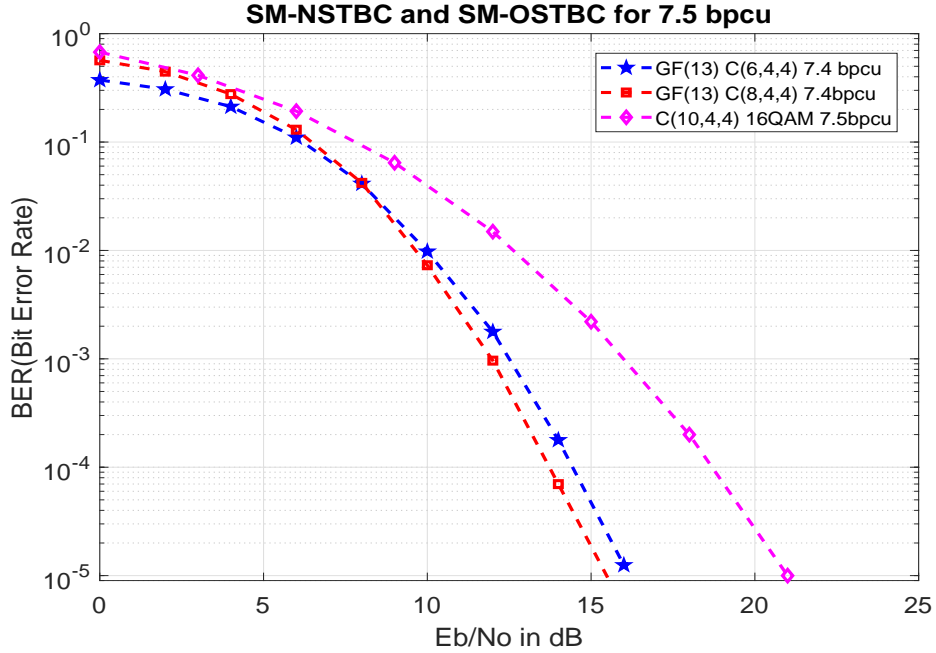
Figure 6.5 BER performance of SM-NSTBC and SM-OSTBC for a spectral efficiency of 7.4 bpcu and 7.5 bpcu respectively.

In the succeeding part of the simulation section, we consider simulations under Imperfect Channel State Information (Imp-CSI) availability over correlated fading scenario. We have considered the channel estimation error given by σ_e^2 values such that $0 \leq \sigma_e^2 \leq 0.99$. In order to understand and obtain the complete effect of Imperfect-CSI, the value of σ_e^2 is kept fixed for all values of SNR (this is assumed in order to understand the complete imperfectness of the manifested channel between source to relay and relay to destination). For spatial correlated scenario the transmit antenna spacing of 0.1λ and receiver antenna spacing of 0.5λ is considered [Mesleh et al. (2010)].

Figure 6.6 shows the performance of SM-NSTBC derived over $GF(5)$ with $C(N_t = 6, N_r = 4, N_a = 4)$ yielding a spectral efficiency of 4.643 bpcu over correlated HAP-MIMO environment for $\sigma_e^2 = 0, 0.5, 0.9$. Figure 6.7 gives the performance comparison of SM-NSTBC and STBC-SM [Basar et al. (2011)] for spectral efficiency of ($\eta = 4$) bpcu. Here we have considered two antenna configuration for the proposed SM-NSTBC scheme derived over $GF(17)$. The antenna configuration utilized here are $C(6,4,2)$ and $C(4,4,2)$. It is observed that both antenna configurations of SM-NSTBC outperforms

Performance of SM-NSTBC GF(5) with N$_t$=6 N$_r$=4 N$_a$=4
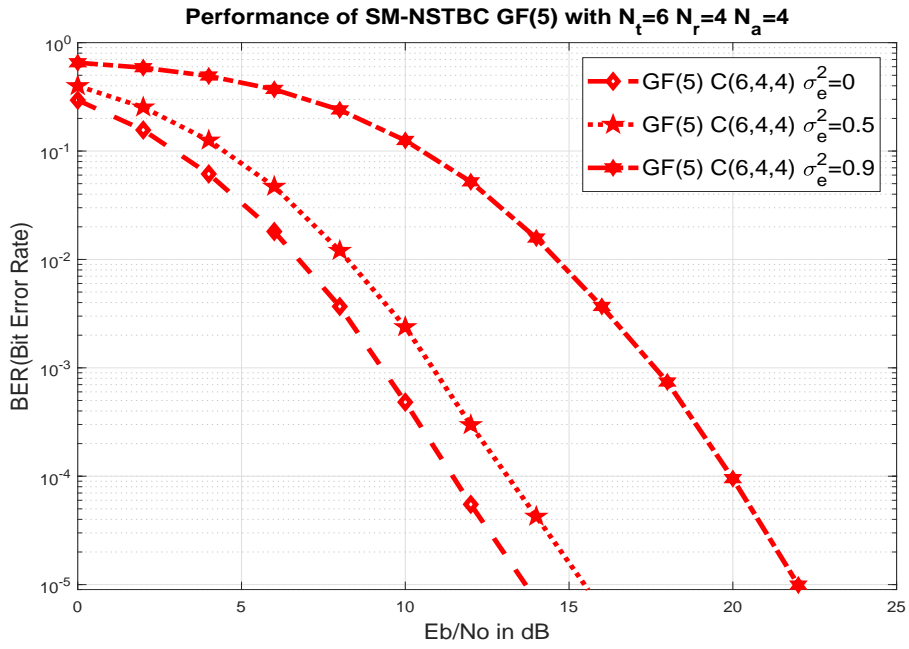
Figure 6.6 Performance of SM-NSTBC with $C(6,4,4)$ over $GF(5)$.

SM-NSTBC and STBC-SM performance
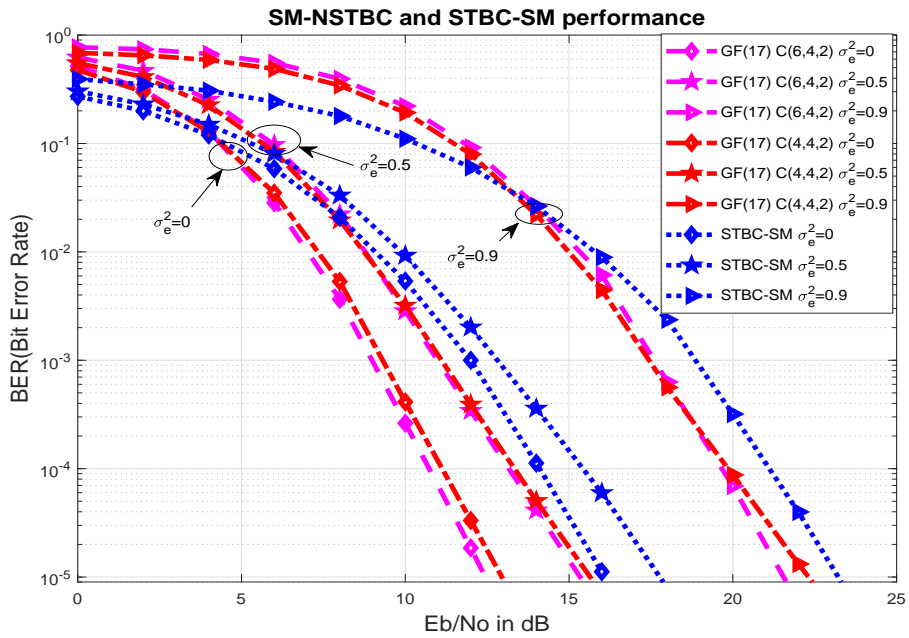
Figure 6.7 Performance of SM-NSTBC and STBC-SM for $\eta = 4$ bpcu.

STBC-SM by ~ 3 dB and ~ 2 dB over correlated HAP-MIMO environment.
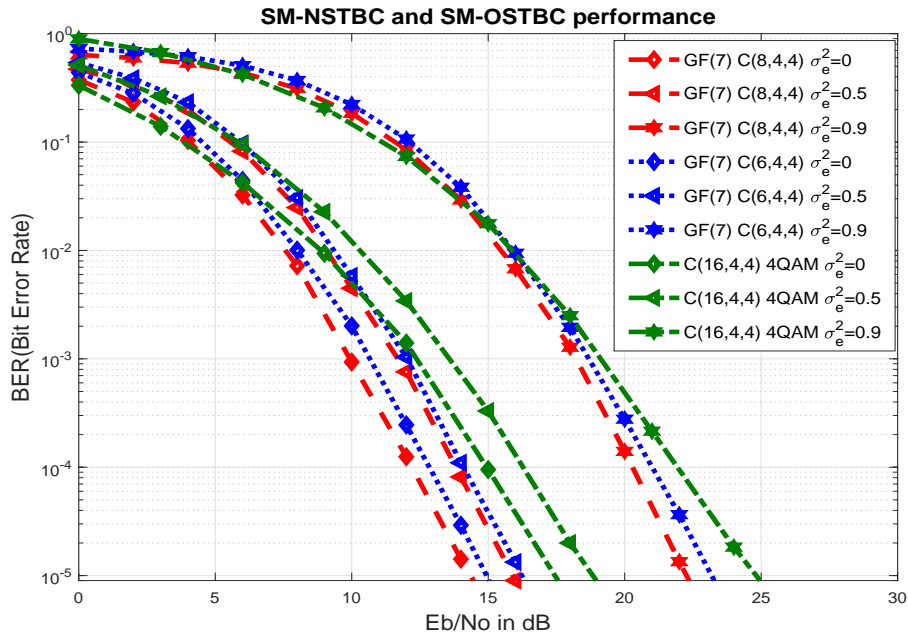
Figure 6.8 BER Performance of SM-NSTBC for $\eta = 5.5$ and SM-OSTBC for $\eta = 6$ bpcu.
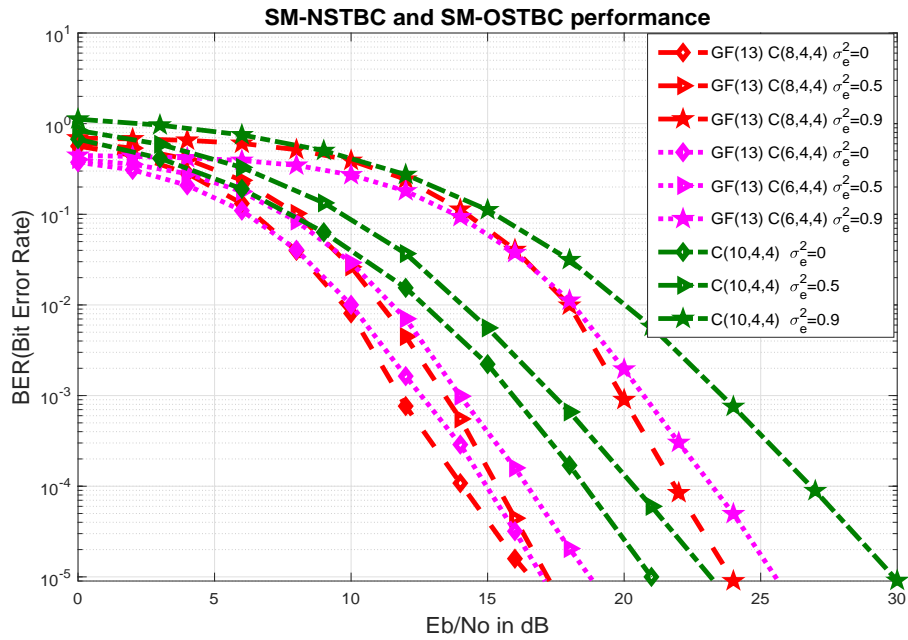
Figure 6.9 Performance of SM-NSTBC and SM-OSTBC for $\eta = 7.5$ bpcu.

In Figure 6.8, the performance of proposed scheme is compared with SM-OSTBC scheme [Le et al. (2014)]. The antenna configuration used for proposed scheme is

$C(8,4,4)$ and $C(6,4,4)$ and the codewords are derived over $GF(7)$. In Figure 6.8, SM-OSTBC attains $\eta = 6$ bpcu for $N_t = 16$ which is very large when compared to proposed SM-NSTBC which utilizes only $N_t = 6$ to achieve $\eta = 5.6$ bpcu and a performance improvement of about ~ 3 dB is observed.

In Figure 6.9, SM-NSTBC yields a spectral efficiency of $\eta = 7.4$ bpcu by incorporating the codewords derived over $GF(13)$ and the SM-OSTBC achieves $\eta = 7.5$ with antenna configuration of $C(10,4,4)$. The proposed SM-NSTBC outperforms SM-OSTBC by approximately 4 dB with $\sigma_e^2 = 0$ and by 6 dB when $\sigma_e^2 = 0.9$. From figure 6.8 and figure 6.9, it can be noted that SM-NSTBC gives a performance improvement over SM-OSTBC by approximately 5dB and approximately 3 dB over highly correlated HAP-MIMO scenario for varying values of spectral efficiency. It is observed that proposed scheme outperforms existing STBC-SM and SM-OSTBC scheme due to the additional structure of codeword design.

Table 6.2 gives the performance comparison of various schemes over correlated fading environment at BER value of 10^{-5}.

Table 6.2 BER comparison values for various scheme with varying values of σ_e^2

η	Scheme	$\sigma_e^2 = 0$	$\sigma_e^2 = 0.5$	$\sigma_e^2 = 0.9$
$\eta = 4$	SM-NSTBC	13 dB	16 dB	22 dB
	STBC-SM	16.5 dB	18.5 dB	23.5 dB
$\eta = 7.5$	SM-NSTBC	17 dB	18.5 dB	26 dB
	SM-OSTBC	21 dB	23 dB	30 dB

6.4 Summary

In this chapter a High Altitude Platform (HAP) MIMO channel is modeled. The performance of full rank SM-NSTBC is proposed to provide reliable communication over a uncorrelated and correlated HAP-MIMO environment. In order to estimate the performance of these proposed codes, Monte-Carlo simulations have been performed over

HAP-MIMO environment. It is observed that, the proposed SM-NSTBC achieves a superior performance of at least 3 dB over SM-OSTBC and STBC-SM schemes for varied spectral efficiencies. Further the correlated HAP-MIMO channel is considered with Imperfect Channel State Information (Imp-CSI). A performance improvement of approximately 2 to 5 dB is observed as compared to SM-OSTBC and STBC-SM for varying spectral efficiencies and for varied values of Imp-CSI. We conclude that, this is another promising technology which can be implemented in future wireless technologies.

Research work carried out till this chapter concentrate on the design of several SM-NSTBC schemes. We have employed the full rank Cyclic codewords to obtain codeword matrices satisfying the full rank property. In the next chapter, we further propose novel implementation and design issues of Space Time (ST) designs derived from the class of Abelian codes. In the succeeding chapter, we have first presented the transform domain characteristics of Abelian codes, followed by a brief description of the rank-distance properties of these codes. Later, the process that needs to be followed to derive full rank codes from the general class of Abelian codes has been discussed. Finally, STBC designs are extracted from certain specified Abelian codes and their performance over wireless channels is quantified.

Chapter 7

A framework for design of full rank NSTBCs from Abelian codes

In this chapter, we have designed a framework which enables the user to design full rank NSTBCs starting from the class of Abelian codes. Cyclic codes are the subclass of Abelian codes. We have initiated the chapter with a brief description of the transform domain characterization of Abelian codes. This description is used to specify a sequence of steps that yields full rank Abelian codes over any base field. The n-length full rank Abelian codes are designed over $GF(q^m)$, where q is a prime and m is order of the field extension. These can also be viewed as $m \times n$ matrices over the base field $GF(q)$. By applying suitable puncturing, the $m \times n$ full rank codeword matrices are transformed into $m \times m$ matrices over the base field $GF(q)$. These $m \times m$ codeword matrices are mapped to complex number field to obtain full rank NSTBCs. A class of Spatially Modulated Non-orthogonal Space Time Block Codes derived from full rank Abelian codes is presented in this chapter. The analytical upper bound is also derived for the proposed scheme. The proposed scheme achieves a performance improvement of minimum 2 dB as compared to competing schemes such as STBC-SM and SM-OSTBC. The proposed Abelian SM-NSTBC provides a performance improvement of ~ 1 dB when compared with Cyclic SM-NSTBC.

7.1   Introduction

Abelian codes are a class of codes which contain Cyclic codes as a sub-class. It is known that every Abelian group can be expressed as a direct product (cartesian product)

of its constituent Cyclic subgroups. An Abelian code is an ideal of the group algebra of an appropriate Abelian group. An Abelian code can be considered as a direct product of the r (r is an integer) constituent cyclic codes. There are two ways of representing an Abelian code namely, character representation and mixed radix representation. We have employed the mixed radix representation in this work because of its simplicity and ease of implementation. The transform domain description for Abelian codes was given by individually by [MacWilliams (1970), Rajan and Siddiqi (1992)]. [MacWilliams (1970)] presented the Character representation and [Rajan and Siddiqi (1992)] derived the Mixed radix representation.

Abelian codes can be considered as direct product of cyclic subgroups. An Abelian code can be represented as product of r consecutive Cyclic codes. Consider a Abelian code constructed as a direct product of cyclic groups $C_0, C_1, \ldots, C_{r-1}$ Cyclic codes where $m_0, m_1, \ldots, m_{r-1}$ denote the order of $C_0, C_1, \ldots, C_r - 1$ respectively. Then the order of Abelian code is defined as $n = m_0 m_1 \cdots m_{r-1}$. The following sub-section gives a brief description of mixed radix representation of Abelian code.

7.1.1 Mixed radix Representation

Let $m_0, m_1, \cdots, m_{r-1}$ be defined as positive integers called as Mixed radixes and n be defined as their product. Thus, $n = m_0 m_1 \cdots m_{r-1}$. Then, any integer i, $(0 \leq i \leq (n-1))$ can be expressed as

$$i = i_0 + i_1(m_0) + i_2(m_0 m_1) + \cdots + i_{r-1}(m_0 m_1 \cdots m_{r-1}) \tag{7.1}$$

Here, $0 \leq i \leq (n-1)$ and $0 \leq i_k \leq m_k - 1$, $k = 0, 1, \cdots, (r-1)$. The integer i is represented by $i = < i_0, i_1, \cdots, i_{r-1} >$ in Mixed radix representation. Throughout this chapter it is assumed that $gcd(n, q) = 1$.

[Berman (1967)] observed that a particular class of Abelian codes provides improved error performance than the class of Cyclic codes of same length, as it has better error correction ability. This has inspired us to investigate the performance of full rank codes derived from Abelian codes when employed as Non-orthogonal Space Time Block structure.

The remaining part of the chapter is organized as follows: Section 7.2, gives a brief description of the transform domain characterization of Abelian codes in mixed

radix representation. This is followed by a discussion of the rank-distance properties of Abelian codes. In section 7.3 the system model of the proposed SM-NSTBC designed with full rank Abelian codes is provided. Section 7.4 gives the theoretical upper bound for the proposed scheme. Simulation results are given in section 7.5. Finally, the significance of the results and the conclusions derived from this body of work are discussed in section 7.6.

Notation: Throughout this paper, matrices and vectors are represented by bold uppercase and lowercase alphabets. Other notations and abbreviations are given below in Table 7.1.

Table 7.1 Abbreviations and Notations

		$\mathscr{C}$	Abelian code
		$Rank_q(\mathscr{C})$	Rank of $\mathscr{C}$ over $GF(q)$
		$\mathscr{Z}(i)$	Gaussian Map
GFFT	Galois Field Fourier Transform	$\zeta(i)$	Eisenstein Map
IGFFT	Inverse Galois Field Fourier Transform	$\mathscr{M}_{m \times m}$	Full rank codeword matrix
STBC	Space Time Block Code	$\mathbf{X}_{SM}$	Spatially modulated codeword matrix
SM	Spatial Modulation	N_t	Number of transmit antennas
STBC-SM	Space Time Block Coded Spatial Modulation	N_r	Number of receive antennas
SM-OSTBC	Spatially Modulated Orthogonal STBC	N_a	Number of active transmit antennas
ML	Maximum Likelihood	n_s	Number of time slots
ABER	Average Bit Error Rate	$C_a(\cdot)$	Antenna configuration from Abelian code
PEP	Pairwise Error Probability	$C(\cdot)$	Antenna configuration from Cyclic code
		η	Spectral Efficiency
		$\mathbf{Y}$	Received matrix
		$\mathbf{H}$	Channel Matrix

7.2 Transform description of Abelian codes

The transform domain description of Cyclic codes as elaborated in [Moon (2005), Blahut (1983)] can directly be scaled up to obtain the transform domain description of Abelian codes as given in [Rajan and Siddiqi (1992)]. Let $\mathscr{C}$ be an n-length Abelian code obtained as the direct product of r Cyclic codes $C_0, C_1, \cdots, C_{r-1}$. Let $m_0, m_1, \ldots, m_{r-1}$ be the respective orders of Cyclic codes $C_0, C_1, \ldots, C_r - 1$. Then the length n of the code-

words corresponding to Abelian code is specified as $n = m_0, m_1, \ldots, m_{r-1}$. Any element $a \in \mathcal{C}$ in mixed radix notation is represented as $a_i = a_{<i_{r-1}, \cdots, i_1, i_0>}$. The Galois Field Fourier Transform of the $n-$length Abelian code is defined as follows.

Let $\mathbf{a} = (a_0, a_1, \ldots, a_{n-1})$ be a codeword of an Abelian code where $a_i, \in GF(q), i = 0, 1, 2, \cdots, (n-1)$. It is assumed that q is prime and $gcd(q, n) = 1$, Let m be the smallest positive integer such that $n | q^m - 1$ and $\alpha_{m_0}, \alpha_{m_1}, \cdots, \alpha_{m_{r-1}}$ be elements of order $m_0, m_1, \cdots, m_{r-1}$ in $GF(q^m)$. The Galois Field Fourier Transform (GFFT) of $\mathbf{a}$ is given by $\mathbf{A} = (A_0, A_1, \ldots, A_{n-1})$ where the $A_j, j = 0, 1, \cdots (n-1)$ are defined by Equation (7.2) [Rajan and Siddiqi (1992), Sripati and Rajan (2004)].

$$A_j = A_{<j_{r-1}, \cdots, j_1, j_0>} = \sum_{i_{r-1}=0}^{m_{r-1}-1} \cdots \sum_{i_1=0}^{m_1-1} \sum_{i_0=0}^{m_0-1} (\alpha_{m_0})^{i_0 j_0} (\alpha_{m_1})^{i_1 j_1} \cdots (\alpha_{m_{r-1}})^{i_{r-1} j_{r-1}} a_{<i_{r-1}, \cdots, i_1, i_0>}$$

(7.2)

Here $\alpha_{m_0}, \alpha_{m_1}, \cdots, \alpha_{m_{r-1}}$ represents the primitive elements of order $m_0, m_1, \ldots, m_{r-1}$. The Inverse Galois Field Fourier Transform is defined as given below [Rajan and Siddiqi (1992)].

$$a_i = a_{<i_{r-1}, \cdots, i_1, i_0>} = \sum_{j_{r-1}=0}^{m_{r-1}-1} \cdots \sum_{j_1=0}^{m_1-1} \sum_{j_0=0}^{m_0-1} (\alpha_{m_0})^{-i_0 j_0} (\alpha_{m_1})^{-i_1 j_1} \cdots (\alpha_{m_{r-1}})^{-i_{r-1} j_{r-1}} A_{<j_{r-1}, \cdots, j_1, j_0>}$$

(7.3)

7.2.1 Rank-distance properties of Abelian codes

Similar to the description of Cyclic code, any $n-$length Abelian code over $GF(q^m)$ can also be viewed as a $m \times n$ matrix over $GF(q)$. The rank of $n-$length Abelian code over $GF(q^m)$ is identified with the rank of obtained $m \times n$ matrix over $GF(q)$. In this subsection the rank-distance property of Abelian codes given [Sripati and Rajan (2004)] are presented.

Theorem 1: Let $\mathcal{C}$ be a Abelian code of length n over $GF(q^m)$ with $A_{<0,0,\ldots,0>}$ being one of the free transform domain components. Then $Rank_q(\mathcal{C}) = 1$.

It can be proved by the definition of transform domain, when $A_{<0,0,\ldots,0>}$ is the only free transform domain component yields a repetition code of form $(x, x, \cdots, x)$ for $x = A_{<0,0,\ldots,0>}$.

Theorem 2 [Sripati and Rajan (2004)]: Consider $\mathcal{C}$ to be a an Abelian code of

114

over $GF(q^m)$. Let $A_{<j_{r-1}q^s,\cdots,j_1q^s,j_0q^s>} \in A_{[j]}$, $(|[j]| = e_j, \ 0 \le s \le e_j - 1)$ be a single free transform domain component and all other transform components be constrained to zero, then the $Rank_q(\mathscr{C}) = e_j$. Here, e_j is order of the q-cyclotomic coset $[j]$.

When A_{jq^s} is the only free transform domain component and all other $n - 1$ components are constrained to zero, then the Inverse Galois Field Fourier Transform (IGFFT) of is described as

$$a_i = a_{<i_0,i_1,\cdots,i_{r-1}>} = \frac{1}{n \ modulo \ p} (\alpha_{m_0})^{-i_0 j_0} (\alpha_{m_1})^{-i_1 j_1} \cdots (\alpha_{m_{r-1}})^{-i_{r-1} j_{r-1}} A_{(j_{r-1},\cdots,j_1,j_0)}$$

(7.4)

By incorporating Theorem 2, we have designed a class of full rank Abelian codes. These codes have the property that when viewed as $m \times n$ matrices over $GF(q)$, all non zero codeword matrices satisfy the full rank property. The codeword construction is illustrated in the example given below.

Example 1: Consider the Abelian group, $G, |G| = n = 26$ expressed as $G = C_0 \times C_1$ where $C_0 = 2$, $C_1 = 13$. $GF(5)$ is the base field. $m = 4$ is the order of field extension. The length n of the codeword, $n|q^m - 1$, where $n = 26$. Let $A_{<1,0>}$ be a free transform domain component and all other components be constrained to zero. Here, $A_{<1,0>}$ belongs to the cyclotomic coset of $\{< 1,0 >< 5,0 >< 12,0 >< 8,0 >\}$ so we get $e_j = 4$. That is the obtained Abelian code is has full rank as $(m = e_j)$.

Codeword Construction: Incorporating theorems from [Sripati and Rajan (2004)], full rank length n Abelian codes are derived. Here, we have constructed full rank Abelian codes from two cyclic codes C_0 and C_1 over $GF(q^m)$. Here $q = \{5, 7, 13\}$ and length of Abelian codes constructed are $n = \{26, 10, 10\}$ respectively. These obtained full rank Abelian codes can be expressed in form of $m \times n$ codeword matrix. This $m \times n$ codeword matrix can be suitably punctured to obtain $m \times m$ full rank codeword matrix.

The process of puncturing depends on the order of Cyclic code considered for Abelian code construction. It is observed by computations that the obtained $m \times n$ codeword matrices when punctured alternately by every m_0 columns $(m_0 = 2)$, obtained punctured $m \times m$ matrix is a full rank. These obtained $m \times m$ codeword matrices are used in the design of NSTBC. This puncturing process is illustrated in the example below.

Example 2: Let us consider an Abelian code $\mathscr{C}$ with length $n = 10$ over $GF(7^4)$. This $\mathscr{C}$ is designed as a direct product of two Cyclic codes C_0, C_1, with orders $|C_0| = 2$ and $|C_1| = 5$. The mixed radix representation of $\mathscr{C}$ is given as $\{< i_1, i_0 > | 0 \le i_1 \le 4, 0 \le i_0 \le 1\}$.

The 7-cyclotomic coset *modulo* 10 are $\{< 0,0 >\}, \{< 0,1 >\}, \{< 1,0 >< 2,0 >< 4,0 >< 3,0 >\}, \{< 1,1 >< 2,1 >< 4,1 >< 3,1 >\}$. Let $A_{<1,0>}$ be the free transform domain component and all other component be constrained to zero. As $A_{<1,0>} \in A_{[j]}(|[j]| = 4)$ the Rank($\mathscr{C}$)=4. So the rank obtained $m \times n$ over $GF(7)$ is also 4.

In this case C_1 with order 5 also has full rank cyclotomic set in $GF(7^4)$, so when we consider columns alternately with order of $C_0 = 2$, here every second column we get full rank $m \times m$ punctured codeword matrix.

Let us consider a random non-zero codeword. The puncturing process is illustrated in the example.

The obtained punctured $m \times m$ codeword matrix has full rank property. Incorporating theorem 2 and the puncturing property, we have designed a set of $q^m - 1$ non-zero $m \times m$ full rank codeword matrices. These obtained full rank codeword matrices over $GF(q)$ are then mapped using complex number field. This mapping is performed by employing rank preserving maps (Gaussian Integer Map for $GF(5), GF(13)$ and Eisenstein Integer Map for $GF(7)$) as described in section 2.4.

$$
\begin{bmatrix}
0 & 0 & 5 & 2 & 6 & 1 & 2 & 5 & 1 & 6 \\
2 & 5 & 1 & 6 & 0 & 0 & 5 & 2 & 6 & 1 \\
1 & 6 & 5 & 2 & 6 & 1 & 4 & 3 & 5 & 2 \\
2 & 5 & 2 & 5 & 2 & 3 & 4 & 4 & 3 & 4
\end{bmatrix}
\rightarrow
\begin{bmatrix}
0 & 5 & 1 & 5 \\
2 & 1 & 0 & 2 \\
1 & 5 & 1 & 3 \\
2 & 2 & 3 & 4
\end{bmatrix}
$$

Table below gives values of q, m, m_0, m_1, n to obtain full rank Abelian codes.

The obtained full rank $m \times m$ codewords over complex number field are employed in the design of proposed Abelian SM-NSTBC scheme. The following section describes

Table 7.2 Values of q, m, m_0, m_1, n

q	m	m_0	m_1	$n \mid q^m - 1$
5	4	2	13	$26 \mid 5^4 - 1$
7	4	2	5	$10 \mid 7^4 - 1$
13	4	2	5	$10 \mid 13^4 - 1$

the system model of the proposed Abelian SM-NSTBC scheme.

7.3 System Models

In the proposed Abelian SM-NSTBC communication system, first the binary information is mapped to the full rank $m \times m$ codeword matrices obtained from full rank $n-$length Abelian code. Once the codeword matrices are obtained, spatial modulation is incorporated depending on the number of active antennas. Let N_t be number of transmit antennas, N_a be number of active transmit antennas and N_r be number receive antennas considered. In our analysis we have considered codewords derived from $GF(q^m)$, $q = 5, 7, 13$, $m = 4$ and the codeword matrices obtained are 4×4 codeword matrices. The total number of active antenna patterns are $\binom{N_t}{N_a}$. Once the active antenna subset is selected the codeword vector from lower two rows are conventionally radiated from the active antennas. The algorithm below gives a brief description of Abelian SM-NSTBC encoding.

Algorithm 6 Abelian SM-NSTBC encoding algorithm

1: Start
2: Consider $2^{\lfloor \log_2 (q^m) \rfloor}$ bits
3: Step 1:Acquire $\mathcal{M}_{m \times m} \in GF(q)$ obtained from full rank Abelian codes
4: Step 2: Obtain matrix
5: $[\mathcal{M}_1]_{m \times m/2}$ antenna selection bits $+ [\mathcal{M}_2]_{m \times m/2}$ information bits
6: Step 3:for count=1:no. of time slots for full codeword transmission
7: Step 4: Antenna selection
8:    $[\mathcal{M}_1]_{m \times m/2} \rightarrow C_1[a(1)a(2) \cdots a(m)]$
9: Step 5: Mapping of Information bits: $C_2[i(1)i(2) \cdots i(m)]$
10:    Obtain suitable rank preserving map $X = \varphi(C_2)$
11: end
12: Step 6: Obtain X_{SM}

The received signal has the form as given in Equation (7.5).

$$\mathbf{Y} = \mathbf{H}\mathbf{X}_{SM} + \mathbf{N} \tag{7.5}$$

Here $\mathbf{Y} \in \mathbb{C}^{N_r \times n_s}$ is the received vector, n_s is the number of time slots required to transmit the whole codeword matrix, $\mathbf{H} \in \mathbb{C}^{N_r \times N_t}$ represents the channel between transmitter and receiver, $\mathbf{X}_{SM} \in \mathbb{C}^{N_t \times n_s}$ is the transmitted symbol vector and $\mathbf{N} \in \mathbb{C}^{N_r \times n_s}$ represents independent and identically distributed (i.i.d) circularly symmetric complex Additive White Gaussian Noise with zero mean and unit variance.

The spectral efficiency for the proposed SM-NSTBC scheme is given by

$$\eta = \frac{\lfloor \log_2 (q^m) \rfloor}{n_s} \tag{7.6}$$

Here $n_s = 2m/N_a$, time slots required to transmit a single SM-NSTBC codeword. At the receiver section ML decoding is employed to estimate the transmitted codeword matrix. The following section gives a brief description the theoretical upper bound for ABER of the proposed Abelian SM-NSTBC scheme.

7.4 Analytical performance

This section gives a analytical description for Average Bit Error Rate (ABER) of the proposed Abelian SM-NSTBC system. An analytical upper bound on the ABER validates the correctness of Monte Carlo simulations performed. A analytical upper bound on ABER is given by [Proakis (1995), Simon and Alouini (2005)].

$$ABER_{NSTBC} \leq \frac{1}{2^{\lfloor \log_2 q^m \rfloor}} \sum_{i=1}^{2^{\lfloor \log_2 q^m \rfloor}} \sum_{j=1}^{2^{\lfloor \log_2 q^m \rfloor}} \frac{d(\mathbf{X}_{SM} - \hat{\mathbf{X}}_{SM})}{2\eta} (P(\mathbf{X}_{SM} \to \hat{\mathbf{X}}_{SM})) \tag{7.7}$$

Here, η is the spectral efficiency of the proposed scheme, $d(\mathbf{X}_{SM} - \hat{\mathbf{X}}_{SM})$ is the number of non-zero elements of the difference matrix of $\mathbf{X}_{SM} - \hat{\mathbf{X}}_{SM}$ and $P(\mathbf{X}_{SM} \to \hat{\mathbf{X}}_{SM})$ represents the Pairwise Error Probability of detecting $\hat{\mathbf{X}}_{SM}$, when $\mathbf{X}_{SM}$ is transmitted and is given below

$$P(\mathbf{X}_{SM} \to \hat{\mathbf{X}}_{SM}) = Pr \left(\|\mathbf{Y} - \mathbf{H}\mathbf{X}_{SM}\|_F^2 > \|\mathbf{Y} - \mathbf{H}\hat{\mathbf{X}}_{SM}\|_F^2 |\mathbf{H} \right) \tag{7.8}$$

The pairwise error probability is evaluated using

The PEP of the system is evaluated in terms of non-zero eigen values of the code-

word matrices [Simon and Alouini (2005), Basar et al. (2012)]. Let $\lambda_{i,j}$ represent the non-zero Eigen values of difference matrix. The closed form solution of PEP can be obtained from [Simon and Alouini (2005)], and is simplified as shown in Equation (7.9).

$$P(\mathbf{X}_{SM} \to \hat{\mathbf{X}}_{SM}) \leq \frac{1}{2} \prod_{l=1}^{L} \frac{1}{\left(1 + \frac{\rho \lambda_{i,j_l}}{4}\right)^{N_r}} \tag{7.9}$$

Here, L represents the total number of non-zero Eigen values ($L = 4$), ρ is the SNR value and λ_{i,j_l} are the individual Eigen values for distance matrix. The analytical upper bound on the Average Bit Error Rate (ABER) is calculated as given in Equation (7.10).

$$ABER_{NSTBC} \leq \frac{1}{2^{\lfloor \log_2 q^m \rfloor}} \sum_{i=1}^{2^{\lfloor \log_2 q^m \rfloor}} \sum_{j=1}^{2^{\lfloor \log_2 q^m \rfloor}} \frac{d(\mathbf{X}_{SM} - \hat{\mathbf{X}}_{SM})}{4\eta} \prod_{l=1}^{L} \frac{1}{\left(1 + \frac{\rho \lambda_{i,j_l}}{4}\right)^{N_r}} \tag{7.10}$$

7.5 Simulation Results

This section gives the simulation results of the proposed Abelian SM-NSTBC scheme. The proposed scheme is represented as $C_a(N_t, N_r, N_a)$ for all simulations. The proposed scheme has been compared with the variants of SM-NSTBC, STBC-SM and SM systems. All performance comparison are carried out for a ABER value of 10^{-5}. It has been observed that for a given spectral efficiency the proposed scheme outperforms other competing scheme by ~ 1.5 dB over Rayleigh fading channel.

Figure 7.1, shows performance of the proposed Abelian SM-NSTBC system which employs 6 transmit antennas, 4 receive antennas and 2 active antenna combinations represented as $C_a(6,4,2)$. For codewords derived from full rank Abelian codes over $GF(q)$ where $q = 5, 7, 13$. The theoretical upper bound is is also presented, the close correspondence between simulation results and upper bound for higher values of SNR. The spectral efficiency achieved by the propsoed scheme for $GF(5)$ is 2.25 bpcu, for $GF(7)$ is 2.75 bpcu and for $GF(13)$ is 3.5 bpcu.

In Figure 7.2 the performance of proposed Abelian SM-NSTBC scheme with $N_t = 6, N_r = 4$ and $N_a = 4$ over $GF(5)$, $GF(7)$ and $GF(13)$ are presented. The proposed scheme is compared with the SM-NSTBC system which employs the codewords derived from full rank cyclic codes. The spectral efficiency attained by both the schemes
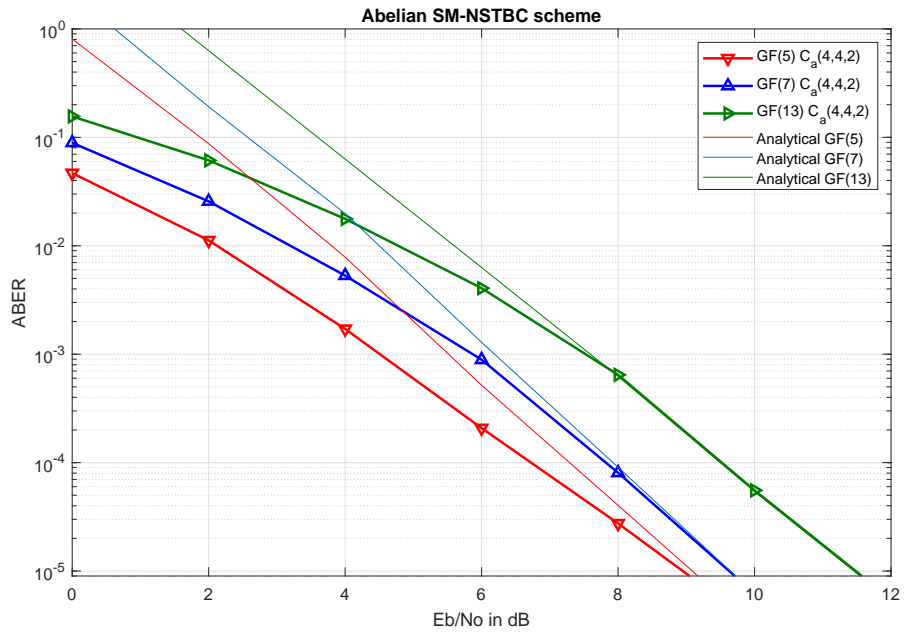
Figure 7.1 ABER performance of Abelian codes for $q = 5, 7, 13$ for $(N_t = 6, N_r = 4, N_a = 2)$
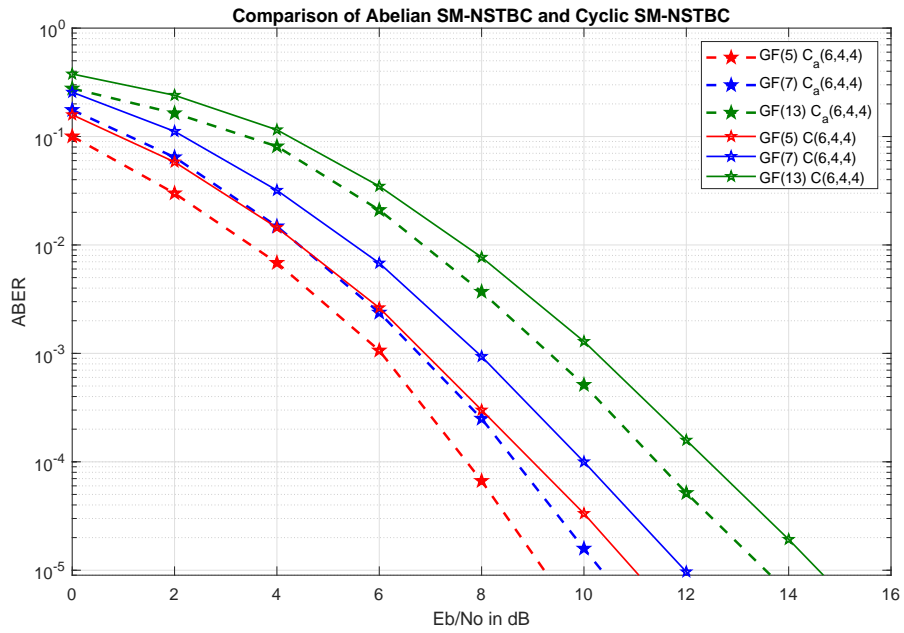

Figure 7.2 Performance comparison of Abelian and Cyclic codewords for $q = 5, 7, 13$ for $(N_t = 6, N_r = 4, N_a = 2)$
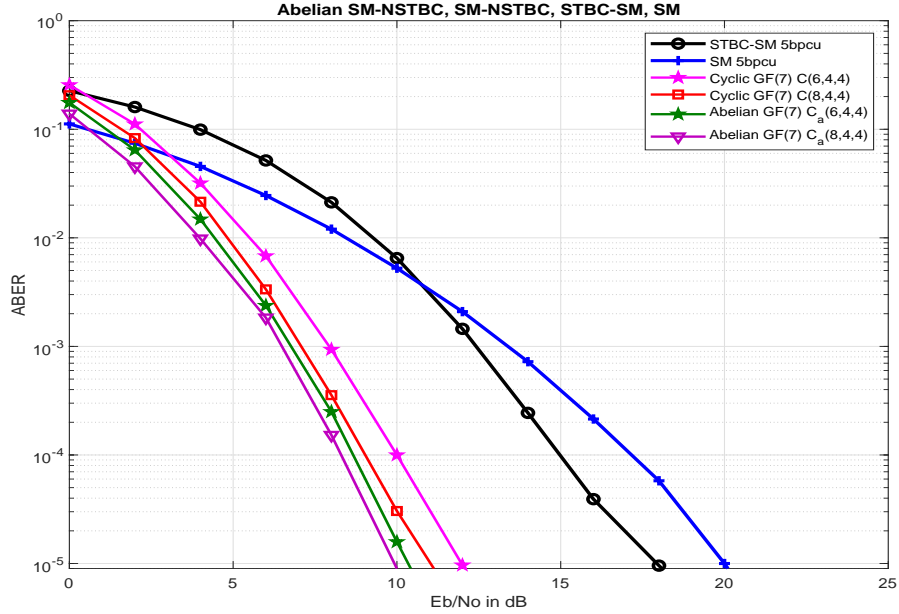
Figure 7.3 ABER comparison of Abelian SM-NSTBC, Cyclic SM-NSTBC, STBC-SM and SM

are 4.5 bpcu, 5.5 bpcu and 7 bpcu for $GF(5)$, $GF(7)$ and $GF(13)$ respectively. It is observed that proposed Abelian SM-NSTBC scheme has a coding gain of minimum 1 dB over SM-NSTBC designed from cyclic codes due to the inbuilt structure of Abelian code.

Figure 7.3 gives the ABER comparison of proposed Abelian SM-NSTBC scheme with Cyclic SM-NSTBC, STBC-SM [Basar et al. (2011)] and SM [Mesleh et al. (2008)] schemes. The spectral efficiency achieved by STBC-SM and SM scheme is 5 bpcu. This performance is compared with Abelian SM-NSTBC with codeword derived over $GF(7)$ and the spectral efficiency of 5.5 bpcu. It is observed that the proposed scheme has a superior performance of ~ 3 dB over STBC-SM and ~ 4 dB over SM scheme.

In Figure 7.4 the ABER performance of proposed scheme is compared with SM-OSTBC [Wang and Chen (2014)] scheme. The SM-OSTBC employs ($N_t = 8$, $N_r = 4$, $N_a = 6$) with 4-QAM and ($N_t = 8$, $N_r = 4$, $N_a = 4$) with 16-QAM, while proposed scheme employs codewords derived over $GF(13)$ and ($N_t = 6, 8$, $N_r = 4$, $N_a = 4$) antenna configuration. The spectral efficiency achieved by above scheme is 7 bpcu. It is
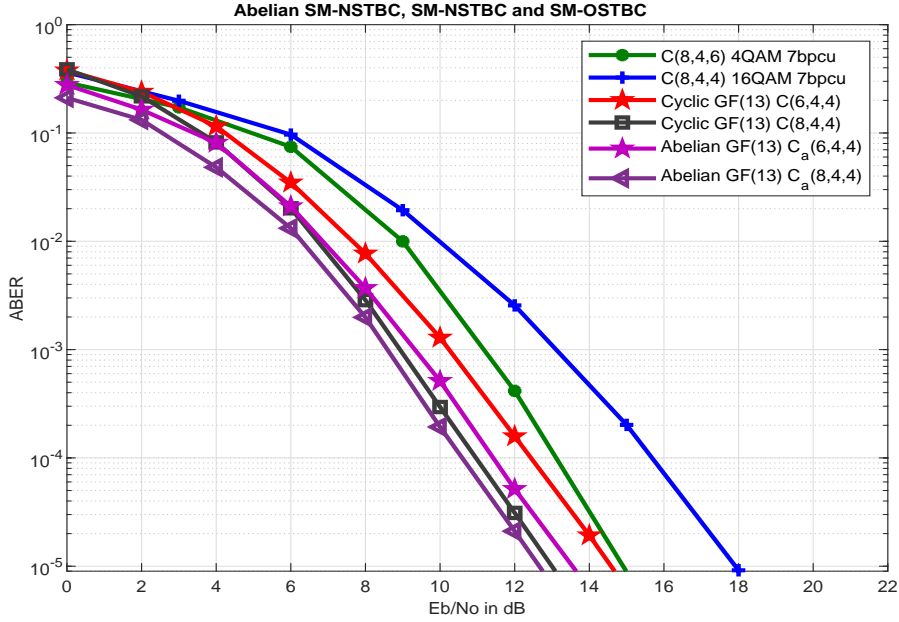
Figure 7.4 ABER comparison of Abelian SM-NSTBC, Cyclic SM-NSTBC and SM-OSTBC

observed that proposed Abelian SM-NSTBC scheme employs less number of transmit and active antennas still has a performance improvement of ~ 3 dB over SM-OSTBC scheme.

The performance of NSTBCs derived from Abelian codes provide a higher performance than NSTBCs derived from Cyclic codes. This improvement in performance is obtained due to the higher coding gain of the Abelian codes. It is observed that Abelian codes achieves a coding gain of minimum of 0.6 dB as when compared with Cyclic codes. The table below shows the coding gain NSTBCs derived from Abelian code and Cyclic code.

7.6 Summary

This chapter gives a brief insight on the transform domain description of Abelian Codes, and their rank distance properties. A novel Spatially Modulated Space Time Block Code designed from the class of full rank Abelian codes over $GF(q^m)$, where $q = 5, 7, 13$ and $m = 4$ is proposed. In the proposed scheme the codewords of Abelian code are

Table 7.3 Performance comparison of Abelian and Cyclic SM-NSTBC system at ABER of 10^{-5} in dB

Constellation Size	Performance of Abelian code at 10^{-5} ABER (dB)	Performance of Cyclic code at 10^{-5} ABER (dB)	Coding gain of Abelian over Cyclic code (dB)
$GF(5)$	9.4	11	1.6
$GF(7)$	10.2	12	1.8
$GF(13)$	13.8	14.4	0.6

mapped into $m \times m$ full rank matrices over the Complex number field by the use of either Gaussian Integer Map (for $q = 5, 13$) or the Eisenstein Integer Map (for $q = 7$). A mathematical upper bound on the ABER for proposed scheme has been derived and the tightness of this bound is verified by Monte-Carlo simulation. The ABER performance of the proposed system is compared with other competing schemes. It is observed that the proposed scheme outperforms Cyclic SM-NSTBC scheme by minimum of 1 dB, SM-OSTBC by ~ 2 dB and STBC-SM by ~ 4 dB. Hence, we can consider Space Time Codes derived from non-binary codes as worthy candidates for designing various SM-NSTBC schemes for various applications.

Chapter 8

Conclusions and Future work

We have started off the research work described in this thesis by revisiting the study of and characterization of full rank Cyclic codes using the Transform domain characterization. Several Cyclic codes with full rank property have been derived and analyzed. These full rank Cyclic codes have been employed to derive Non-Orthogonal Space Time Block Codes. Full rank Cyclic codes from primary base fields ($q = 5, 7, 13, 17$) have been synthesized and incorporated throughout the thesis to obtain STBC designs for several modern applications. A thorough study of modern MIMO techniques such as Spatial Modulation and Space Time Block Codes has inspired us to develop the novel Spatially Modulated Non-orthogonal Space Time Block Codes (SM-NSTBC). The NSTBCs designed in the thesis have full rank property, and are derived over a base field of $GF(q)$, where $q = 5, 7, 13, 17$. The codeword matrices of the synthesized codes have been translated into equivalent matrices over the complex number field by rank preserving maps. Gaussian Integer Map is used for $q = 5, 13, 17$ and Eisenstein Integer Map is used for $q = 7$. The full design parameters and performance analysis for the proposed SM-NSTBC scheme are presented in Chapter 3. It is observed that the proposed SM-NSTBC scheme provides a performance improvement of a minimum of ~ 1.5 dB and ~ 1 when compared with STBC-SM and SM-OSTBC.

In the second contributory chapter (chapter 4) the concept of receive spatial modulation is explored. In this scheme, only a subset of receive antennas for a given time interval. The process of activating only a subset of receive antenna is achieved by implementing the precoding technique. In order to ensure the accuracy of the precoder, the availability of perfect channel state information at the transmitter is assumed. We

125

have proposed the concept of Precoded SM-NSTBC, where NSTBC is derived from full rank cyclic code derived over extension Galois field of $GF(q^m)$, and represented in primary Galois field as a matrix over $GF(q)$. In order to achieve receive spatial modulation, a zero-forcing precoding technique is employed. The performance of the proposed scheme is evaluated over both uncorrelated and spatially correlated Rayleigh fading environments. It is observed that the proposed scheme outperforms precoded SM-OSTBC and STBC-SM by approximately 2 dB to 7 dB in an uncorrelated and spatially correlated fading environment.

In chapter 5, the idea of cooperative communication is designed and explored. A cooperative communication system provides the benefits virtual MIMO system. The information is conveyed from source to destination with the assistance of geographically available intermediate relays. The most commonly employed relay technique that is employed in practice is Amplify and Forward. This has been employed in this thesis. We have proposed a SM-NSTBC-AF scheme in which the dual-hop cooperative communication link, as well as direct link between source and destination have been made available. The analytical upper bound on the ABER provided by this composite cooperative communication link is estimated. Monte Carlo simulations have shown that the performance of the proposed SM-NSTBC-AF scheme has performance improvement of ~ 3 dB over STBC-SM and ~ 2dB improvement over SM-OSTBC scheme employing Cooperative AF link.

In chapter 6, the modeling of a High Altitude Platform (HAP) is given. HAP have gained huge attention due to its advantages of easy restoration, quick installment as a remote base station. HAP ensures high quality of service in practical scenarios where establishing a whole base station is not feasible and not cost-effective. The performance of SM-NSTBC is evaluated over the HAP environment in this chapter. Further, the proposed scheme is compared with a conventional techniques of SM-OSTBC and STBC-SM. Later the performance is assessed over correlated HAP environment in the presence of Perfect and Imperfect Channel State Information. It is observed that the proposed scheme outperforms the competing by a minimum of 3 dB in the presence of Perfect CSI and by 2 dB in Imp-CSI availability.

126

In chapter 7, a new class of STBCs derived from Abelian codes has been designed. Their application in the field of MIMO wireless communication has been explored. The transform domain characterization of Abelian codes has been employed to specify Abelian codes possessing full rank property. After synthesizing Abelian codes possessing full rank property, STBCs derived from these codes have been proposed. An expression for the overall ABER presented by these codes has also been derived. Their performance has been studied using Monte Carlo simulations has been determined and this has been compared with conventional designs and designs derived from full rank Cyclic codes.

8.1   Future work

- Full rank cyclic codes with higher values of q can be designed. Such designs will be able to provide higher rates. We have documented the performance of these codes with the use of ML detection and have also explored the low complexity sphere decoding technique. The more specific full rank code decoding techniques, such as soft decoding for RS codes, can be designed and employed in the proposed NSTBC system.

- The study in this thesis constitutes the codewords derived $(n, 1)$ full rank Cyclic and Abelian codes. This concept can further be explored for codewords derived from (n, x), for $x > 1$ and its suitable implementation in MIMO systems can be examined as future works.

- Precoding aided SM-NSTBC is designed in chapter 4, which demonstrates the receive spatial modulation technique. We have used the zero-forcing precoding technique to achieve receive spatial modulation. The scheme can be examined by incorporating different precoding techniques. Further, as only a subset of receive antennas are activated, one can consider designing a low complexity receive spatial modulation (Ordered Block MMSE) decoding technique instead of a Brute force ML decoder.

- The field of cooperative communication is expanding very rapidly nowadays. We have explored the concept of Amplify and forward technique, one can extend the study by evaluating the performance of a decode and forward technique. Further, the concept of AF can be explored by varying the number of relays and antenna configurations at the source and destination nodes. The idea of cooperative communication can be more judiciously studied by adopting a selection algorithm, which would select one of two available relaying techniques (AF and/or DF) depending on the channel parameters (hybrid selection).

- The application of these full rank codewords derived from Abelian codes and Cyclic codes can further be explored for other applications in wireless systems operating over a block fading environment.

Appendix A

Gaussian and Eisenstein Mapping

The rank preserving maps employed throughout these thesis are Gaussian Integer Map and Eisenstein Integer Map [Huber (1994b)] and [Huber (1994a)].

Gaussian Integer Map [Huber (1994b)]: A prime number q which is in the form of $q = 4K + 1$, can be expressed as $q = u^2 - v^2$ for suitable u and v. These are known as Gaussian integers which are represented by $\omega = u + iv; u, v \in Z$ [Huber (1994b)]. This map is defined as follows:

$$\mathscr{Z}_i = i \bmod \Pi = i - \left[\frac{i\Pi'}{\Pi\Pi'}\right]\Pi; \qquad i = 0, 1, \ldots, q - 1 \tag{A.1}$$

Here, $\Pi = (u + iv)$ and $\Pi' = (u - iv)$, $[\cdot]$ stands for rounding of operation to the nearest integer. The values of Gaussian Integer Map and the constellation diagram for $q = 5, 13, 17$ is as follows.

Table A.1 Gaussian Map exponent for $\mathscr{Z}_{2+i}$ for $GF(5)$

s	0	1	2	3	4
$\mathscr{Z}_{2+i}$	$2 + i$	1	i	$-i$	-1

Table A.2 Gaussian Map exponent for $\mathscr{Z}_{3+2i}$ for $GF(13)$

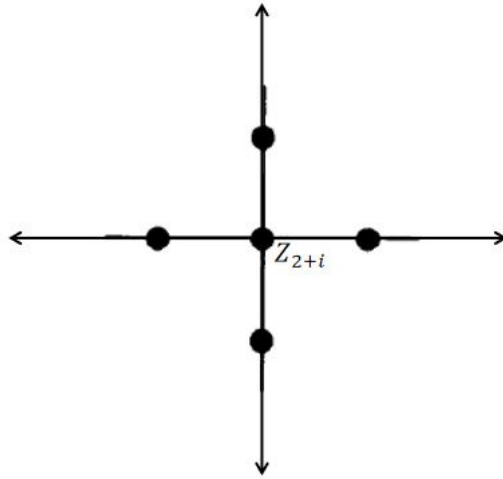| s	0	1	2	3	4	5	6	7	8	9	10	11	12
$\mathscr{Z}_{3+2i}$	$3 + 2i$	1	$1 + i$	$2i$	$-i$	$1 - i$	2	-1	$-1 - i$	$-2i$	i	$-1 + i$	-2

Figure A.1 Constellation for $GF(5)$ [Huber (1994b)]
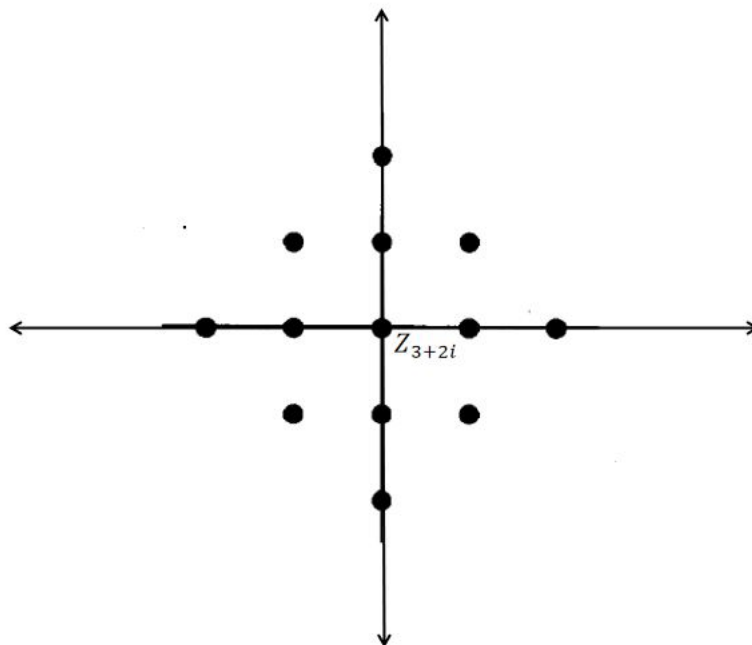
Figure A.2 Constellation for $GF(13)$ [Huber (1994b)]

130

Table A.3 Gaussian Map exponent for $\mathscr{Z}_{4+i}$ for $GF(17)$

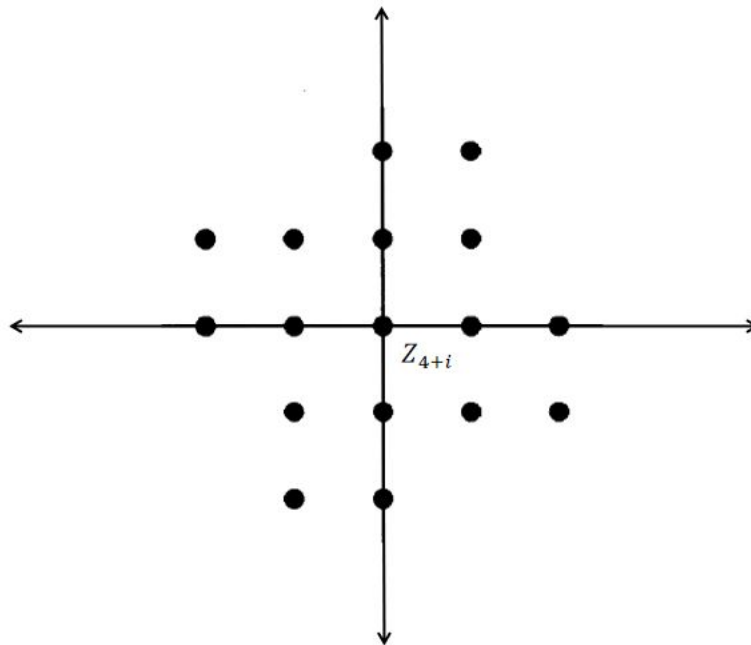| s	0	1	2	3	4	5	6	7
$\mathscr{Z}_{4+i}$	$4+i$	1	$1+i$	$2i$	$-1-2i$	i	$-1+i$	-2
8	9	10	11	12	13	14	15	16
$2-i$	-1	$-1-i$	$-2i$	$1+2i$	$-i$	$1-i$	2	$-2+i$

Figure A.3 Constellation for $GF(17)$ [Huber (1994b)]

Eisenstein Integer Map [Huber (1994a)]: A rank preserving map for $GF(q)$, (q is a prime) which can be expressed as $q = 1$ *mod* 6 was given in [Huber (1994a)] . The Eisenstein-Jacobi integer can be expressed as $\omega = \alpha + \rho\beta$, where ρ is a complex number given by $\rho = (-1 + i\sqrt{3})/2$, the Eisenstein-Jacobi prime is given by $q = \alpha^2 + 3\beta^2$. The mapping for Eisenstein map is given as following:

$$\zeta(i) = i \mod \Pi \triangleq i - \left[\frac{i\Pi^*}{\Pi\Pi^*}\right] \Pi \; for \; i = 0, 1, 2, \ldots, q-1 \tag{A.2}$$

Where $\Pi = \alpha + \beta + \rho 2\beta$ and $\Pi^* = \alpha + \beta + \rho^2 2\beta$. The values of Eisenstein Integer Map and the constellation diagram for $q = 7$ is as follows.

Table A.4 Eisenstein Map exponent for $\zeta_{3+2\rho}$ for $GF(7)$

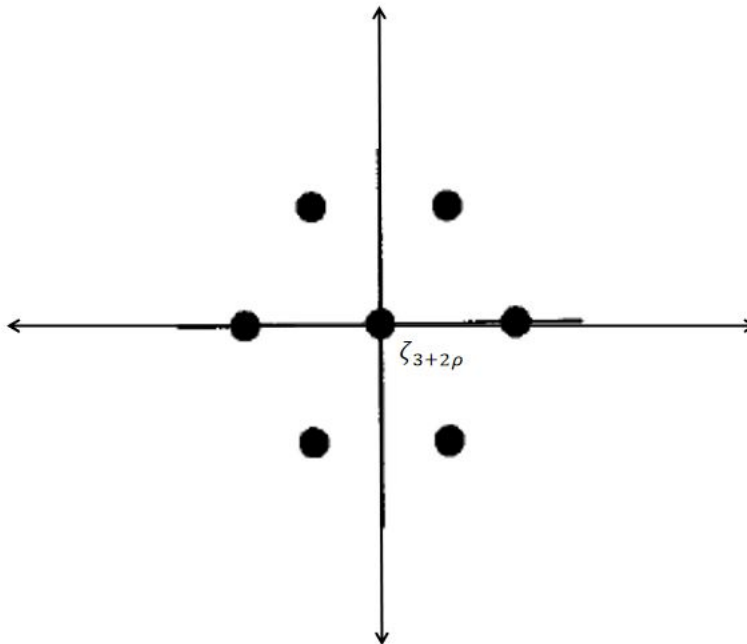| s	0	1	2	3	4	5	6
$\zeta_{3+2\rho}$	$3+2\rho$	1	$1+\rho$	ρ	-1	$-1-\rho$	$-\rho$

Figure A.4 Constellation for $GF(7)$ [Huber (1994a)]

Bibliography

Alamouti, S. M. (1998). A simple transmit diversity technique for wireless communications. *IEEE Journal on selected areas in communications*, 16(8), 1451–1458.

Alkhawaldeh, S. A. (2018). Layered spatial modulation. *EURASIP Journal on Wireless Communications and Networking*, 2018(1), 233.

Alsmadi, M. M., Canbilen, A. E., Ikki, S. S., Basar, E., Gultekin, S. S., and Develi, I. (2018). Imperfect csi and improper gaussian noise effects on ssk: Optimal detection and error analysis. In *2018 IEEE Global Communications Conference (GLOBE-COM)*, 1–6. IEEE.

Altın, G., Aygolu, U., Başar, E., and Celebi, M. E. (2016). Outage probability analysis of cooperative spatial modulation systems. In *2016 23rd International conference on telecommunications (ICT)*, 1–5. IEEE.

Altın, G., Aygölü, Ü., Basar, E., and Çelebi, M. E. (2017). Multiple-input–multiple-output cooperative spatial modulation systems. *IET Communications*, 11(15), 2289–2296.

Babaei, M., Basar, E., and Aygölü, Ü. (2016). A cooperative spectrum sharing protocol using stbc-sm at secondary user. In *2016 24th Telecommunications Forum (TELFOR)*, 1–4. IEEE.

Başar, E. and Aygölü, Ü. (2009). High-rate full-diversity space-time block codes for three and four transmit antennas. *IET communications*, 3(8), 1371–1378.

Basar, E., Aygolu, U., Panayirci, E., and Poor, H. V. (2011). Space-time block coded spatial modulation. *IEEE Transactions on Communications*, 59(3), 823–832.

Basar, E., Aygolu, U., Panayirci, E., and Poor, H. V. (2012). Performance of spatial modulation in the presence of channel estimation errors. *IEEE Communications Letters*, 16(2), 176–179.

Berman, S. (1967). Semisimple cyclic and abelian codes. ii. *Cybernetics*, 3(3), 17–23.

Blahut, R. E. (1983). *Theory and practice of error control codes*. Addison-Wesley.

Blahut, R. E. (2003). *Algebraic codes for data transmission*. Cambridge university press.

Chen, S., Wang, W., Zhang, X., and Sun, Z. (2009). Performance analysis of ostbc transmission in amplify-and-forward cooperative relay networks. *IEEE Transactions on Vehicular Technology*, 59(1), 105–113.

Cho, Y. S., Kim, J., Yang, W. Y., and Kang, C. G. (2010). MIMO-OFDM wireless communications with Matlab. *John Wiley & Sons*.

Delsarte, P. (1978). Bilinear forms over a finite field, with applications to coding theory. *Journal of Combinatorial Theory, Series A, Elsevier*, 25(3), 226–241.

Foschini, G. J. (1996). Layered space-time architecture for wireless communication in a fading environment when using multi-element antennas. *Bell labs technical journal*, 1(2), 41–59.

Foschini, G. J. and Gans, M. J. (1998). On limits of wireless communications in a fading environment when using multiple antennas. *Wireless personal communications*, 6(3), 311–335.

Gabidulin, E. M. (1985). Theory of codes with maximum rank distance. *Problemy Peredachi Informatsii, Russian Academy of Sciences, Branch of Informatics, Computer Equipment and Automatization*, 21(1), 3–16.

Godkhindi, S., Goutham Simha, G., and Acharya, U. S. (2019). Spatially Modulated non Orthogonal Space Time Block Code: Construction and design from cyclic codes over Galois Field. *Physical Communication, Elsevier*, page 100735.

Goutham Simha, G. D. (2018). *Design and implementation of modulation and detection strategies for Spatial Modulation MIMO systems*. PhD thesis, NITK, Surathkal, India.

Goutham Simha, G. D., Raghavendra, M., Shriharsha, K., and Acharya, U. S. (2017). Signal constellations employing multiplicative groups of gaussian and eisenstein integers for enhanced spatial modulation. *Physical Communication*, 25, 546–554.

Gradshteyn, I., Ryzhik, I. M., Jeffrey, A., and Zwillinger, D. (2007). Table of Integrals. *Series, and Products, Alan Jeffrey and Daniel Zwillinger (eds.), Seventh edition (Feb 2007)*, 885.

Helmy, A. G., Di Renzo, M., and Al-Dhahir, N. (2016). Enhanced-reliability cyclic generalized spatial-and-temporal modulation. *IEEE Communications Letters*, 20(12), 2374–2377.

Huber, K. (1994a). Codes over eisenstein-jacobi integers. *Contemporary Mathematics*, 168, 165–165.

Huber, K. (1994b). Codes over gaussian integers. *IEEE Transactions on Information Theory*, 40(1), 207–216.

Jeganathan, J., Ghrayeb, A., Szczecinski, L., and Ceron, A. (2009). Space shift keying modulation for mimo channels. *IEEE transactions on wireless communications*, 8(7), 3692–3703.

Kramer, G., Gastpar, M., and Gupta, P. (2005). Cooperative strategies and capacity theorems for relay networks. *IEEE Transactions on Information Theory*, 51(9), 3037–3063.

Laneman, J. N., Tse, D. N., and Wornell, G. W. (2004). Cooperative diversity in wireless networks: Efficient protocols and outage behavior. *IEEE Transactions on Information theory*, 50(12), 3062–3080.

Laneman, J. N. and Wornell, G. W. (2000). Energy-efficient antenna sharing and relaying for wireless networks. In *WCNC*, 7–12.

Le, M.-T., Ngo, V. D., Mai, H.-A., Tran, X. N., and D Renzo, M. (2014). Spatially modulated orthogonal space-time block codes with non-vanishing determinants. *IEEE Transactions on Communications*, 62(1), 85–99.

Li, J., Wen, M., Cheng, X., Yan, Y., Song, S., and Lee, M. H. (2016). Generalized precoding-aided quadrature spatial modulation. *IEEE Transactions on Vehicular Technology*, 66(2), 1881–1886.

Li, X. and Wang, L. (2014). High rate space-time block coded spatial modulation with cyclic structure. *IEEE Communications Letters*, 18(4), 532–535.

Luo, J., Wang, S., Wang, F., and Zhang, W. (2018). Generalized precoding-aided spatial modulation via receive antenna transition. *IEEE Wireless Communications Letters*, 8(3), 733–736.

Lusina, P., Gabidulin, E., and Bossert, M. (2003). Maximum rank distance codes as space-time codes. *IEEE Transactions on Information Theory*, 49(10), 2757–2760.

MacWilliams, M. F. (1970). Binary codes which are ideals in the group algebra of an abelian group. *Bell System Technical Journal*, 49(6), 987–1011.

Mans, R., Simha, G. G., and Sripati, U. (2017). Abelian codes over eisenstein-jacobi integers for mimo systems. In *2017 International Conference on Advances in Computing, Communications and Informatics (ICACCI)*, 1909–1912. IEEE.

M.Blaum, P. F. and van Tilborg, H. (1998). Array codes. *Handbook of Coding Theory, vol. 1, Elsevier*, 295–461.

Mesleh, R., Di Renzo, M., Haas, H., and Grant, P. M. (2010). Trellis coded spatial modulation. *IEEE Transactions on Wireless Communications*, 9(7), 2349–2361.

Mesleh, R., Haas, H., Sinanovic, S., Ahn, C. W., and Yun, S. (2008). Spatial modulation. *IEEE Transactions on Vehicular Technology*, 57(4), 2228.

Mesleh, R., Hiari, O., Younis, A., and Alouneh, S. (2017). Transmitter design and hardware considerations for different space modulation techniques. *IEEE Transactions on Wireless Communications*, 16(11), 7512–7522.

Mesleh, R., Ikki, S., and Alwakeel, M. (2011). Performance analysis of space shift keying with amplify and forward relaying. *IEEE Communications Letters*, 15(12), 1350–1352.

Mesleh, R. and Ikki, S. S. (2012). On the effect of gaussian imperfect channel estimations on the performance of space modulation techniques. In *2012 IEEE 75th Vehicular Technology Conference (VTC Spring)*, 1–5. IEEE.

Mesleh, R. and Ikki, S. S. (2013). Performance analysis of spatial modulation with multiple decode and forward relays. *IEEE Wireless Communications Letters*, 2(4), 423–426.

Mesleh, R., Ikki, S. S., Aggoune, E.-H. M., and Mansour, A. (2012). Performance analysis of space shift keying (SSK) modulation with multiple cooperative relays. *EURASIP Journal on Advances in Signal Processing*, 2012(1), 201.

Mohammed, A., Mehmood, A., Pavlidou, F.-N., and Mohorcic, M. (2011). The role of high-altitude platforms (haps) in the global wireless connectivity. *Proceedings of the IEEE*, 99(11), 1939–1953.

Moon, T. K. (2005). *Error Correction Coding: Mathematical Methods and Algorithms*, 750. John Wiley & Sons.

Mozaffari, M., Saad, W., Bennis, M., Nam, Y.-H., and Debbah, M. (2019). A tutorial on UAVs for wireless networks: Applications, challenges, and open problems. *IEEE Communications Surveys & Tutorials*.

Nosratinia, A., Hunter, T. E., and Hedayat, A. (2004). Cooperative communication in wireless networks. *IEEE communications Magazine*, 42(10), 74–80.

Öztoprak, Ö. C., Yarkin, F., Altunbas, I., and Basar, E. (2017). Performance analysis of Space Shift Keying for af relaying with relay selection. *AEU-International Journal of Electronics and Communications*, 81, 74–82.

Proakis, J. G. (1995). *Digital Communications*. McGraw-Hill, 3rd edition.

Puchinger, S., Stern, S., Bossert, M., and Fischer, R. F. (2016). Space-time codes based on rank-metric codes and their decoding. In *Wireless Communication Systems (ISWCS), 2016 International Symposium on*, 125–130. IEEE.

Rajan, B. S. and Siddiqi, M. (1992). Transform domain characterization of abelian codes. *IEEE transactions on information theory*, 38(6), 1817–1821.

Roth, R. M. (1991). Maximum-rank array codes and their application to crisscross error correction. *IEEE transactions on Information Theory*, 37(2), 328–336.

Serafimovski, N., Sinanovic, S., Di Renzo, M., and Haas, H. (2011). Dual-hop spatial modulation (dh-sm). In *2011 IEEE 73rd Vehicular Technology Conference (VTC Spring)*, 1–5. IEEE.

Simha, G. G., Koila, S., Neha, N., Raghavendra, M., and Sripati, U. (2017). Redesigned spatial modulation for spatially correlated fading channels. *Wireless Personal Communications*, 97(4), 5003–5030.

Simon, M. K. and Alouini, M. S. (2005). *Digital communication over fading channels*, 95. John Wiley & Sons.

Som, P. and Chockalingam, A. (2013). End-to-end ber analysis of space shift keying in decode-and-forward cooperative relaying. In *2013 IEEE wireless communications and networking conference (WCNC)*, 3465–3470. IEEE.

Spencer, Q. H., Swindlehurst, A. L., and Haardt, M. (2004). Zero-forcing methods for downlink spatial multiplexing in multiuser mimo channels. *IEEE transactions on signal processing*, 52(2), 461–471.

Sripati, U. (2004). *Space time block codes for MIMO fading channels from codes over finite field*. PhD thesis, IISc Bangalore, India.

Sripati, U. and Rajan, B. S. (2003). On the rank distance of cyclic codes. In *IEEE International Symposium on Information Theory, 2003. Proceedings.*, page 72. IEEE.

Sripati, U. and Rajan, B. S. (2004). On the rank distance of Cyclic and Abelian codes. *National Conference of Communication*, 410–414.

Sripati, U., Rajan, B. S., and Shashidhar, V. (2004). Full-diversity stbcs for block-fading channels from cyclic codes. In *Global Telecommunications Conference, 2004. GLOBECOM'04. IEEE*, 1, 566–570. IEEE.

Stavridis, A., Sinanovic, S., Di Renzo, M., and Haas, H. (2012). Transmit precoding for receive spatial modulation using imperfect channel knowledge. In *2012 IEEE 75th Vehicular Technology Conference (VTC Spring)*, 1–5. IEEE.

Su, W. and Xia, X.-G. (2003). On space-time block codes from complex orthogonal designs. *Wireless Personal Communications*, 25(1), 1–26.

Sudheesh, P., Sharma, N., Magarini, M., and Muthuchidambaranathan, P. (2018). Effect of imperfect csi on interference alignment in multiple-high altitude platforms based communication. *Physical Communication,Elsevier*, 29, 336–342.

Sugiura, S., Chen, S., Haas, H., Grant, P. M., and Hanzo, L. (2011). Coherent versus non-coherent decode-and-forward relaying aided cooperative space-time shift keying. *IEEE Transactions on Communications*, 59(6), 1707–1719.

Sugiura, S., Chen, S., and Hanzo, L. (2010). Coherent and differential space-time shift keying: A dispersion matrix approach. *IEEE Transactions on Communications*, 58(11), 3219–3230.

Tarokh, V., Seshadri, N., and Calderbank, A. R. (1998). Space-time codes for high data rate wireless communication: Performance criterion and code construction. *IEEE transactions on information theory*, 44(2), 744–765.

Telatar, E. (1999). Capacity of multi-antenna gaussian channels. *European transactions on telecommunications, ETT*, vol.10(6), 585–595.

Varshney, N., Goel, A., and Jagannatham, A. K. (2016). Cooperative communication in spatially modulated mimo systems. In *2016 IEEE Wireless Communications and Networking Conference*, 1–6. IEEE.

Varshney, N., Krishna, A. V., and Jagannatham, A. K. (2015). Selective df protocol for mimo STBC based single/multiple relay cooperative communication: End-to-end

performance and optimal power allocation. *IEEE Transactions on Communications*, 63(7), 2458–2474.

Viterbo, E. and Boutros, J. (1999). A universal lattice code decoder for fading channels. *IEEE Transactions on Information theory*, 45(5), 1639–1642.

Wang, L. and Chen, Z. (2014). Correction to "spatially modulated orthogonal space-time block codes with non-vanishing determinants". *IEEE Transactions on Communications*, 62(10), 3723–3724.

Wang, L., Chen, Z., and Wang, X. (2014). A space-time block coded spatial modulation from (n, k) error correcting code. *IEEE Wireless Communications Letters*, 3(1), 54–57.

Yang, D., Xu, C., Yang, L.-L., and Hanzo, L. (2011). Transmit-diversity-assisted space-shift keying for colocated and distributed/cooperative mimo elements. *IEEE Transactions on Vehicular Technology*, 60(6), 2864–2869.

Yang, L.-L. (2011). Transmitter preprocessing aided spatial modulation for multiple-input multiple-output systems. In *2011 IEEE 73rd Vehicular Technology Conference (VTC Spring)*, 1–5. IEEE.

Yeoh, P. L., Elkashlan, M., and Collings, I. B. (2011). Selection relaying with transmit beamforming: a comparison of fixed and variable gain relaying. *IEEE Transactions on Communications*, 59(6), 1720–1730.

Younis, A. (2014). Spatial modulation: Theory to practice. *The University of Edinburgh*.

Zajic, A. (2012). Mobile-to-mobile wireless channels. *Artech House*.

Zhang, R., Yang, L.-L., and Hanzo, L. (2013). Generalised pre-coding aided spatial modulation. *IEEE Transactions on Wireless Communications*, 12(11), 5434–5443.

Journal Publications:

- **Godkhindi Shrutkirthi S.**, Goutham Simha G.D.,U Shripathi Acharya," Spatially Modulated Non Orthogonal Space Time Block Code: Construction and Design from cyclic codes over Galois Field", Physical Communication, Elsevier, Volume 35, August 2019, 100735.

- **Godkhindi Shrutkirthi S.**, Goutham Simha G.D.,U Shripathi Acharya, "Generalized designs for Precoded Receive Spatial Modulation derived from Non-Orthogonal Space Time Block Codes.", Telecommunication systems, Springer (Under Review)

- **Godkhindi Shrutkirthi S.**, Goutham Simha G.D., R Prasad Naik, U Shripathi Acharya, "Design and performance analysis of cooperative SM-NSTBC with amplify and forward relaying.", IEEE Transactions on Wireless Communications (Under Review)

Conference Papers

- **Godkhindi Shrutkirthi S.**, Goutham Simha G.D.,U Shripathi Acharya, "A MIMO SM-NSTBC scheme for High Altitude Platform communication systems: Study and Analysis.". 6th International Conference on Signal Processing and Integrated Networks (SPIN-2019), IEEE.

- **Godkhindi Shrutkirthi S.**, Goutham Simha G.D.,U Shripathi Acharya, "Performance of SM-NSTBC for correlated HAP fading channels with Imperfect-CSI. ", International Conference on Optical and Wireless Technologies (OWT-2019), Springer proceedings.

BIO-DATA

Name : Godkhindi Shrutkirthi S.

Email Id : shrutakirtig@gmail.com

Mobile : +91-9925207723

Date of Birth : 25-June-1991

Address : Dept of Electronics and Communication Engineering NITK, Surathkal.

Educational Qualifications and Teaching Experience:

Degree	Year of Passing	University
B.E.	2013	GTU Gandhinagar, BIT, Vadodara.
M.tech.	2015	GTU Gandhinagar,GCET Vallabh Vidyanagar, Anand.
Research Scholar	2015-2020	National Institute of Technology Karnataka, Surathkal.